NTNU – Trondheim
Norwegian University of
Science and Technology

Wellbore Stability and the Thermal Effects Analysis for a North Sea Exploration Well

Inocencio Prazeres

Petroleum Geosciences
Submission date: June 2015
Supervisor: Andreas Bauer, IPT

Norwegian University of Science and Technology
Department of Petroleum Engineering and Applied Geophysics

NTNU – Trondheim
Norwegian University of
Science and Technology

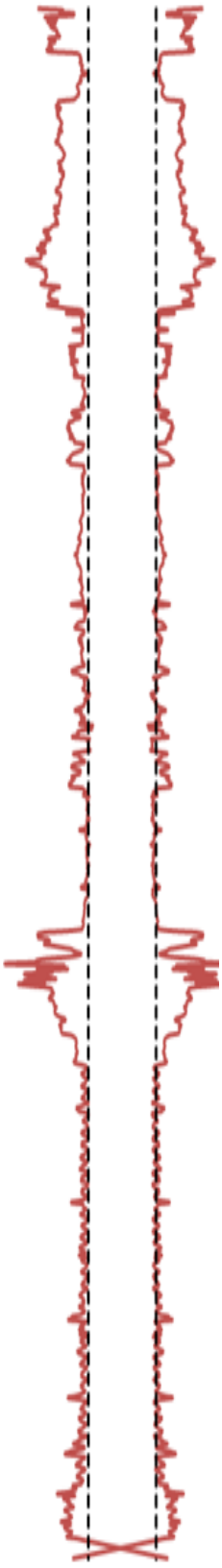

Wellbore Stability and the Thermal Effects Analysis for a North Sea Exploration Well.

Inocencio Prazeres

NTNU Norwegian University of Science and Technology

Faculty of Engineering Science and Technology

Wellbore Stability and the Thermal Effects Analysis for a North Sea Exploration Well

Inocencio Prazeres

Supervisor │ Andreas Bauer, SINTEF Petroleum Research

Co-Supervisor │ Per Horsrud, STATOIL

Spring │ 2015

Department of Petroleum Engineering and Applied Geophysics

Prefácio

Esta tese foi feita como conclusão do Mestrado em Geofísica, na NTNU (Universidade Norueguesa de Ciência e Tecnologia, Instituto de Tecnologia do Petróleo (IPT).

A pesquisa para esta tese foi interessante. No entanto, a linha de abordagem acabou por se tornar em batalhas contra equações diferenciais parciais (PDE) (equação da difusão), e o estresse (estresse da crusta terrestre). Embora o material recolhido e as informações foram mais do que suficiente, os desafios foram decidir sobre quais pressupostos seria o melhor a fazer abordagens e como lidar com estes.

A escrita desta tese foi uma tarefa muito difícil, ao invés de processo interessante devido ao número considerável de questoues a serem coberto. Aqui, não pode expressar as longas noites sem dormir, o estresse induzido pela frustração ou vice versa, a esperança de bons resultados e a tristeza e cansaço em cada tentativa fracassada. No processo de escrita eu aprendi muito e minhas concepções iniciais sobre a instabilidade de pocos mudaram e de que maneira! Lidei com uma série de questoes, numa tentativa de dar a esta tese uma ampla perspectiva sobre instabilidade de pocos.

A tese foi feita exclusivamente pelo autor; a maior parte do texto, no entanto, baseia-se na pesquisa de outros, e eu fiz o meu melhor para fornecer referências a essas fontes.

Inocencio Prazeres

Trondheim, Primavera 2015

Preface

This thesis has been made as a completion of Master Degree in Geophysics, at NTNU (Norwegian University of Science and Technology, Institute of Petroleum Technology (IPT).

The research for this thesis has been an interesting. However, the line of approach turned out to be battles against PDEs (Partial differential equations) (Diffusion Equation) and Stresses (Earth stress). Although the collected material and information have been extremely comprehensive, challenges was to decide on which assumptions would be the best to make approaches and to how to handle these.

Writing this thesis has been a very difficult task, rather than interesting process because of the considerable number aspects to cover. And it cannot express the long sleepless nights, the frustration induced stress and vice-versa, the hope for good results and the sadness and tiredness with each failed attempt. In the process of writing I have felt I have learned a lot and my initial conceptions of Wellbore Stability have certainly changed! I have dealt with a lot of subjects, in an attempt to give this thesis a broad perspective on Wellbore Stability.

The thesis has been made solely by the author; most of the text, however, is based on the research of others, and I have done all my best to provide references to these sources.

Inocencio Prazeres

Trondheim, spring 2015

I. Acknowledgments

Quite a few people have helped me in a number of ways to complete this work. First, and foremost, I would like to express the deepest appreciation to Andreas Bauer my supervisor from SINTEF Petroleum Research AS, for his patient guidance, support, useful and openly critiques during this project. His insights and enthusiastic encouragement have been inspirational, and I feel lucky to have had him as my supervisor.

I would like to offer my special thanks to Per Horsrud from Statoil for his input, advice, unconditional assistance and support, as well as his efforts on helping me to gather all relevant data required for this project.

I am highly indebted to STATOIL to provide me with data and for their financial support to complete this thesis.

In addition I am particular grateful to SINTEF Petroleum Research AS in general and in particular to Idar Larsen and Erling Fjaer for their insights which greatly changed my wellbore stability concepts and understanding of software and results interpretation.

Thanks also to Jose Frey Martinez, Nils Erik Janbu and Manuel Seque all from STATOIL, they have been a great collaborator throughout this project. Extended thanks to the people in ANTHEI 2013/2015 group and to the IPT department staff who have been helpful over the years. I thank Adeleye Mike Mayowa, whose support and friendship helped me through quite a few difficult days.

Finally, I thank my family for their support over this time. My parents have always been there for me, and that has always been a great source of comfort.

II. Abstract

A good understanding the wellbore stability process is crucial for a safe and effective drilling of deep wells, wellbore instability is one of the key problems that engineers encounter during drilling. Wellbore instability are often caused by either failure of the rock around the hole due to high stresses, low rock strength, inappropriate drilling practice or chemical effects.

The demand for wellbore stability analyses during the drilling phase of a field arise from economic considerations and the increasing use of deviated, extended reach and horizontal wells, all of which are highly susceptible to the problem.

This paper presents a review of the causes, indicators and diagnosing of wellbore instability types and respective problems and summarizes main results of a stability study for a North Sea well, and particularly explore the thermo-poroelastic effect on wellbore stability, more specifically focusing on the effect of temperature on wellbore stability.

Further point is that apart from failure of the rock around the hole due to high stresses, low rock strength, inappropriate drilling practice or chemical effects. The wellbore instability are quite often a result of a combination of above factors plus thermal effects, as shown by the evidences that thermal regimes considerably affects the stress, as it was found that while drilling, changes in formation temperature resulting in thermally induced stress and pore pressure changes that may lead to fracturing and or borehole collapse.

The results show that thermal stress occurs because the temperature near and around the wellbore is changed by the mud in the well, and then the stress distribution is changed and eventually impact the wellbore stability. So, based on the thermoelasticity theory numerical computation for thermal stress is conducted and the results simulated for the temperature field around the borehole, then the thermal stress distribution is obtained as a function of time. Further, the thermal stress is stacked with the pure mechanical stress near wellbore. Finally, the effect of the thermal stress effect on the wellbore stability is analysed by use of the Mohr-Coulomb criterion for the any drilling condition and any time. The simulated results shows that the thermally induced stress around the borehole may make the total effective stress to increase. In addition, the thermal effect on the stresses around the borehole is important. Since the cooling effect can not only reduce the compressive radial and hoop stresses, but also the vertical stresses. This stress reduction can have an impact on wellbore stability during drilling stage as well as promoting hydraulic fracture initiation in the rock formation during the stimulation stage.

Cooling may induce small fractures and cause the mud leak to these. Closure of these fractures on reheating is responsible for the transient pressure build up and back flow, which is not true kick indicator.

The analysis was carried out using PSI (SINTEF Borehole stability Software) at five different depths for each hole section, giving recommended mud weight values as output as well as failure and collapse probabilities. With those recommended mud weights, the magnitude of circumferential stress and the radial stress distribution have been shown for those corresponding depths. These have been evaluated as well with more convenient empirical formulas and the results compared to the calculated output.

The results also shows that no significant thermal induced wellbore stability related issues were encountered during drilling of this well, and the best drilling plan to minimize the risk of wellbore instabilities, stuck pipe and accelerate the drilling process by flagging the intervals in which geologic risks such as pore pressure, fracture pressure and other instabilities can threaten the borehole integrity.

Contents

List of Illustrations

List of tables

1. Introduction

The drilling for hydrocarbon exploration and production is a challenging task, it can cause unexpected or unknown behaviour of rock which is often the cause of drilling problems, and this problems drive up the drilling costs.

Drilling operations cause stress concentration around the borehole which may lead to borehole collapse near wellbore area, because some of stressed rock materials are now replaced by mud that cannot support in situ formation stresses. The stress imbalance pops up as rock is removed from the hole, replaced with drilling fluid, and the drilled formations are exposed to drilling fluids causing instabilities around the borehole.

These instability problems can lead to stuck pipe, reaming operation, side tracking etc. which are costly expensive and time consuming. In fact, the factors of instability are very complicated and some of them have been playing much more important role than others, but some of them a little role such as, thermal effects.

However, there may be several effects of temperature on the wellbore stability, and it may play an important role. First, thermal stress induced by heating or cooling of the rock alters the effective stress distribution in the rock near hole, and these stresses can be compressive or tensile depending on whether the temperature of the drilling fluid is higher or lower than the in situ temperature. Second, thermal effect is associated with the low permeability of shale, although there is thermal stresses in high-permeability rocks. Heating / cooling results in a change in total stress, and, for low-permeability rocks, a change in pore pressure; the latter results in a change in effective stress. Since the thermal expansions of the rock and the pore fluid are different. In the process of drilling, under the effects of the drilling fluid pressure in the borehole, the pore pressure and temperature can change due to the circulation of the drilling mud and the heat exchange with the host rock , these changes in pressure and temperature will affect significantly the thermo-elastic properties distributions around the wellbore which causes effective stress concentration near the borehole, and the stability of the borehole can be affected, and easily causing borehole collapse and sticking issues.

The thermal effects is the repeated cycle (consisting of alternate cooling and reheating) effects during the drilling process. So, the wellbore may be subjected to the fatigue, failure especially in shale. Thus, the effect of temperature is time dependent effect in sense that the longer the formation is in contact with the drilling fluid the further away from the hole the temperature perturbation will diffuse.

Increasing need for energy has increased the demand for oil resources, and revealed a need for better understanding of complex geological environment and non-conventional reservoirs and generally, complex geological environment and non-conventional reservoirs means higher temperature and pressure reservoirs, as well as greater difficulties. A number of reservoirs with temperature over 150 ºC have been drilled in many regions across the world, particularly in North Sea.

Presently it is quite common to drill high temperature wells, and it becomes difficult to maintain the stability as the depth of the wellbore increases due to the high in-situ stresses encountered at depth, as changing the formation temperature can additional thermally induce pore pressure which can significantly causes high stress concentration around the borehole affecting the stability.

However, drilling operations cause changes in wellbore temperatures that can significantly causes stress redistribution around the borehole, and the stability can be affected. Since wellbore temperatures are influenced by numerous factors, including ambient temperature, geothermal static temperature, wellbore configuration, drilling fluid properties, cement properties, circulating parameters, and the mud-circulating system.

A Wellbore stability study must consider many factors, and it requires a quite comprehensive analysis in order to resolve the issues, and in many cases the optimal strategy to prevent or mitigate the risk of these troubles or even borehole collapse is to apply integrated predictive methods that can, help to optimize the mud density, chemistry, rheology, the selection of filter cake building additives, and possibly temperature. Wellbore stability predictive models may also be used to design appropriate completions.

The purpose of the present study was to focuses on thermal induced stress and their effect on wellbore stability by incorporating the developed wellbore temperature model, and calculating the redistributed stress state accompany it with an adopted failure criterion, and determine the required mud density to optimize the well trajectory for future drilling operations and field development.

Successful drilling depend on developing a good plan, continually updating it in light of new information and keeping the involved personnel informed on timely basis. The plan must include procedures to follow under normal circumstances and the methods for dealing with the most likely and most severe problem that may be encountered. With a proper well defined drilling process, sufficient data and tools for interpretation, successfully drilling should be a routine process.

Here the words analysis and model / modelling is used interchangeably to define the process of getting information about how the wellbore will behave without actually testing it in real life, to develop data as a basis for making economical or technical decisions. However what is generally meant by modelling is much broader than what is generally meant by analysis.

For practical reasons and to reduce the length of the manuscript and enhance readers understanding of the analysis results relevant / essentials figures and tables are placed in the report while supportive ones are placed in the appendix section.

2. Wellbore stability Analysis

2.1. General Background

Drilling wells under increasingly complex geologic conditions has revealed a need for better understanding of borehole stability issues. It is conservatively estimated that wellbore instability results in substantial economic losses to the industry of about US$ 8 billion per year (Offshore Magazine – Dodson Jan 2004. Why bother with PPwD?)

Wellbore instability is the main concern of drilling operations, resulting in higher than necessary drilling costs, extra rig time and sometimes in a loss of parts of or even the whole well. Wellbore instabilities make the data acquisition very difficult as well as the interpretation (Maury and Sauzay, 1987). A bad hole condition alters artificially the annulus zone thereby altering the depth of investigation of most of the logging tools. The shape of the borehole can be strongly modified giving an elongated hole in one direction, diameter reduction in the other direction and also almost circular caving in places.

Lots of innovative technologies have been applied in the oil industry, such as re-entry horizontal wells, extended reach drilling and multilaterals from a single well. These have definitely increased the demand for wellbore stability studies. Recently, technological advances have been pushing the boreholes to reach beyond 9000 m below the sea level in deep-water. World record well C-26 (9327 m) in the Oseberg field in the Norwegian sector of the North Sea.

Highly inclined, extended-reach wells may have to remain open over long periods of time, not only during the drilling phase but also over the life time of a reservoir. New challenges arose since the increasing use of horizontal wells, drilling in naturally fractured media, in very deep formations, high pressure and high temperature conditions and in difficult geological

conditions, where wellbore stability is a major issue. For example, a 9327 m deep well was drilled in Oseberg field in the Norwegian sector of the North Sea, and some types of wellbore instabilities (stuck pipes, cavings, pack-off, breakouts) were observed (Okland and Cook, 1998). Some wellbore instabilities associated with complex geologic conditions, where the stress regime was controlled by active faults, are reported in the Cusiana field (Colombia), the Pedernales field (Venezuela), (Willson et al., 1999).

When a borehole is drilled in a naturally fractured formation, excessively high mud density allows the drilling fluid to penetrate into fractures network and flowrate through the fracture will be large when the normal effective stress on the fracture joints gets smaller and the joints openings become much larger. The friction applied on the blocks around the well diminishes, and these blocks become looser and more prone to be eroded by the mud, and intensifying ovalization (Santarelli et al., 1992).

When this occurs, the fractured blocks are no longer subject to the mud overbalance pressure, and the destabilized blocks can cave into the wellbore as a result of swabbing the formation when tripping (Willson et al., 1999). When a borehole crosses a fault, drilling mud may invade the discontinuity plane. Apart from mud losses, penetration of the fluid reduces the normal stress and induces a displacement along the crack planes which shears the well, as shown in **Fig.1.**

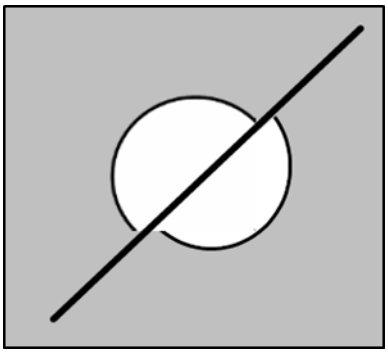

Figure 1 Schematic representation of borehole shearing when crossing a discontinuity.

The consequences can quickly become dramatic and could lead to partial or even total loss of the well. Two case histories in Aquitaine, France were described that resulted in the loss of the wells and the need for the drilling of two new wells, costing in the range of US$30 million (Maury and Zurdo, 1996).

Wellbore instability can result in lost circulation where tensile stresses have occurred due to high drilling mud pressure **(Fig.2)**; breakouts and hole closure in case of compressive and shear failures. During drilling phase an open hole is supported by drilling mud pressure to keep wellbore from collapse. If the mud weight is lower than the shear failure stress or collapse stress, the shear failure and compressive failure occur in the wellbore in the minimum far-field stress direction, causing hole collapse or breakout. If the mud weight exceeds the rock tensile strength, the tensile fracture is induced in the maximum far-field stress direction.

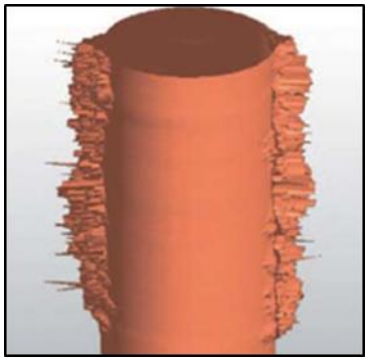

Figure 2 Figure 2 Schematic plot of stress-induced wellbore instability. Due to high mud weight. Results from an Ultrasonic Borehole Imager logging tool demonstrating wellbore breakout aligned along the plane of least horizontal stress. © Schlumberger

Consequently, this may cause drilling fluid losses into the formation or lost circulation**. Fig.3** (Martino and Chandler, 2004), shows a typical wellbore instability due to breakout and drilling induced tensile fracture.

Figure 3 Breakout in a circular tunnel with a radius of R = 1.75 m in the Underground Research Laboratory, Canada. The maximum breakout occurred in the minimum stress direction and the maximum hole radius is 1.3R. The in-situ stresses are σ_3 = 14 MPa and σ_1 = 55MPa (Martino and Chandler, 2004).

In the Cusiana field in Colombia, even though some measures to prevent borehole instability were taken, extensive breakouts in fissile and naturally fractured shales – of up to 22" in $12^1/_4$" hole – occurred (Willson et al., 1999). The instability in the Cusiana field were mainly because of abnormally high tectonic stresses induced by an active thrust-faulting environment.

There are several phases in the life of a well, i.e., drilling, completion, production, etc. and borehole instabilities can be encountered in all these phases. In the drilling phase, the main concerns are to determine the mud composition and density (mud weight) which will maintain the integrity of the well, without the loss of drilling fluids. During the completion and stimulation stage, the reservoir must be connected to the well via perforations. This operation could fail if the rock adjacent to the cemented casing is non-brittle, and this is due to the fact that these material at a very low strain rate have a small region of elastic behaviour and a large region of ductile behaviour before they fracture, and the reason is at low strain rates more time is available for individual atoms to move and therefore ductile behaviour is favoured, blocking the perforations and restrain the flow. Prior to full production, downhole tests include open-hole logging, fluid sampling, etc. It is possible to induce wellbore failure and casing collapse during these processes, i.e., the well PTS 5 gas well located southwest of France, the cement of the 10 ¾ in casing was in poor condition then casing collapsed caused by reduction in internal well pressure (Maury and Zurdo, 1996). As

hydrocarbons are depleted, the drained region compacts which could induce solids production, Casing damage, surface subsidence and wellbore failure. All these phases in the life of a well, integrated borehole stability analyses are important to ensure the reservoir economical production and minimize the costly problems induced by the wellbore instabilities.

2.2. Fundamentals

Underground formations are always in a stressed state, mostly due to overburden and tectonic stresses. Stress is the pressure or tension exerted on a material object, and in terms of earth science it means the force that cause earth's crust to change its shape or volume. So as earth's plates move and push against each other (or collide) they are exerting forces. On the other hand, sedimentary basins may be exposed to sedimentary subsidence, sea-level changes and tectonic forces creating repeated cycles of elevation and depression, all these geological activities and events will affect the in situ stresses.

In order to predict wellbore stability, stress components and distributions near the wellbore due to drilling perturbation need to be analysed. Applying rock failure criteria wellbore stress and rock strength can, then, be compared to determine rock failures, such as shear failure, tensile failure etc. Finally, a mud weight range can be determined to avoid wellbore shear, compressive, and tensile failures. This mud weight range is the safe mud weight window for drilling.

2.2.1. Stress determination

Stress is a concept that is fundamental to wellbore stability analysis. Knowledge of the rock stress and its directions is critical for planning best orientations of wells. Stress determination relies on indirect measurements. The vertical stress may be estimated by assuming an average overburden density gradient to be inserted in **Eq. (2.1)** in some cases, borehole density log data exist from surface to depth, permitting a more direct computation.

$$\sigma_v = \int \rho g * dz \qquad (2.1)$$

2.2.2. Stresses around boreholes

When a well is drilled into a formation, stressed solid material is removed. The borehole wall is then supported only by the fluid pressure in the hole. As this fluid pressure generally does not match the in situ formation stresses, there will be a stress redistribution around the well. Knowledge of the stresses around a well is therefore essential for discussions of well problems.

The most common procedure for calculating the stress concentration around the wellbore is utilizing the Kirsch equations. To find the stress state at the arbitrarily oriented wellbore, it is necessary to transform in-situ stresses to a new Cartesian coordinate system. Only after this transformation, we can derive the stress state near the vicinity of the wellbore using the Kirsch concept. The transformation of the equations from the Cartesian coordinate system to the cylindrical system results in **Eq. 2.2,** bellow which is the Kirsch (1898) equation for the stress component around the borehole wall.

The equations presented bellow (the whole section 2) if not referred can be found in a literature such as Fjaer et al (2008) mostly and Jaeger and Cook (1976). I will be focusing on the main equations without going into detailed derivation.

$$\sigma_r = \frac{\sigma_x+\sigma_y}{2}(1-\frac{R_w^2}{r^2}) + \frac{\sigma_x-\sigma_y}{2}(1+3\,\frac{R_w^4}{r^4}-4\,\frac{R_w^2}{r^2})cos2\theta + \tau_{xy}(1+3\,\frac{R_w^4}{r^4}-4\,\frac{R_w^2}{r^2})sin2\theta + P_w\frac{R_w^2}{r^2}$$

$$\sigma_\theta = \frac{\sigma_x+\sigma_y}{2}(1+\frac{R_w^2}{r^2}) - \frac{\sigma_x-\sigma_y}{2}(1+3\,\frac{R_w^4}{r^4})cos2\theta - \tau_{xy}(1+3\,\frac{R_w^4}{r^4})sin2\theta - P_w\frac{R_w^2}{r^2}$$

$$\sigma_z = \sigma_z - v[2(\sigma_x-\sigma_y)\frac{R_w^2}{r^2}\cos2\theta + 4\,\tau_{xy}\frac{R_w^2}{r^2}sin2\theta] \qquad (2.2)$$

$$\tau_{r\theta} = \frac{\sigma_x - \sigma_y}{2}(1 - 3\,\frac{R_w^4}{r^4} + 2\,\frac{R_w^2}{r^2})sin2\theta + \tau_{xy}(1 - 3\,\frac{R_w^4}{r^4} + 2\,\frac{R_w^2}{r^2})\cos2\theta$$

$$\tau_{\theta z} = (-\tau_{xz}\sin\theta + \tau_{yz}\cos\theta)(1 + \frac{R_w^2}{r^2})$$

$$\tau_{rz} = (\tau_{xz}\cos\theta + \tau_{yz}\sin\theta)(1 - \frac{R_w^2}{r^2})$$

The angle $\boldsymbol{\theta}$ is the azimuth angle relative to the x-axis, and in this case measured relative to the direction of the major horizontal stress, then $\boldsymbol{\theta}$ is zero in the direction of σ_H. Since the angle $\boldsymbol{\theta}$ varies between the maximum and minimum value. Fjaer et al., (2008), the tangential stress at the borehole will do the same.

At some point away from the hole, the stresses have their initial values, since the presence of the hole cannot be sensed. At the borehole wall ($r=R_w$), the well pressure Pw is always balanced by a radial stress component:

$\sigma_{r\,=\,P_w}$ When ($r=R_w$) and $\sigma_r \;=\; \sigma_h$ when ($r\rightarrow\infty$)

Then following the condition ($r=R_w$), at the borehole the equations **(2.2)** are reduced to equations **(2.3)**

$\sigma_{r\,=\,P_w}$

$\sigma_{\theta\,=\,\sigma_x+\sigma_y\,-2(\,\sigma_x-\,\sigma_y)cos2\theta-4\tau_{xy}sin2\theta\text{-}P_w}$

$$\sigma_{z=\,\sigma_v} - \nu\big(2\,\sigma_x - \,\sigma_y\big)cos2\theta + 4\tau_{xy}\,\sin2\theta \qquad (2.3)$$

$$\tau_{r\theta} = 0$$

$$\tau_{\theta z} = 2(-\tau_{xz}\sin\theta + \tau_{yz}\cos\theta)$$

$$\tau_{rz} = 0$$

If the borehole wall is assumed impermeable (like in the presence of a perfect mud cake, or like during drilling shale), and the shale drilled with Oil based mud. Which means that the pore pressure is not influenced by the well pressure (Constant pore pressure). Then for a vertical hole in an isotropic horizontal stress field, taking into account that the angle $\boldsymbol{\theta}$ is zero, which make the third terms of $\boldsymbol{\sigma_r, \sigma_\theta, \sigma_z}$ in equation **2.2** equal to zero, and the second term will also be zero due to difference of the isotropic stress, then the principal stresses around the borehole can be reduced to equations **2.4-2.6**.

$$\sigma_r = \sigma_h(1 - \tfrac{R_w^2}{r^2}) + \tfrac{R_w^2}{r^2}P_w \qquad (2.4)$$

$$\sigma_\theta = \sigma_h(1 + \tfrac{R_w^2}{r^2}) - \tfrac{R_w^2}{r^2}P_w \qquad (2.5)$$

$$\sigma_z = \sigma_v \qquad (2.6)$$

The equations **2.4 – 2.6** are the general solution for the linear elastic model vertical well isotropic stress condition which may be simplified to equations **2.7 – 2.9** at the borehole wall since at the borehole wall the ratio $\frac{R_w^2}{r^2}$ is equal to 1.

$$\sigma_{r\,=\,P_w} \qquad (2.7)$$

$$\sigma_{\theta=}\,2\sigma_h - P_w \qquad (2.8)$$

$$\sigma_{z\,=\,\sigma_v} \qquad (2.9)$$

Where:

$$Pw = \rho_w \mathrm{g}D \qquad (2.10)$$

If the horizontal stress field is anisotropic, then the tangential and axial stress with vary with direction along the circumference of the borehole:

$$\sigma_{r = P_w} \quad (2.11)$$

$$\sigma_{\theta = \sigma_H + \sigma_h - 2(\sigma_H - \sigma_h)cos2\theta - P_w} \quad (2.12)$$

$$\sigma_{z = \sigma_v} - 2v_{fr}(\sigma_H - \sigma_h)cos2\theta \quad (2.13)$$

The **Eq. (2.12)** shows that the tangential stress at the borehole wall varies between the maximum and minimum value. Fjaer et al., (2008)

$$\sigma_{\theta,min} = 3\sigma_H - \sigma_h - P_w \quad (2.14)$$

and the minimum value

$$\sigma_{\theta,max} = 3\sigma_h - \sigma_h - P_w \quad (2.15)$$

Where the maximum value occurs in the direction of σ_h and the minimum value in the direction of σ_H. (Fjaer et al., 2008) the variation in tangential stress around the borehole is illustrated in **Fig.4**

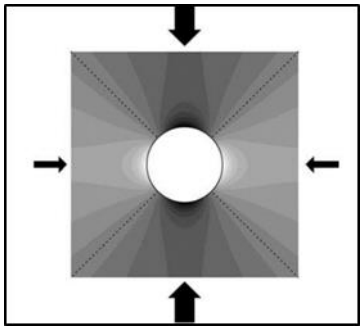

Figure 4 Change in tangential stress due to the drillout of a borehole in anisotropic far field stresses. White is increase in tangential stress, black is decrease in tangential stress. The dotted lines shows the contours of no change. Fjaer 1992

Now let's assume that the borehole wall is permeable, (the pore pressure at the borehole wall is equal to the well pressure). Then pore pressure equilibrium is installed and in addition to mechanical equilibrium, the stress solutions near the borehole also incorporate fluid flow equilibrium. In this case for effective stresses we must use Pw rather than P_f. For a vertical borehole in an isotropic stress field, the stresses at the borehole wall in this case are given as:

$$\sigma_{r = P_w} \quad (2.16)$$

$$\sigma_{\theta = 2\,\sigma h - P_w - 2\eta(P_w - P_f)} \quad (2.17)$$

$$\sigma_{z = \sigma_v} - 2\eta(P_w - P_f) \quad (2.18)$$

$$\eta = \alpha \frac{1-2\nu_{fr}}{2(1-\nu_{fr})} \quad (2.19)$$

$$P_f = P_w \quad (2.20)$$

2.2.3. Failure Criteria

One of the factors playing a key role during wellbore-stability analyses is the selection of a rocks failure criterion. An appropriate failure criterion should be applied for representing the true in-situ failure conditions. There are three main different shear failure criterion available: The first category considers only the minimum and maximum principle stresses while, the second category takes into account the effect of the intermediate principle stress. The most universal criterion representing the first category is the Mohr-Coulomb rock failure criterion.

The failure occurs when the value of the maximum shear stress (τ_{max}), developed on a specific plane, is enough to overcome the formation cohesion (S_0) and frictional force, the compressional failure occurs. Therefore, the Mohr-Coulomb compressional failure depends only on two principal stresses, the maximum (σ_1) and minimum (σ_3) principal stresses. The Mohr-Coulomb criterion can be described as in equation **2.21**.

Besides this criterion, there is Drucker-Prager criterion like Mohr-Coulomb, but accounts for intermediate principal stress (σ_2), and Modified Lade criterion, which is basically the same as the Drucker-Prager. Others failure criterion exists like Tresca criterion which can be considered as a special case of the Mohr–Coulomb criterion, with φ = 0 in equation **2.21**, which lead to $|\tau| = S_0$ (Mohr-Coulomb for frictionless material), and the Griffith criterion which is based on crack growth in two dimensional model. The results of the stability analysis will also depend on the choice of the failure criteria.

There are three main types of failure that apply to rocks in the Earth: Shear failure, tensile failure, and compactive failure. Holt (2008)

Here the Mohr–Coulomb criterion for shear failure will be used since it's a simple and handy criterion broadly used, but it is not necessarily the most representative criterion for all materials and it is well known that Mohr-Coulomb failure model is a conservative model (Khan et al 2012), meaning it shows worse than it is. Considering the amount of uncertainty in this study, it could be safer to consider results from Mohr-Coulomb model.

Shear failure is most often described by the Mohr-Coulomb failure criterion.

$$\tau = S_0 + \sigma_n tan\varphi \qquad (2.21)$$

The Mohr-Coulomb criterion can also be written in terms of principal stresses:

$$\sigma_1 = C_0 + \sigma_3 tan^2\beta \qquad (2.22)$$

$$\beta = 45^0 + \frac{\varphi}{2} \qquad (2.23)$$

$$C_0 = 2S_0 \, tan\beta \qquad (2.24)$$

In the presence of pore pressure we write the Mohr-Coulomb criterion in terms of an effective stress as follows:

$$\sigma'_\theta = C_0 + \sigma'_r \, tan^2\beta \qquad (2.25)$$

$$\sigma'_r = \sigma_r - \alpha \, P_f \qquad (2.25.1)$$

In the formula above the effective stress coefficient (α) for failure is equal to 1.

There are several conditions for which the borehole may fail, depending on the magnitudes of the principal stresses: The drilling fluid density (Pw) is too low, such that $\sigma_r = P_w$ becomes the smallest principal stress. We see from **Eq. (2.7** and **2.9)** that depending on the relative magnitude of σ_h and σ_v , either σ_θ or σ_z will become the largest principal stress at the borehole wall and that is where failure will be initiated, or when the stress on wellbore wall exceeds the formation shear strength, in the case where $\sigma_\theta > \sigma_z > \sigma_r$ the borehole will collapse, so the collapsing pressure can be calculated and is given by the Mohr-Coulomb criterion. **Eq. (2.25).**

In theory there are six different possibilities for shear failure summarized in **Table 1**, depending on which of the principal stress components at the borehole wall are largest and smallest (Fjaer et al., 2008).

Table 1 Conditions for shear failure in vertical boreholes with isotropic far-field horizontal stress and impermeable borehole wall. Fjaer et al,.2008

Case	$\sigma_1 \geqslant \sigma_2 \geqslant \sigma_3$	Borehole failure occurs if
a	$\sigma_\theta \geqslant \sigma_z \geqslant \sigma_r$	$p_w \leqslant p_f + \frac{2(\sigma_h - p_f) - C_0}{1 + \tan^2\beta}$
b	$\sigma_z \geqslant \sigma_\theta \geqslant \sigma_r$	$p_w \leqslant p_f + \frac{\sigma_v - p_f - C_0}{\tan^2\beta}$
c	$\sigma_z \geqslant \sigma_r \geqslant \sigma_\theta$	$p_w \geqslant p_f + 2(\sigma_h - p_f) - \frac{\sigma_v - p_f - C_0}{\tan^2\beta}$
d	$\sigma_r \geqslant \sigma_z \geqslant \sigma_\theta$	$p_w \geqslant p_f + \frac{2(\sigma_h - p_f)\tan^2\beta + C_0}{1 + \tan^2\beta}$
e	$\sigma_r \geqslant \sigma_\theta \geqslant \sigma_z$	$p_w \geqslant p_f + (\sigma_v - p_f)\tan^2\beta + C_0$
f	$\sigma_\theta \geqslant \sigma_r \geqslant \sigma_z$	$p_w \leqslant p_f + 2(\sigma_h - p_f) - (\sigma_v - p_f)\tan^2\beta - C_0$

By referring to the well pressure required to fulfil the Mohr-Coulomb criterion in the case of an impermeable borehole wall with $\sigma_\theta > \sigma_z > \sigma_r$ can be written:

$$P_{w,\min} = P_f + \frac{2(\sigma_{h-P_f}) - C_0}{1 + tan^2\beta} \quad (2.26)$$

Or for $\sigma_z > \sigma_\theta > \sigma_r$

$$P_{w,min} = P_f + \frac{\sigma_v - P_f - C_0}{tan^2\beta} \quad (2.27)$$

Then, if the well pressure falls below the value given by **Eq. (2.26** and **2.7)**, shear failure will occur at the borehole wall.

If the borehole wall is permeable and a steady state pore pressure profile has been reached, then the solutions for the limiting well pressures are worked out by combining the borehole principal stresses **(Eq. (2.17, 2.18))** with the Mohr-Coulomb criterion. Here the minimum effective stress at the borehole wall now is 0, because the pore pressure equals the well pressure. For the two cases above $\sigma_\theta > \sigma_z > \sigma_r$ and $\sigma_z > \sigma_\theta > \sigma_r$ one finds:

$$P_{w,min} = \frac{2\sigma_h - 2\eta P_f - C_0}{2 - 2\eta} \quad (2.28)$$

And

$$P_{w,min} = \frac{\sigma_v - 2\eta P_f - C_0}{1 - 2\eta} \quad (2.29)$$

Usually the horizontal stresses are anisotropic; i.e. $\sigma_H > \sigma_h$. Then for anisotropy field case, means that we have to use the borehole stresses in **Eq. (2.12** and **2.13)** for the case of an impermeable borehole wall. Since the tangential and axial stresses change with position along the circumference of the hole, we have to search the maximum values for these stresses for the two cases above $\sigma_\theta > \sigma_z > \sigma_r$ and $\sigma_z > \sigma_\theta > \sigma_r$. The results is that we can use the same equations as **(2.26)** and **(2.27)** above, but replacing $2\sigma_h$ with $3\sigma_H - \sigma_h$

Tensile failure occurs if the minimum principal stress (σ_3) becomes sufficiently negative.

$$\sigma_3 \leq -T^* \quad (2.30)$$

In the presence of pore pressure, the condition for tensile failure is:

$$\sigma_3' = \sigma_3 - P_f = -T^* \quad (2.31)$$

Tensile failure may take place in two different ways:

By hydraulic fracturing, resulting from a high well pressure that creates a sufficiently negative effective tangential stress;

$$\sigma'_\theta = -T^* \quad (2.32)$$

For the case of an impermeable borehole wall and an anisotropic horizontal stress field, the fracturing pressure is found by use of **Eq. (2.12** and **2.13)**. The minimum values of the tangential stress now control the orientation of the fracture, which means that the fracture will initiate at θ = 0 and 180°; i.e. parallel to the maximum in situ horizontal stress. The fracturing pressure is then:

$$P_{w,max}^{Frac} = 3\sigma_h - \sigma_H - P_f + T^* \quad (2.33)$$

Tensile failure may also occur by the well pressure becoming lower than the pore pressure, so that the radial effective stress becomes sufficiently negative;

$$\sigma'_r = -T^* \quad (2.34)$$

2.3. Wellbore instabilities

Wellbore instability is usually caused by a combination of factors which may be broadly classified as being either controllable or uncontrollable (natural) in origin, some of the factors can be summarized below. More detailed review on this topic can be found on McLellan et al., (1994a).

Uncontrollable factors

Naturally fractured or faulted formations

Natural fracture system in the rock can often be found near faults. Rock near faults can be broken into large or small pieces. If they are loose they can fall into the wellbore and jam the string in the hole. **Fig.5** shows possible problems as result drilling a naturally fractured or faulted system. This mechanism can occur in tectonically active zones.

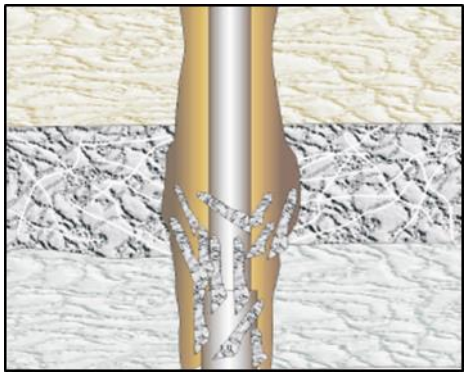

Figure 5 drilling through naturally fractured or faulted. (Pasic et al,. 2007)

Hole collapse problems may become quite severe if weak bedding planes intersect a wellbore at unfavourable angles. Such fractures in shales may provide a pathway for mud or fluid invasion that can lead to time-depended strength degradation, softening and ultimately to hole collapse (Willson et al., 1999).

The instability in fractured formation probably result from opening of joints communicating with the borehole and subsequent invasion of the fracture network by the drilling fluid circulating in the well and consequent loosening of the correspondent fractured blocks make it possible for them to be eroded from the wall (Santarelli et al,. 1992).

Mobile formations

Mobile formation squeezes into the wellbore because it is being compressed by the overburden forces. Mobile formations behave in a plastic manner, deforming under pressure. The deformation results in a decrease in the wellbore size, causing problems of running Bottom hole assembly (BHA), logging tools and casing **(Fig.6).** A deformation occurs because the mud weight is not sufficient to prevent the formation squeezing into the wellbore. This mechanism normally occurs while drilling salt and certain types of shale. An appropriate drilling fluid and maintaining sufficient drilling fluid weight are required to help stabilize these formations.

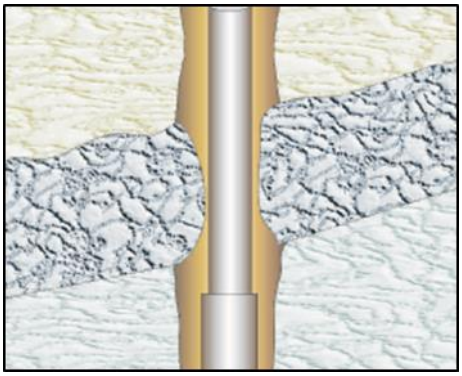

Figure 6 Drilling through mobile formations. (Pasic et al,. 2007)

Unconsolidated formations

Unconsolidated formation falls into the wellbore because it is loosely packed with little or no bonding between particles. The collapse of formations is caused by removing the supporting rock as the well is drilled. It happens in a wellbore when little or no filter cake is present. The un-bonded formation (generally sand), cannot be supported by hydrostatic pressure as the fluid simply flows into the formations, sand or gravel then falls into the hole. An adequate filter cake is required to help stabilize these formations.

Induced Over-Pressured Shale Collapse

Induced over-pressured shale collapse occurs when the shale assumes the hydrostatic pressure of the wellbore fluids after a number of day's exposure to that pressure. When this is followed by no increase or a reduction in hydrostatic pressure in the wellbore, the shale, which now has a higher internal pressure than the wellbore, collapses in a similar manner to naturally over-pressured shale. This mechanism normally occurs in water based drilling fluids, after a reduction in drilling fluid weight or after a long exposure time during which the drilling fluid was unchanged.

Controllable factors

Mud density

The mud density or the equivalent circulating density (ECD), is usually the main tool at the driller's disposal to guarantee the initial stability of an open wellbore **(Fig.7 and Fig.8 Left)**. The supporting pressure offered by the static or dynamic fluid pressure during drilling, will determine the stress concentration present in the wellbore surrounding. Because rock failure is dependent on the effective stress, the consequence for stability is highly dependent on whether and how rapidly fluid pressure penetrate the wellbore wall. That is not to say however, that high mud densities are always optimal for avoiding instability in a given well over time (Oort, 2003). In the absence of an efficient filter cake, such as in fractured formations, a rise in a bottom hole pressure may be detrimental to stability and can

compromise other criteria, e.g., formation damage, differential sticking risk, mud properties, or hydraulics (McLellan, 1994a).

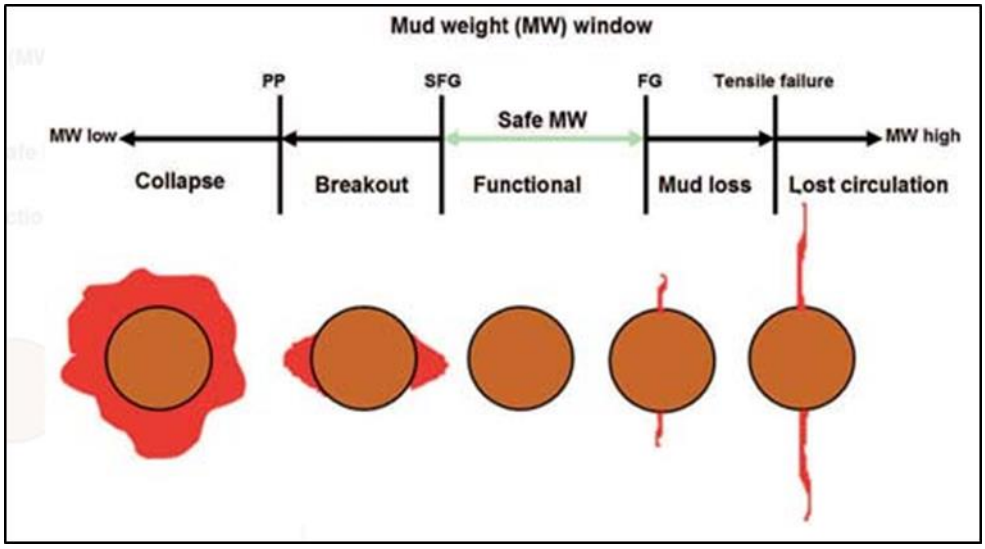

Figure 7 Effect of mud weight on the stress in wellbore wall. Safe mud pressure is vital for the stability of a well. Too low a mud pressure can lead to wellbore collapse; too high a mud pressure can create wellbore fracturing and losses. © Knowledge Systems

Well Inclination and Azimuth

Inclination and azimuth of a well with respect to the principal in-situ stresses can be an important factor affecting the risk of collapse and/or fracture breakdown occurring **(Fig.8 Right)**. This is particularly true for estimating the fracture breakdown pressure in tectonically stressed regions where there is strong stress anisotropy (McLellan, 1994a).

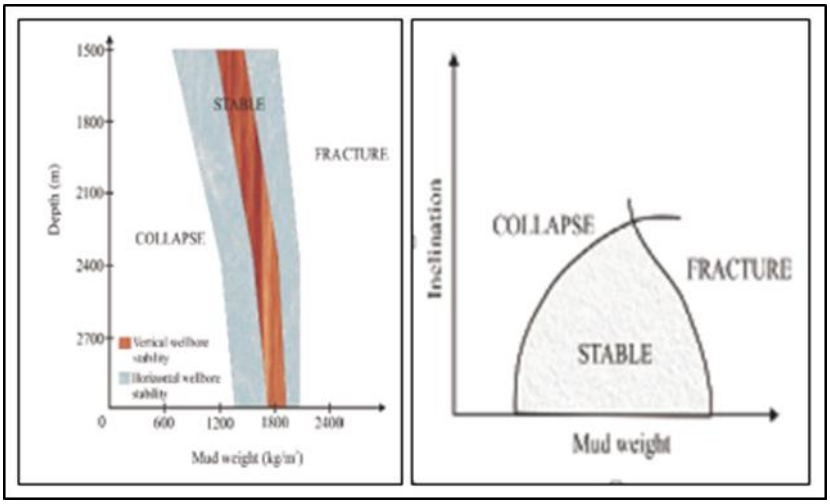

Figure 8 Effect of the well depth (Left) and the hole inclination (Right) on Wellbore stability. (Left)Pasic et al,. 2007) and (Right) Bradley 1979)

Drilling fluid temperature

If there is temperature difference between fluid and formation, the temperature will propagate by diffusion into the rock. Rocks, like most other materials expand or shrink when temperature is changing. In a borehole geometry, thermal expansion is restricted (except for radial direction) (Fjaer et al., 2002). Drilling fluid temperatures, and to some extent, bottom hole producing temperatures changes can give rise to thermal concentration or expansion stresses which may be detrimental to wellbore stability.

The thermal induced stress at an impermeable borehole wall caused by changing in temperature are given by **Eq. (2.35).**

$$\sigma_T = \frac{E_{fr}}{1-v_{fr}} \alpha_T (Tw - T_{\mathrm{f}}) \quad (2.35)$$

Then the thermoelastic stresses at the borehole wall will be given by:

$$\sigma_r = P_w \quad (2.36)$$

$$\sigma_\theta = 2\sigma_h - P_w + \sigma_T \quad (2.37)$$

$$\sigma_z = \sigma_v + \sigma_T \quad (2.38)$$

The reduced mud temperature causes a reduction in the near-wellbore stress concentration, thus preventing the stresses in the rock from reaching their limiting strength (McLellan, 1994a; Maury and Guenot, 1995). This acts as a strengthening of the borehole with respect to collapse.

The drilling fluid is usually (at t = 0) colder than the formation to be drilled, when circulation starts. The fluid and formation temperatures will gradually adjust, depending on the circulation rate. After the circulation stops, the formation near the well will gradually heat up. Maury and Sauzay (1987) found that this could explain delayed failure. Shortly after drilling the borehole is stable. However, as the temperature increases, the tangential and axial stresses at the borehole wall will both increase by the same amount as:

$$\Delta\sigma_\theta = \Delta\sigma_z = \frac{E}{1-\nu} \alpha_T (T_w - T_f) \quad (2.39)$$

It is apparent from **Eq. (2.39)** that cooling the fluid will tend to reduce axial stress and the hoop stress and thus enable the hole to withstand lower well pressure.

Cooling of a low permeability rock like shale will also influence the pore pressure, due to a larger thermal expansion coefficient* for the fluid than for the solid parts of the rock. Maury and Guenot, (1995). Thus, cooling reduces the pore pressure, which in general improves stability.

Perkins and Gonzalez (1984) gave analytical expressions for the stress change resulting from a cylindrical cooled zone of arbitrary height. In the limit of small diameter to height ratio (d/h → 0), they found

$$\Delta\sigma_r(\Delta \mathrm{T}) = \Delta\sigma_\theta(\Delta T) = \frac{E}{2(1-\nu)} \alpha_T (T_{cool} - T_0) \quad (2.40)$$

For the opposite limiting case (d/h → ∞) which is applicable to the situation after some time when the cooled region has grown considerably into the reservoir, the result is:

$$\Delta\sigma_r(\Delta \mathrm{T}) = \Delta\sigma_\theta(\Delta T) = \frac{E}{(1-\nu)} \alpha_T (T_{cool} - T_0) \quad (2.41)$$

The above equations (**2.40-2.41**) assume that **ΔT** is constant along the borehole axis (**Z**), so for the d/h → 0 case $\Delta\sigma_z(\Delta \mathrm{T}) = \sigma_T$ (in equation 2.35). The expressions (2.40-2.41) constitute good approximations for more general situations (**equation 2.35**) if the spatial variations of **ΔT** along the borehole axis is weak compared to the spatial variations along the radial direction, then in the d/h → 0 case $\Delta\sigma_z(\Delta \mathrm{T}) \cong 0$ when r → ∞. As pointed out by Perkins and Gonzalez (1984) stresses are relatively constant throughout the inner region while outer stresses are not very sensitive to vertical position but they decrease as radial distance increases.

Physical/chemical fluid-rock interaction

There are many physical/chemical fluid-rock interaction phenomena which modify the near-wellbore rock strength or stress. The significance of these effects depend on a complex

interaction of many factors including the nature of the formation (mineralogy, stiffness, strength, pore water composition, stress history, temperature), the presence of a filter cake or permeability barrier is present, the properties and chemical composition of the wellbore fluid, and the extent of any damage near the wellbore (McLellan, 1994a; Mody and Hale, 1993).

Since the pore fluid in the shale has chemical activity given by the type and amount of dissolved ions. If the surface of the rock is exposed to a fluid with different chemical activity, water molecules will move into or out of the shale to compensate this disturbance, thus creating disturbance in pore pressure at the surface given as by Mody and Hale, 1993 in **Eq. (2.42).**

$$\Delta p = C_n T_f \ln \frac{\alpha_{df}}{\alpha_{sh}} \tag{2.42}$$

This disturbance (commonly called osmotic pressure*) will propagate into the rock with the same consequences. If $\alpha_{df} < \alpha_{sh}$ we will have that $\Delta p < 0$ which is good for borehole stability since that increase the effective support of the drilling fluid on the borehole wall. However, if the rock surface does not act as perfect membrane (a membrane that allow only water molecules to pass) ions will also move through the surface and gradually change the activity of the shale towards that of the drilling fluid. And then after while the pore pressure shift is reduced to $\sigma \Delta p$ where $\boldsymbol{\sigma}$ is a number (called membrane efficiency) between zero and one. (Fjaer et al., 2008).

In 1993 Mody and Hale implemented osmotic potential* theory into a rock mechanics model for borehole stability. They added the osmotic potential through a stress term equivalent to the poroelastic contribution seen in **Eq. (2.17, 2.18):**

The osmotic potential ΔΠ (from e.g. Marine and Fritz, 1981) is:

$$\Delta \Pi = \frac{RT}{V_w} ln \frac{\alpha_{w,df}}{\alpha_{w,sh}} \tag{2.43}$$

$$\sigma_r = Pw \tag{2.44}$$

$$\sigma_\theta = 2\sigma_h - Pw + \alpha \frac{1-2\nu_{fr}}{1-\nu_{fr}} \Delta \Pi \tag{2.45}$$

$$\sigma_z = \sigma_v + \alpha \frac{1-2\nu_{fr}}{1-\nu_{fr}} \Delta \Pi \tag{2.46}$$

The activity denotes the effective concentration of water in a solution, so that α_w = 1 for fresh water, while α_w < 1 for salt water. Adding salt to the drilling fluid so that $\alpha_{w,df} < \alpha_{w,sh}$ sets up an osmotic potential $\Delta \Pi$ < 0, which will tend to drive water out of the shale and hence acts as an effective pore pressure reduction. This has an instantaneous stabilizing effect on the borehole.

The chemical interaction between shale and drilling fluid primarily leads to a significant reduction of the maximum allowed drilling fluid density because of potential for tensile failure. This is related to potassium or calcium from the drilling fluid exchanging with larger hydrated sodium ions in the shale (smectite) resulting in a change in the size of the mineral structure. Thus the rock may shrink or expand depending on which ion moves in either potassium or calcium, leading to changes tangential (hoop), axial and radial stress near the borehole (Nes et al., 2012).

The consequences for a borehole will be similar to the effect of the difference in temperature giving shift in the axial and hoop stress at the borehole wall, this means that it may be modelled similarly; **Eq. (2.47, 2.49)** Fjaer et al., 2002

$$\sigma_r = Pw \tag{2.47}$$

$$\sigma_\theta = 2\sigma_h - Pw\ - \frac{E}{1-\nu}\ \Delta\varepsilon_{ch} \tag{2.48}$$

$$\sigma_z = \sigma_v - \frac{E}{1-\nu}\ \Delta\varepsilon_{ch} \tag{2.49}$$

2.3.1. Indicators of borehole instability

A list of the indicators of wellbore instability which are primarily caused by wellbore collapse during the drilling, completion or production of a well is shown in **Table 2**. They are classified in two groups: direct and indirect causes. Direct symptoms of instability include observations of over gauge or under gauge hole, as readily observed from calliper logs. Caving from the wellbore wall, circulated to surface, and hole fill after tripping confirm that spalling processes are occurring in the wellbore. Large volumes of cuttings and/or cavings, in excess of the volume of rock which would have been excavated in a gauge hole. Provided the fracture gradient was not exceeded and vuggy or naturally fractured formations were not encountered, a requirement for a cement volume in excess of the calculated drilled hole volume is also a direct indication that enlargement has occurred (McLellan et al., 1994a).

Table 2 Indicators of wellbore instability. Resumed from Pasic et al,.2007

Indicators of wellbore instability	
Direct indicators	Indirect indicators
Hole Overgauge	High torque and drag (friction)
Hole Undergauge	Stuck pipe
Excessive volume of cuttings	Poor logging response
Excessive volume of cavings	Excessive drillstring vibrations
Cavings at surface	Increased circulating pressures
Hole fill after tripping	Excessive doglegs
Excess cement volume required	Hanging up of drillstring, casing

2.3.2. Borehole-instability prevention

Total prevention of borehole instability is unrealistic, because restoring the physical and chemical in-situ conditions of the rock is impossible. However, the drilling engineer can mitigate the problems of borehole instabilities by adhering to good field practices. These practices include:

- Proper mud-weight selection and maintenance.
- Use of proper hydraulics to control the equivalent circulating density (ECD).
- Proper hole-trajectory selection.
- Use of borehole fluid compatible with the formation being drilled.

Additional field practices that should be followed are:

- Minimizing time spent in open hole.
- Using offset-well data (use of the learning curve).
- Monitoring trend changes (circulating pressure, torque and drag, fill-in during tripping).

- Collaborating and sharing information between all the intervenient.

2.3.3. Borehole instability while drilling

Borehole instabilities that occur during the drilling phase are usually manifested as tight hole / stuck pipe incidents and lost circulation. The first typically represent significant (5-10%) part of drilling costs, mainly because it takes time to get loose / ream the hole while the second are potentially dangerous, thus representing a safety risk that has to be avoided. **Fig.2** and **6** illustrates in a schematic manner different instability problems that might occur.

Tight hole/stuck pipe

Tight hole / Stuck pipe situations occur primarily in shale, often in high pore pressure zones, and in smectite (swelling clay mineral) rich formations.

There are three main reasons why the drill string gets stuck during drilling operations:

- Hole collapse in shale, usually caused by shear failure of the rock around the hole. This may lead to brittle failure with the formation of a breakout. The fragments that are created by the failing borehole fall into the hole and block the motion of the string, while the hole actually is enlarged. Hole collapse may also be more plastic, with the hole shrinking and the drill string getting stuck as a result of that. Finally, hole collapse in shale may also be due to tensile failure when the well is in underbalance (well pressure < pore pressure).

- The mud may not be able to clean the hole by removing drill cuttings and produced caving in a sufficiently effective way.

- The tool may also get stuck in reservoir sections by so-called differential sticking, which is caused by a too large pressure overbalance between the well and the reservoir.

Lost circulation

Lost circulation means that a significant amount of drilling fluid is lost into the formation. The reason for mud losses is either that mud is lost into existing, natural fractures, or that new fractures are induced as a tensile failure (hydraulic fracturing; e.g. (**Eq. 2.33**) by too high pressure in the borehole. The mud loss may also lead to a temporary pressure drop in the well, since a part of the mud column is disappearing into the formation. As a consequence, pore fluid may flow into the well from permeable layers higher up, and In the presence of gas, this may lead to a rapid increase in well pressure and a high risk of a blowout. This is a potentially dangerous situation that may result in loss of lives and equipment.

The main solution is to keep the mud weight sufficiently low that fluid loss does not occur; i.e. below the limit for fracture initiation for in non-fractured formations, and below the fracture reopening pressure in naturally fractured formations.

2.4. Wellbore Stability Tools Background

Oil and gas is a fascinating industry for a myriad of reasons: It has changing technology, dynamics in the variety of operational way and a hint of unpredictability where a twist of fate can turn the game around. This industry has a history spanning many tens of years and specialized procedures, tools / technology for borehole instability issues which have also existed for a quite some time now.

Despite the fact that drilling operations have not changed much, technological and scientific progress has made possible planning and preventing instability issues that could not have been implemented years back and made a large contribution to oil industry.

WBS tools are widely-used, and oftentimes, even minor drilling operations is done with the mandatory application of these tools. They have become significantly less dangerous, and the control over their usage is applied effectively. This can be attributed to the invention of the WBS software, development of new drilling fluid system, use of annular pressure while drilling and monitor of downhole vibrations, which facilitated their application while drilling.

It should be emphasized that there has been a radical transformation in the way drilling is carried out today compared to years ago. Most of this can be attributed to new scientific innovations like using of rotary steerable system for drilling efficiency and optimized hole quality and reduce the risk of stuck pipe as well as addition of coating / plugging material like silicates and methyl glycoside. However modern technology are not yet in the clear. They still face challenges like the ones arose from a more sophisticated well trajectories as well as from complex geologic environments.

There lots of software for WBS, in each moment, we are presented with the opportunity to choose from an array of options ranging from Wellcheck for Baker, Logtech from SLB Drillwork-predict for Halliburton and PSI from SINTEF Pretroleum Research AS. They all bear some superficial similarities (input data), but the differences between them are clear. So, when we want to make a choice based on facts and objective reasoning exclusively, we need to methodically analyse and compare each product based on the criteria that we value. It doesn't matter what software you decides to choose, the result is 100% guaranteed but the accuracy and the shortcomings are different.

2.4.1. PSI software

PSI is a computer based wellbore stability software developed at SINTEF. The model implemented in the PSI software combines inputs describing formation conditions, properties and well data to predict the stability of the well. PSI estimates the probability for failure around the wellbore wall at some distance away from the wellbore wall. Since the model was developed based on a combination of well-established analytical solutions, approximate solutions and some numerical solutions the results is very fast enabling even while drilling updates. The software allows the stresses analysis and pore pressure around the well and the correspondent stability versus time since drilling.

The model takes into account rock and fluid properties affecting the well stability over time. Some features it can handle are: formation stresses, well orientation and drilling fluids. Precisely the model take into account:

- Mud chemistry-osmosis and ion exchange
- Inclination and azimuth
- Strength anisotropy
- Plasticity and
- Temperature

The input parameters needed to run a well stability prediction are:

- Formation conditions (in situ stress, pore pressure and temperature).
- Well data (Inclination and azimuth, well diameter, physical and chemical properties of the drilling fluid, mud temperature).
- Formations properties (mineralogy, porosity, diffusion constant, strength parameters, elastic parameters, thermos-elastic parameters, poro-elastic parameters, chemo-elastic parameters, plastic parameters).

The stability will depend on the degree of uncertainty of all above parameters, but some input are more important than others. The user should use all possible sources for input parameters such as:

- Direct measurement when available
- Extra information from small sample test if available.
- Indirect measurement combined with acceptable correlation

It is a must the data should be consistent and when extracting different parameters the same basic model should be used.

For the analysis the software used is an academic (student) version, which is closely related to the professional (commercial) version, and there is no difference at all in terms of functions. The academic version is only meant for training purposes, but the features and functionality are the same with that of professional version. The academic version of the software is an older version of the most current variant (the professional version). While the previous have limited functionality in some form, in this case inability to handle log based data. and only single depth based data, and up to five single depth based data, which can pose great degree of difficulties when comes to interpret the results since it extrapolates what is happening in between two depths.

2.4.2. Wellbore Stability Methodology

Several factors play key roles when it comes to analysing wellbore instability problems during drilling and completion operations. The wellbore instability issues as caused by rock-fluid interactions, complex stress conditions, wellbore inclination and orientation, lack of appropriate drilling and operating practices, pressure alterations, and temperature change. In addition, the presence of faults, unconformities, stress alterations due to fluid flow into a formation and formation anisotropy can also impact on the formation to cause an unstable behaviour. In other words, a combination of these factors influence failure at the wellbore.

The first step in diagnosing wellbore-stability problems is to confirm the existence of wellbore-stability issues. Then, the causes of possible rock failure can be narrowed down by excluding the key operational factors that did not create the problems. One of the techniques to narrow this search is to carry out a comparative study using the data analysis for wells drilled with and without wellbore-stability issues. If one of the factors was identical for both unstable and stable well cases, we can temporarily exclude the specific factor from the data processing with an assumption that this factor did not play a significant role in rock failure. At the end of this elimination process, only a limited number of parameters will be identified as contributing to the wellbore failure. Thus, unless a complex wellbore-stability dataset is available, the diagnostic analysis only helps in identifying possible factors without offering any solution.

In order to perform a wellbore stability analysis there is a numbers of parameters have to be accounted for. These parameters are related to formation properties, formation conditions and the well data.

Formation properties includes the Mechanical and the Petrophysical parameters. The key parameters are the strength in terms of UCS and the friction angle.

Formation conditions includes the in-situ principal stresses as well as pore pressure and formation temperature, in addition to this fracture pressure is also required.

Wellbore data includes the well inclination and azimuth, mud temperature, borehole diameter in addition to mud type and composition.

Here follows a series of data that provide information about some major input parameters to the wellbore stability analysis and their possible sources of deduction. The vertical stress (σ_v) can be estimated from overburden pressure which is computed from well density logs and pseudo density from seismic velocity. It can be achieved by integrating the density well log with respect to vertical depth and the equation **2.1** can be re-written in the following equation: **(Eq. 2.49)**

$$\sigma_v = g[\int_0^b \rho_{sea} * dz + \int_b^z \rho_b * dz] \quad (2.49)$$

2.4.2.1. Overburden Stress

The overburden stress, also called vertical stress is a lithostatic pressure exerted on formation from the weight of overlying rock and soil. The magnitude of overburden stress **(S_v),** is equivalent to integration of rock densities from the surface to the depth of interest **(Eq. 2.49).** Thus, it is essential to take into account that the bulk density value can be affected by near-wellbore washouts and water-shale adverse interactions that will result measuring a lower than actual bulk density value (van Oort et al., 2001). The "stress arching" (the ability of the overburden to shield the vertical stress above the depleting reservoir zone leading to the formation of a stress arch with increasing load on the sides of the depleting areas) effect can cause a difference between the calculated overburden stress and the actual one. In this study, due to the small values of dip angles and assuming that the production is at the early stage with no depletion effect yet, the "stress arching" effect does not have a significant impact on the overburden stress and has not been considered.

Some of the practical problems associated with the computation of overburden stress **(S_v)** using the above equation **(Eq. 2.49)** relate to the fact that density logs readings can be affected by the borehole conditions, which may bring uncertainty to the overburden stress **(S_v)** computation. Plus the fact that density log is often not recorded all the way up to the seabottom. Hence it is necessary to extrapolate densities to obtain the overburden stress as a function of depth.

It was shown in the North Sea that shallow bulk density values can be higher than the ones seen in sedimentary basins around the world, due to ice loading (Fjaer 2008). Density logs from the exploratory wells around North Sea showed densities above 2.0 g/cc as shallow as 500m depth.

Therefore, for this analysis, the average density for shallow zones, where log data was not available, the densities was assumed to be the same as the average of the first 100m where results from density logs were available. As such, the bulk density was assumed to be 2.01 g/cc for the zone from the sea floor to the beginning of the logged interval (indicated by the red dashed line, in **Fig.9**. And then the overburden stress gradient **(Sv) (Fig.10)** was estimated from this assumption using **(Eq. 2.49).** It is possible that this method may overestimate the bulk density, in turn overestimating the overburden stress as well.

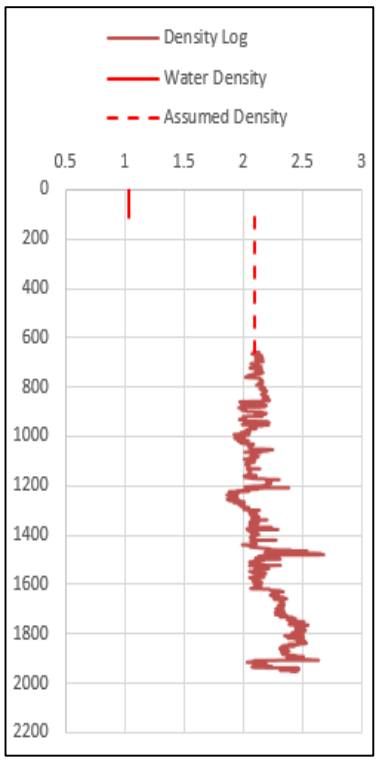

Figure 9 Assumption for density at shallow zones, where log data was not available.

Principal horizontal stresses (Maximum and minimum) are more difficult to determine. The most common method is to create a hydraulic fracture from a borehole, and measure the pressure required to generate the fracture as well as the fracture closure pressure, these pressures are directly related to the in situ stresses, with minimum horizontal stress given by the fracture closure pressure. The hydraulic fracturing method is employed both onshore and offshore.

Other techniques like Anelastic strain recovery (ASR), the technique based on the anelastic behaviour (creep) occurring after unloading of a rock, and Overcoring exists and they are detailed discussed in Fjaer et al., (2008).

2.4.2.2. Pore Pressure

Pore pressure **(PP)** value is a fundamental input into minimum horizontal stress calculation. In a general case, pore pressure is a critical parameter for successful drilling operations, reservoir characterization, and production optimization. However, in order to solve wellbore-stability problems encountered during drilling, it is critical first to determine pore pressure not only in the productive intervals, but also in the overburden intervals.

The pore pressure estimation in low permeable shale is more difficult, particularly in case of interbedded shales contacting partially to deplete zones. (Nes et al., 2005) otherwise it can be estimated from compaction analysis using acoustic velocity and offset well log data including formation test data for sandstone reservoirs as an input.

The normal trend (Eaton) and explicit methods (Holbrook, Bower) are commonly used in the oil industry for pore pressure prediction. Eaton method of pore pressure prediction will be used here considering it is the most common method with the data that is available for this study.

The Eaton method for pore pressure **(PP)** prediction relates changes in pressure to changes in sonic compressional velocity (Inverse of the compressional travel time) of the measurements. The basic assumption of the Eaton method is that a ratio of compressional velocity obtained from regions of normal and abnormal pressure is related to the ratio of normal and abnormal pressure to the region through an exponent that can be determined empirically (Eaton, 1975). This methodology is the most commonly used for pore pressure prediction.

The method estimates pore pressure from the ratio of acoustic travel time in normally compacted sediments to the observed acoustic travel time. Pore pressure is estimated using the equation below, **(Eq. 2.50),** and the results shown in **figure 10.**

The normal compaction curve is the trend line of certain rock properties with depth of burial at normal hydrostatic pressure. Normally compacted formations will have its properties following a certain trend with depth of burial **(Fig 10)**. The normal compaction curve is required to identify any overpressure related indications from the sonic log. A normal compaction curve is also required for pore-pressure prediction from the Eaton (1975) method used here. The hydrostatic pressure (Normal pore pressure) (PPn) is equal to the vertical height of a column of water extending from the surface to the zone of interest.

$$PP = S_v - (S_v - PPn)\left(\frac{DTC_n}{DTC_o}\right)^3 \quad (2.50)$$

$$PPn = g\rho_{water}D \quad (2.51)$$

In the **equation 2.50**, DTC_n is the compressional acoustic travel time from the normal compaction trend at the depth of investigation, and DTC_o is the observed (the logged) compressional acoustic travel time from the sonic log, the units is given in μs/f or s/m for DTC and psi/ft or Kpa/m for PP.
Where DTC is the measured sonic travel time, at the desired depth of interest, which corresponds to the depths at which the $\mathbf{S_V}$ is determined.
The DTC_n in equation 2.50 is plotted using the equation 2.52 (Desbrandes, 1985). With D being vertical depth and a & b determined manually with the points sorted before using the least square method in Microsoft excel (Desbrandes, 1985)

Ln (DTC_n) = (a * D) + b

DTC_n = Exp ((a * D) + b) (2.52)

a: = INDEX (LINEST(Y,Ln(D),1)

b: = INDEX (LINEST(Y,Ln(D),2)

With **c** being the **Slope** and **b** the **Intercept**, **D** is the true vertical depth (m), **Y** is the natural logarithm of transit time in the initial and final pivot depth.

Note that, although this method of predicting pore pressures has been proven effective in some environments, most notably the North Sea, it should be used with caution in regions with ongoing rapid sedimentation such as deep water Gulf of Mexico. This is because the general formulation of the Normal Compaction Trend underestimates sediment velocities at low effective stresses (Zoback 2007).

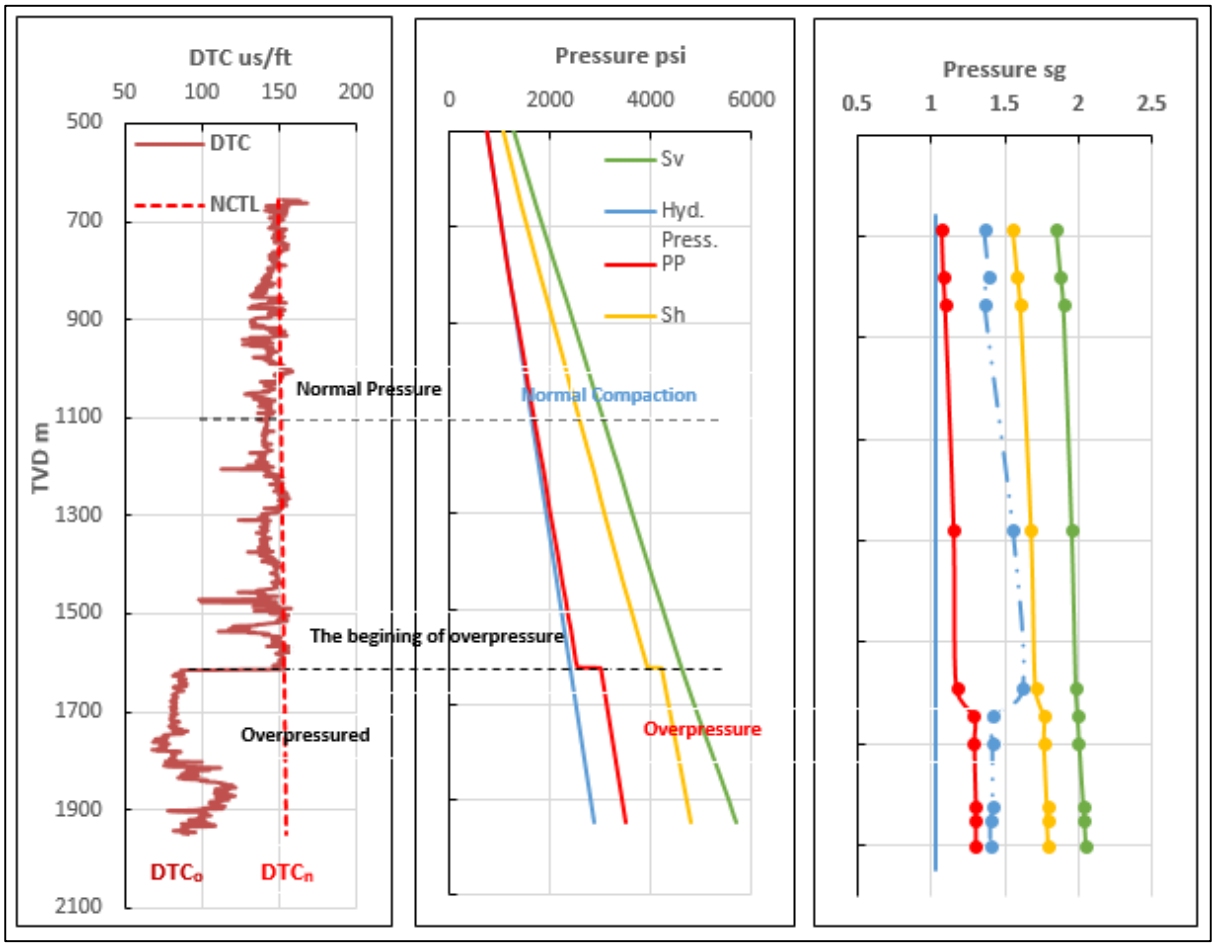

Figure 10 Trend line approach (Left) and its correlation with pressure gradient (Centre) and (Right) Plot showing the pressure gradient. The legend is the same as the centre plot but here the dash dot dot blue line represent the Optimum weight which was averaged from lower and upper limit MW.

The major problem with all trend-line methods is that the user must pick the correct normal compaction trend **(fig 10 left)**. Sometimes are too few data to define the normal compaction trend. Unfortunately, if the normal compaction trend is defined over an interval with elevated pore pressure, the method will give the wrong (too low) pore pressure.

When the pore pressure is equal to the hydrostatic pressure profile **(Fig 10 centre),** the pore pressure is referred to as normal pore pressure (PP_n). Abnormal formation pressure refers to formation pressure that is higher (overpressure) or lower (underpressure) than hydrostatic pressure. Here, a water density value of 1.03 g/cc (0.45 psi/ft) was used as the average water density.

2.4.2.3. Minimum horizontal stress calculation

The least horizontal stress **(S_h)** is the essential parameter for planning borehole stability. This stress (S_h or $\boldsymbol{\sigma_h}$) value can be read from the available XLOT data results performed with flowback. **Fig.11** shows a type curve of these tests (Zoback, 2007), which refers to a fully carried out LOT test and in such cases the fracture closure pressure (FCP) is a better measure of the least principal stress. The various terms associated with such a test are explained in details in *Zoback, M. D. 2007 Reservoir Geomechanics. Chapter 7*. The maximum horizontal stress (σ_H) can be estimated from indirect methods such as analysis of tensile fractures and breakouts from combination of image and calliper logs. Rock strength can be estimated from velocity, porosity data and calibrated from core data.

According to Oort et al. (2001), the most accurate value of the minimum horizontal stress corresponds to the fracture closure pressure during the Extended Leak-off Tests (XLOT). Since there are only one available XLOT data for the well, the Eaton method was used to calculate the minimum horizontal stress **(S_h)** from the Poisson's ratio properties that can be obtained from the compressional and shear slowness and vertical stress as shown on **(Eq. 2.53),** and that was assumed to be equal to the magnitude of the fracture pressure, but in order to determine the more absolute stress values, data from more accurate method like the XLOT technique from several offset wells were used for model calibration.

$$S_h = \frac{v}{1-v}(S_v - PP) + PP \qquad (2.53)$$

The problem with Eaton's method is that it assumes a constrained basin which is free from tectonics effects and assuming a constant Poisson ratio, which is not true since Poisson ratio change even due to a loading compaction, so the values for minimum horizontal stress from Eaton's methods is used when there is no other option. These calculations indicate the likely values of the vertical and horizontal natural in-situ stress components based on the application of elasticity theory to an isotropic rock.

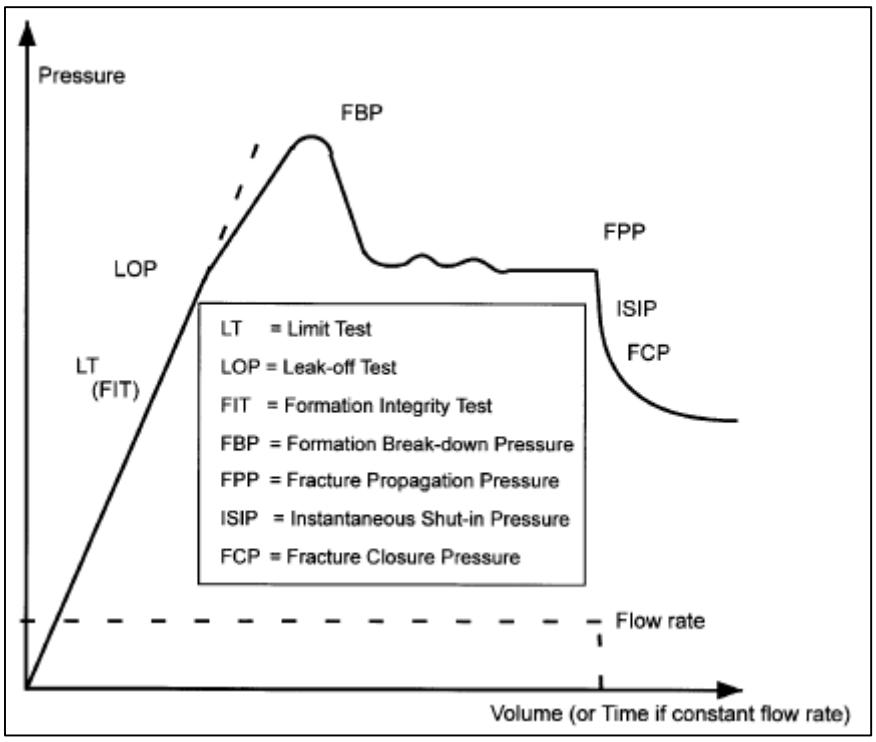

Figure 11 Schematic illustration of an XLOT (Zoback 2007). The various terms associated with such a test are detailed explained in Zoback, M. D. 2007 Reservoir Geomechanics. Chapter 7.

2.4.2.4. Rock mechanical properties

Rocks responses are functions of their mechanical properties, the pressure of the fluids within, and the magnitudes and orientations of the forces that are applied (Bell, 1996).

Static strength and deformation properties are considered to be the most representative of actual material behaviour. Unfortunately, collection of this data is costly in time and money as these methods require core samples from the formation for testing and only represent the material properties at that specific location. At the other hand, dynamic stiffness and deformation properties can be calculated from sonic well logs and provide a complete view of material characteristics along the entire wellbore (Fjaer and Holt, 1999).

Sonic logging tools measure acoustic wave travel times, i.e. compressional travel time and shear travel time, which together with density log measurements provide the elastic properties. In an elastic, isotropic, homogenous solid rock the elastic moduli can be determined from travel time of the compressional waves (DTC) and travel time of the shear waves (DTS)

However, due to lack of laboratory rock mechanic testing the rock mechanical properties could not be calibrated. Therefore calibration is necessary to reduce such uncertainty in rock mechanical properties characterization and to get the absolute value of the parameter.

2.4.2.4.1. Young Module and Poisson Ratio

Once the velocities are measured, Poisson's ratio (ν) can be calculated and combined with density measurement, Young's modulus (E) is calculated from Poisson's ratio and density. Therefore the quality of reservoir's stress analysis can be related to the basic measurements of compressional velocity (1/DTC), shear velocity (1/DTS) and formation density (Coates and Denoo, 1980).

Rock stiffness inputs such as Poisson's ratio (ν), young module (E) and uniaxial compressive strength (UCS) was estimated from processed sonic data of the drilled well. All these log derived parameters should be compared with available core data of the reservoir section, to check for comprehensive match with each other.

Using the concept of elastic moduli equations described by Clark (1966), the dynamic compressive modulus (M), shear modulus (G), bulk modulus (K) along with the dynamic Young modulus (E) and Poisson's ratio (ν) were calculated using the below relations **(Eq. 2.54-2.58).** The results of the calculations are shown in **figure 12**.

Young's Modulus is a measure of a stiffness of material, material resistance against being compressed by uniaxial stress, while Poisson's ratio is a measure of lateral expansion relative to longitudinal contraction and Shear module is a measure of the sample's resistance against shear deformation (Fjaer, et al., 2008). However the simple equations related to log derived measurement to rock mechanical properties are not valid when elastic anisotropy is encountered.

$$M = \rho \left(\frac{1}{\mathrm{DTC}}\right)^2 \quad (2.54)$$

$$G = \rho \left(\frac{1}{DTS}\right)^2 \quad (2.55)$$

$$K = M - \left(4 * \frac{G}{3}\right) \quad (2.56)$$

$$E = \frac{9*G*K}{G+3*K} \quad (2.57)$$

$$\nu = \frac{1}{2}\left[\frac{\left(\frac{DTS}{DTC}\right)^2 - 2}{\left(\frac{DTS}{DTC}\right)^2 - 1}\right] \quad (2.58)$$

The dynamic rock stiffness calculated from log data are representative of the undrained properties, the different stiffness properties characterize the drained and undrained

response, and the definition of elastic modulus such Bulk modulus, Poisson ratio must include drained or undrained. Drained Young modulus may be calculated from drained Bulk modulus and Shear modulus. Theoretically the Shear modulus is not affected by the drainage condition, hence, dynamic undrained and drained Shear moduli is expected to be the same, since the shear modulus for the fluid is zero. The porous Bulk material is stiffer for undrained conditions because the fluid resists compression as well as the framework. The induced pore pressure opposes the applied stresses that produced it (Wang 2000). The relationship between the drained and undrained Bulk modulus is given in Wang, H.F (2000) in the theory of linear poro-elasticity with applications to geomechanics. The undrained Poisson ratio is larger than drained value because an increase in fluid pressure will decrease the vertical strain and increase the lateral strain, for an incompressible material the undrained Poisson's ratio would be 0.5 (Wang 2000).

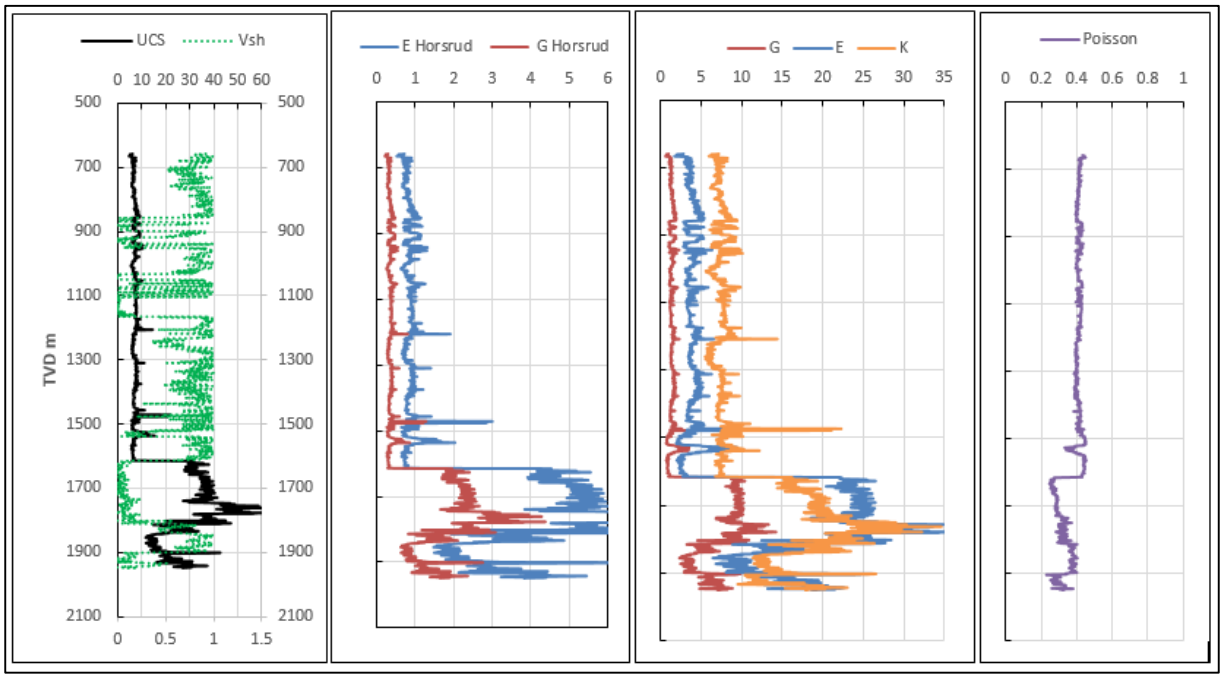

Figure 12 Plot showing the calculated rock parameters. The UCS is given in MPa, E in GPa, G in GPa and K in GPa. And the comparison between G, E Horsrud and G, E. The E and G Horsrud was obtained by using the empirical Horsrud (2001) correlation while E, K and G was obtained by using the acoustic travel time and density

Eventually, these have been evaluated with other like Fjaer (2008) equations **2.20-2.24** and the results fitted into to the input parameters to check for uncertainty of the model and improve the calculated output.

In addition the rock mechanical parameters above was calculated using Horsrud (2001) empirical correlation available using the compressional wave transit time from the sonic log, for young moduli and shear moduli available **fig 12**, the correlations can be written as follow **(Eq. 2.59-2.60);** here the DTC is travel time of compressive acoustic wave in µs/ft, and E and G are in GPa.

$$E=0.076(304.8/DTC)^{3.23} \quad (2.59)$$

$$G=0.030(304.8/DTC)^{3.30} \quad (2.60)$$

The above correlations **(2.59-2.60)** predict very low Young and Shear moduli for high travel times (DTC ≥ 125 us/ft) and high Young and Shear moduli for low travel times, when compared to the ones derived from sonic data, and appear to probably underestimate the data since the values of **E** and **G** are too low when compared to the core measurement reference value given for **E** at 1589 m which is 1.6 GPa. It should be noted that in the

porosity context of this correlation were derived, then here the cause for different reading might be the difference in porosity of the rocks. However it is important to bear in mind that the validity of any of these correlations is best judged in terms of how well it would work for the rocks for which it was initially tested.

2.4.2.4.2. Rock Strength

The rock strength value is defined as the peak stress level during a deformation test after which the sample weakens (Zoback, 2007). The strength of rock usually termed as UCS or C_0 depends on how it is confined. When core samples are not available for laboratory testing, various correlations are performed to simulate the rock value. Rock strength value has long been related to other rock measureable value from logging or drilling data. The basis for these relations is the fact that many of the same factors that affected rock strength also affect elastic moduli and other parameters, such as porosity (Zoback, 2007).

For rock strength calculations from sonic data, there are lot of published empirical correlation available. In this case, it had been observed that the Horsrud (2001) correlation to derive rock strength from compressive sonic velocity gave the reasonable correlation. The empirical equations for Uniaxial Compressive Strength (UCS) as a function of sonic velocity are as follows **(Eq. 2.61);** this is an empirical correlation valid only for shale, where DTC is travel time of compressive acoustic wave in μs/ft, and UCS are in MPa.

$$UCS = 0.77\ (304.8/DTC)^{2.93} \qquad (2.61)$$

Each of the above calculations results is shown in the table 6, and it shows the advantage of making assumptions and using empirical correlations when making study with only limited available data. However the outcome usually oversimplifies representations of the real problem being studied, and become source of uncertainty.

However, core plugs of the non-reservoir formation (mudstones and shales), are rarely available for laboratory testing. So the analysis of the calibrated rock strength parameters in shale based on the well log depends solely on the empirical correlation formulation, type and resolution of the log data.

The probability of shear and tensile failure, is calculated on the basis of the local stresses, pore pressure and selected shear failure criterion. Here the Mohr-Coulomb shear failure criterion is applied.

The stress conditions around the borehole are estimated from general equations for borehole failure in a linearly elastic rock (Fjaer et al., 2008) as presented above.

The input data into the software can be provided directly when available from laboratory testing on cores or cuttings. The quality of the predicted stability is directly linked to the quality of the input data describing the well and formation conditions and properties. However sometimes only log or and seismic data is available. In such case various experimental correlations can be used.

To estimate shale mechanical parameters, sonic log data are a primary source. Since shales are generally anisotropic due to their micro- and macrostructure, acoustic velocities generally depend upon the direction of propagation relative to the shale bedding planes (Nes et al., 2013). This must be accounted for when using sonic log data obtained from deviated wells.

All the analyses have been evaluated with the PSI Software and more convenient empirical formulas have been used and the results fitted to the calculated output.

3. Thermal effects on wellbore stability

3.1. Case study from a North Sea well.

3.1.1. Fundamental Overview

The wellbore stability study presented here was completed on a North Sea well. In the North Sea, several challenges exist with both complex structures and varying depositional environments. Establishing a detailed wellbore stability model will be helpful for casing point selection, mud weight selection, identification of potential weak formations and unstable well path trajectories, as well as improve bit design. The wellbore stability model developed for this investigation include data collected from one North Sea well, **Table 3** shows an overview of the log from the well. Drilled vertically to a total depth of 1950 m, with oil based mud, and in an homogeneous isotropic rock submitted to principal in-situ stresses assumed to be vertical (S_v), and horizontally isotropic (S_H=S_h). The assumption of horizontal isotropic stress was based on Horsrud (2015) quote: “In the North Sea and most of the Norwegian Continental Shelf there is no indications of significant horizontal stress anisotropy, this is experience from drilling and stability of producing through oriented perforations”

The borehole wall is assumed to be impermeable and this assumption is reinforced by the concept from Chen and Ewy (2005) which states that: Impermeable borehole wall can occur when an oil based mud is used to drill the water wet shales due to the high capillary entry pressure.

For confidentiality reasons details about the well (name, geology etc) were not provided.

Table 3 Overview of the log collected from the well.

Log Curve	CALI	DTC	DTS	GR	RHOB	VSH	Sv*	PP*	Shmin*
Units	in	µs/ft	µs/ft	API	g/cc	-	sg	sg	sg

The log curve are defined as follow: Cali (Calliper), DTC (Sonic compressional wave travel time), DTS (Sonic shear wave travel time), GR (Gamma Ray), RHOB (Bulk Density), VSH (Shale Volume), Sv (Overburden Gradient), PP (Pore Pressure Gradient), Shmin (Minimum Horizontal Stress Gradient).

**Expected value estimated from an offset well data.*

To determine intervals that may be influenced by the wellbore-stability issues, a detailed analysis of the available well logs (sonic data) was conducted. A detailed investigation was carried out on well-logging data to diagnose the troubles that may be encountered during the drilling, since this is a tight well and the only data available is sonic data, this was done by looking on the calliper log for possible wash out zone (overgauge) in shale, **Fig.13.**

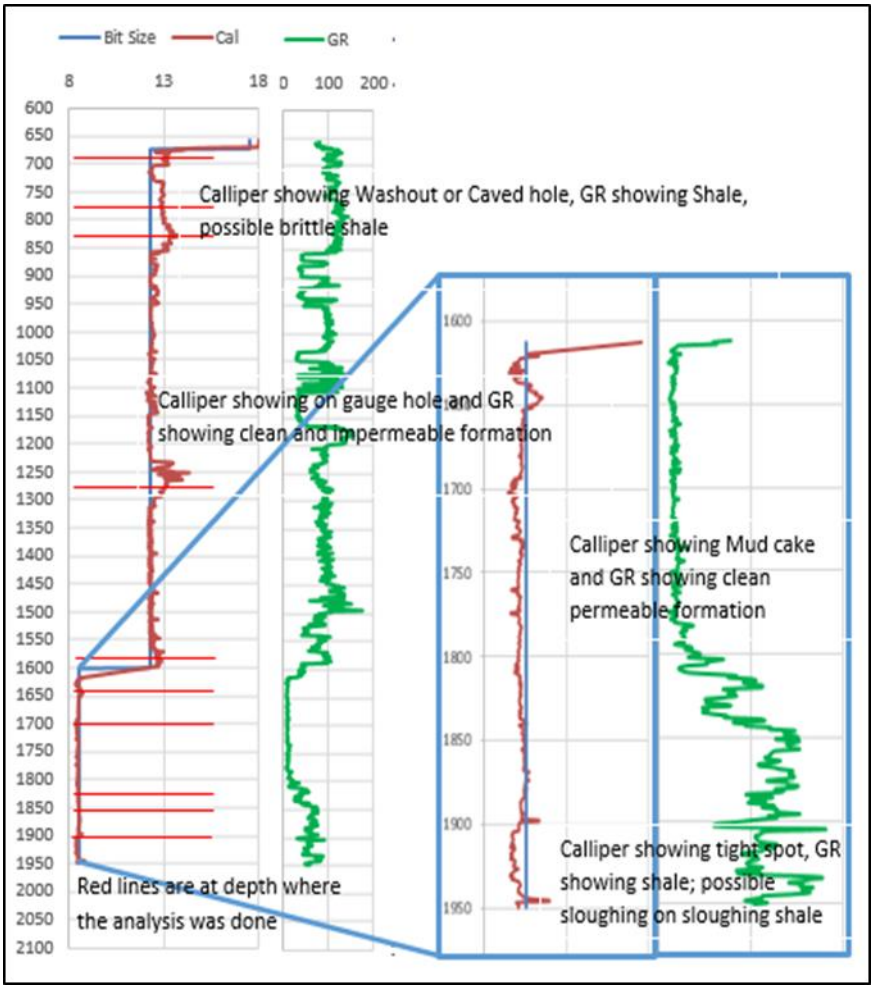

Figure 13 Depth where the analysis has been carried out, and mud cake thickness, possible cavings / possible hole instability

The input data acquisition is an important part of wellbore-stability analysis, and the required input data we used in this analysis are listed below:

- Formation acoustic properties from sonic log (DTC and DTS)
- Rock mechanical properties (Dynamic Poisson's ratio, Dynamic Young's modulus and uniaxial compressive strength of the formation)
- Overburden stress
- Pore pressure
- Minimum horizontal stress

Methodologies used to obtain the input data and results are described above in **section 2.4.**

3.2. Thermal effect theory and background

Increasing need for energy has increased the demand for oil resources, and resulting in increasing focus on the complex geology environment and unconventional reservoirs. Generally, complex geology is related to higher temperature and pressure, and a number of reservoirs under this conditions have been drilled worldwide, particularly in North Sea.

Field evidences indicates that thermal regimes in wellbore considerably affects the wellbore stability. The affected formation temperature in the vicinity of the wellbore could result in different formation rock behaviour and consequent wellbore stability problems. Temperature change will lead to the variation of rock volumes according to thermal expansion

phenomenon, the formations around the borehole cannot expand freely due to the limitation of the borehole liquid column and surrounding rock. In another words if the material is constrained, such that it cannot change its size / volume, a thermal stress will build up when the temperature increases. Then, additional ‘‘thermal stress’’ will be generated on the surrounding rock of the borehole wall, and, the stress around the borehole will change (Detournay and Cheng 1988; Chen and Ewy, 2005).

Studies on the thermal effects on borehole stability could date back to the early XX century, when the drilling fluid temperature and drilling fluid cooling measures were considered during the drilling of geothermal wells in the former Soviet Union (Li, 2004: The study on HT/HP wellbore stability). Several studies (Maury and Guenot (1995); Detournay and Cheng (1988); Chen and Ewy, (2005) and Perkinz and Gonzalez (1984)) have been conducted regarding the thermal stress effect on the wellbore stability, and some researchers have proposed methods to model this effect and the consequent response. Maury and Guenot (1995) have pointed out that thermal stress is one of the reasons for borehole instability and they demonstrated, in an experiment, that a stress of 0.4 MPa will be generated for medium to hard rocks and 1.0 MPa for hard rocks when the temperature rises by 1 ºC. Perkins and Gonzalez (1984) used the analytical solutions to determine the stress resulting from temperature and pressure changes around the wellbore during the injection process. They concluded that injecting large volume of liquid that is cooler than the in situ reservoir can have larger effect on lateral earth stress reducing the tangential stress around the injection well, while increasing the injection pressure tend to increase the tangential stress. However there was no wellbore included in their model.

Great research on the temperature distribution due to drilling fluid circulation in a well has been carried out by Chen and Ewy (2005) on the thermal effects for permeable and impermeable boundary condition on an inclined borehole. They used the analytical solution and verified in real time domain using finite difference methods to solve the fully coupled temperature and pore pressure equation.

For this analysis, the finite differential equation was solved numerically to know the temperature distribution with time in the formation and the numerical results simulated for the temperature field near the borehole wall.

3.3. Temperature distribution around the borehole

During drilling process, one of the key factor that affects borehole stability, is the variation of formation temperature which in turn cause the changes in pressure. While drilling, the drilling fluid continuously exchanges heat with the formation in the circulation process, which can be manifested by the constant variation of the drilling fluid temperature and formation temperature around the borehole. If there is temperature difference between fluid and formation, the temperature will propagate by diffusion into the formation. And the rocks formations, like most other materials expand or shrink when temperature is changing, thus giving rise to the thermal concentration or expansion stresses. Thus, the thermally induced stress can be caused by difference in thermal expansion coefficient of the rock formation. The stress variations as result of temperature changes is the product of difference in thermal strain and material stiffness, the thermal effect is proportional to rock stiffness as pointed out by Maury and Guenot (1995), which means that it is more significant in hard than soft rocks. It is also proportional to the thermal expansion coefficient, (Fjaer et al, 2008).

The induced thermal field can have a pronounced effect on the pore pressure response, if the temperature increase significantly, excess pore pressure can develop because of the fact that volumetric expansion of the fluid in the pores in greater than the solid rock; the difference between thermal expansion for the fluid and the solid creates the induced pore pressure (Fjaer, 2010), and the main effect of temperature changes is the pore pressure variation which in turns produce changes in the effective stress redistribution around the borehole, and the stability of the borehole can be affected.

As the temperature variation caused by radial heat conduction around the borehole is sharp and the temperature variation of the formation far away from the borehole is gentle. The heat transfer process is done by diffusion, and in the diffusion analysis ones wish to know the temperature distribution, which represents how temperature varies with position in the medium. Then the governing equation for heat transfer follows the classical two dimensional heat diffusion equation, **Eq. (3.1).** However for the surrounding rock, because the temperature gradient in the radial direction is much greater than that in the vertical direction in the near region of the wellbore, the derivative of the temperature with respect to depth can be ignored (Raymond 1969), and the equation become as the equation bellow.

$$\frac{\partial T}{\partial t} = \propto \left(\frac{1}{r}\frac{\partial T}{\partial r} + \frac{\partial^2 T}{\partial r^2}\right) \quad (3.1)$$

Where: $\propto = \frac{k}{\rho C_p}$ (3.1.1)

As it has been remarked, the induced thermal field can have a pronounced effect on the pore pressure response, because of the fact that volumetric expansion of the fluid in the pores in greater than the solid rock, then the difference between thermal expansion for the fluid and the solid creates the induced pore pressure; thus, if the temperature increase significantly, excess pore pressure will build up. Then the fully coupled diffusivity equation for temperature and pore pressure can be expressed as bellow, (Chen and Ewy, 2005)

$$\frac{\partial P}{\partial t} = \propto_0 \left(\frac{1}{r}\frac{\partial P}{\partial r} + \frac{\partial^2 P}{\partial r^2}\right) + \mathrm{c}\frac{\partial T}{\partial t} \quad (3.2)$$

$$\propto_0 = \frac{2\delta G B^2 (1+v)^2 (1-v)}{9(1-v_u)(v_u - v)} \quad (3.3)$$

$$c = \frac{\propto_0}{\delta}\left[\frac{2\alpha_T (v_u - v)}{B(1+v_u)(1-v)} + \emptyset(\alpha_{T_{fl}} - \alpha_T)\right] \quad (3.4)$$

$$\delta = \frac{\mathrm{k}*}{\mu} \quad (3.4.1)$$

$$B = \frac{K_f}{K_f + \frac{\emptyset}{a}K_{fr}} \quad (3.4.2)$$

The equations **3.1** and **3.2** are diffusion equations (temperature and pressure) for cylindrical coordinates. In the **equation 3.2** the first term with $\propto_0$ as coefficient represent the pressure diffusion and the second term with **c** as a coefficient denotes the temperature diffusion and here represent the effect of temperature variation on pore pressure changes. If the first term is sufficiently larger than the second the influence of temperature on pore pressure is negligible, which may happens in high permeability formation and the pressure changes may considered independent of temperature changes (Chen and Ewy, 2005). In another words equation **(3.4.2)** indicates that the pore pressure changes will depends linearly on both the deformation of the porous solid and the variation of fluid content. If the term **B** (also called "Skempton **B** parameter": the ratio of the induced pore pressure to the variation of confining pressure under undrained conditions; It has been argued that the realistic range of variation for **B** is [0,1] (Rice and Cleary, 1976)) in the equation **3.4.2** gets sufficiently high (Incompressible situation) **B=1** then the $\propto_0$ term in the equation **3.2** will dominate over the **c** term, and the equation **3.3** gets larger than equation **3.4.** or in another case, we may consider an infinitely compressible situation which corresponds to **B = 0** then the equation **3.3** will be zero and less than equation **3.4** which is the opposite and occur in low permeable formation like shales when the first term of the equation **3.2** gets smaller than the second term an in here the pore pressure will be a steady state function of temperature change.

The permeability coefficient term characterizes the diffusive transport property of the system. All these constants can be measured experimentally in the laboratory.

3.3.1. Modelling Temperature Distribution

Drilling is a dynamic process, circulation of the “cold / hot” mud into the well results in the stress alteration at the borehole wall due to the rock temperature change. Since the heat is transferred in the direction of decreasing temperature and cross the Area perpendicularly. The starting point is focused in the heat diffusion equation. From this equation the objective is solve and analyse the heat flux distribution, the temperature distribution and the temperature gradient of formation. Since most of the tools for wellbore stability analyses has no feature for thermal analyses problem. Then the problem will be solved numerically, based on calculations after specifying the proper boundary conditions.

This **Eq. (3.1)** is a partial differential equation which provides the temperature distribution in the medium, and the **Eq. (3.2)** denotes the pore pressure diffusion and represent the pore pressure changes caused by the temperature variations. To analyse the temperature and pressure fields around a borehole, it is necessary to solve the equation numerically or analytically. Here we use numerical method for modelling the temperature and pressure fields of the borehole and calculate the total stress resulting from this variation based on the thermoelasticity and poroelasticity theory. This method of heat and pressure transfer (diffusion) has been popularized and applied constantly.

However, such a solution of the temperature distribution depends on the physical conditions existing at the boundaries of the medium. In this situation the temperature at the borehole wall is known for any instant, and the temperature is considered to be constant at the boundary (borehole wall) between borehole fluids and surrounding rock and one may for simplicity assume that the temperature remains the same in the far field formation for a relatively long period. And the conditions can be briefed the condition with the expressions:

$T(r_0,0)=T_{w,}$ $T(r_\infty,t)=0$

$P(r_0,0)=P_f(T)$, $P(r_\infty,t)=0$

The temperature distribution in the formation around the borehole is a complicated process, and can be determined by the rate of heat convection of the formation pore fluid and the rate of heat exchange between the fluid and the host rock, (Chen and Ewy, 2005).

The temperature and pressure fields around the borehole, was determined through dispersing the governing equations **Eq. (3.1-3.2)** using the numerical method for differential equation. The numerical method model was developed in Microsoft Excel Software using the following assumptions:

- The temperature flow was assumed to be symmetric around the vertical axis of the borehole
- There was no temperature flow in the vertical direction
- The physical and thermal properties of the rocks was uniform throughout the formation
- There was no heat generation within the rock.

The method determines temperatures at discrete grid points. The temperature at each grid point is based on previous temperature at the grid point and current and previous temperature at neighbouring grid points (Crank and Nicholson, 1947). Outlining the procedure on how to solve the differential equations by numerical method converting them into finite difference equations employing explicit and implicit techniques is not the purpose of this thesis and for more in depth knowledge please refer to: Crank J. and Nicholson, P. 1947. A practical method for numerical evaluation of solutions of partial differential equations of the heat conduction types.

3.4. Thermal induced stress and pore pressure analysis

Since the thermal effect is usually not considered as a factor in most of the conventional borehole stability models, it will be analysed here, and based on the numerical method model developed for modelling the temperature fields around the borehole and formation during drilling process. The temperature distribution is analysed.

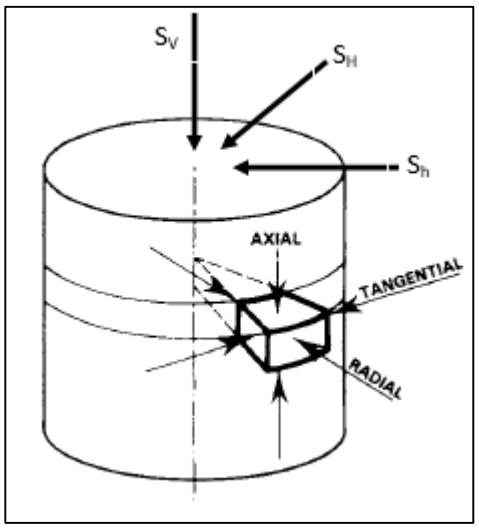

Figure 14 Principal stress configuration at the borehole wall. Vertical (S_v), and horizontally isotropic (S_H=S_h) (Modified from Maury and Sauzay 1987)

Given the above borehole conditions in **3.1.1,** with the parameters calculated in **section 2.4.2**, the principal stress at borehole wall **(Fig.14),** is analysed for thermal effect at 1589 m depth. And the stresses at a point of the borehole wall are given by equations **(2.4-2.6)**

The temperature changes generate additional stress **Eq. (2.35)** and strain **Eq. (3.14)** concentration on borehole wall on the basis of the original balance. Maury and Sauzay (1987) found that, as the temperature increases, the tangential and axial stresses at the borehole wall will both increase by the same amount, **Eq. (2.39).** And the additional thermally induce factors around the borehole resulting from temperature variation is calculated based on thermoelasticity theory. Thus, heating or cooling the borehole wall will add or reduce extra thermally induced changes in stress affecting both the tangential and the axial stress **Eq (3.7-3.9).**

Note that in situ state of stress and internal pressure in the well govern the stress distribution around the wellbore as well as the mode of failure. The thermal stresses must be evaluated taking into account the pre-existing stresses at the borehole wall.

$$\Delta\sigma_r = \sigma_r = P_w \quad (3.7)$$

$$\Delta\sigma_z = \sigma_z + \sigma_z(\Delta T) \quad (3.8)$$

$$\Delta\sigma_\theta = \sigma_\theta + \sigma_\theta(\Delta T) \quad (3.9)$$

Where: σ_r, σ_z and σ_θ are from equations **2.7, 2.8 and 2.9** respectively, and $\sigma_z(\Delta T)$ and $\sigma_\theta(\Delta T)$ is the equations **2.39**. Which account for stresses around the borehole in a vertical well with impermeable borehole wall. The impermeable borehole wall assumption was made due to the presence of mud cake on sands as seen on calliper log **fig.13** and non-permeability on shales.

The radial stress is equal to well pressure. The maximum additional tangential and axial stress are at the borehole wall. Then the thermally induced stress for any distance away from the wellbore wall is given by the following equations, (Yan, C. et al,. 2013).

$$\sigma_r = \frac{E\alpha_m}{3(1-\nu)}\frac{1}{r^2}\int_{R_w}^{r}\Delta T(r',t)r'\partial r' \quad (3.10)$$

$$\sigma_\theta = \frac{E\alpha_m}{3(1-\nu)}[\Delta T(r,t) - \frac{1}{r^2}\int_{R_w}^{r}\Delta T(r',t)r'\partial r'] \quad (3.11)$$

$$\sigma_z = \frac{E\alpha_m}{3(1-\nu)}\Delta T(r,t) \quad (3.12)$$

As stated earlier, the induced thermal field can have a pronounced effect on the pore pressure response, due to the difference between thermal expansion for the fluid and the

solid creates the induced pore pressure. However, two mechanisms play a key role in this interaction between the temperature change, pore pressure and stresses changes:

(i) an increase of temperature induces a dilation of the rock, which will lead to changes in stress an pore pressure, and (ii) changes in stress will cause a compression of the rock and give a rise of pore pressure, but only if the fluid is prevented from escaping the pore network (Detournay and Cheng, 1993).

Now, based on the constitutive theory of Biot (1941) which predicts that for an isotropic rock, changes in pore volume, and therefore pore pressure, will only be caused by changes in mean stress. For the case analysed here which is impermeable borehole (constant pore pressure); no communication between borehole pressure and formation pressure, meaning that the average of stresses around the borehole will be a constant, independent of **r** since the mean stress **(equation 3.12.1)**, at that specific point is a function of local temperature. This means that the elastic rearrangement of the stresses around a wellbore does not result in any volumetric changes and thus pore pressure changes.

$$\sigma^{-} = \frac{\sigma_r(\Delta T)+\sigma_z(\Delta T)+\sigma_\theta(\Delta T)}{3} \quad (3.12.1)$$

And since, the pore pressure and thermal effects are related, increase (changes) in pore pressure Equation **(3.13)** will produce the same effect as increasing (changing) temperature **equation (3.14).**

$$\varepsilon\text{vol} = -\frac{\alpha}{K}\Delta P_f = -\frac{3\alpha(1-2\nu)}{E}\Delta P_f \quad (3.13)$$

$$\varepsilon\text{vol} = -3\alpha_T \Delta T \quad (3.14)$$

In a linear elastic, isotropic rock, a temperature increase of ΔT results in the same (total) stress and strain changes as a pore-pressure increase of **equation (3.15)**

$$\Delta P_f = -\frac{E\alpha_T}{\alpha(1-2\nu)}\Delta T \quad (3.15)$$

Additionally the stress concentration around the borehole wall cause an immediate increase in pore pressure, (Detournay and Cheng, 1988) which dissipate with time. And this happens due to the redistribution of the formation stresses gives a rise in the volumetric strain (Fjaer, 2008)

Based on the research from Maury and Guenot (1995) If the thermal stress contribution is ignored then there may be errors in predicting the safe mud window, resulting in borehole collapsing o fracturing.

The possibility of wellbore pressure invasion, which allows some pressure penetration into borehole wall and the formation, was not considered here meaning that the pore pressure changes will not be dependent upon both the wellbore pressure and temperature changes but only on temperature changes, since the well is impermeable.

In realistic case there is no impermeable borehole condition since there is always small amount of filtrate from oil base mud penetrate into the formation and then will change the in situ pore pressure. For that case, once the pore pressure profile is known the radial, tangential and axial stresses may be calculate and expressing the stresses variation due to pore pressure changes is: **Eq. (3.16-3.18),** ((Nguyen, D. 2010)

$$\sigma_r = \frac{a(1-2\nu)}{1-\nu}\frac{1}{r^2}\int_{R_w}^{r}\Delta P(r,t)r\partial r \quad (3.16)$$

$$\sigma_\theta = -\frac{a(1-2\nu)}{1-\nu}\left[\frac{1}{r^2}\int_{R_w}^{r}\Delta P(r,t)r\partial r - \Delta P(r,t)\right] \quad (3.17)$$

$$\sigma_z = \frac{a(1-2\nu)}{1-\nu}\Delta P(r,t) \quad (3.18)$$

However, this is not this case since the borehole wall here assumed fully impermeable, the wellbore pressure invasion between the wellbore pressure and formation pressure will be

restricted completely and the thermally induced pore pressure will become the full pore pressure solution. On this basis and using the superposition principle, the stresses around the borehole considering the thermal effects, can be obtained by superposing in situ mechanical, and thermal induced stress effects, then the thermoporoelasticity model is obtained. Equations **(3.10-3.12)** and **(3.16-3.18)** are added onto the pure elastic model stress components at the borehole wall **Equations 2.7-2.9**, to get equation **3.19-3.21** at the borehole wall where borehole instability generally occurs, (Fjær et al. 2008) or Eqs. **(3.22-3.24)** at some distance away (around) from the borehole wall which is the thermoporolelastic model equation.

$$\sigma_r = Pw \tag{3.19}$$

$$\sigma_\theta = 2\sigma_h - Pw + \sigma_\theta(\Delta T) + \sigma_\theta(\Delta P) \tag{3.20}$$

$$\sigma_z = \sigma_v + \sigma_z(\Delta T) + \sigma_z(\Delta P) \tag{3.21}$$

$$\sigma_r = \sigma_h\left(1 - \frac{R_w^2}{r^2}\right) + \frac{R_w^2}{r^2}P_w + \frac{E\alpha_m}{3(1-\nu)}\frac{1}{r^2}\int_{R_w}^{r}\Delta T(r,t)r\partial r + \frac{a(1-2\nu)}{1-\nu}\frac{1}{r^2}\int_{R_w}^{r}\Delta P(r,t)r\partial r \tag{3.22}$$

$$\sigma_\theta = \sigma_h\left(1 + \frac{R_w^2}{r^2}\right) - \frac{R_w^2}{r^2}P_w + \frac{E\alpha_m}{3(1-\nu)}\left[\Delta T(r,t) - \frac{1}{r^2}\int_{R_w}^{r}\Delta T(r,t)r\partial r\right] + \frac{a(1-2\nu)}{1-\nu}\left[\frac{1}{r^2}\left[\int_{R_w}^{r}\Delta P(r,t)r\partial r - \Delta P(r,t)\right]\right] \tag{3.23}$$

$$\sigma_z = \sigma_v + \frac{E\alpha_m}{3(1-\nu)}\Delta T(r,t) + \frac{a(1-2\nu)}{1-\nu}\Delta P(r,t) \tag{3.24}$$

The effects of pore pressure and temperature difference of the rock on borehole rock stress can be obtained by analysing the above equation, then study their effects on safety mud density window by analysing stress variation of the borehole wall. Then the combined effect of such thermal stress and the original stress of the borehole wall may exceed the rock strength and cause the borehole to collapse or fracture when the circulation occurs.

3.5. Thermal effects results and discussion

3.5.1. Thermal effects Results

Here the partial differential equations was converted into ordinary differential equations which was solved using numerical method. Based on the established numerical method, the temperature difference between the borehole wall and formation during the mud circulation process was modelled, and the temperature changing into the formation during the drilling of a North Sea well is analysed, in a vertical well simulated with temperature difference of 50 ºC, being well temperature of 114ºC and formation temperature of 64ºC.

In order to analyse the effects of temperature changes on borehole stability, the rock mechanics parameters are taken from at 1589 m depth **(See table 4A for input data).**

Table 4A Input parameters used for modelling the Temperature distribution

Input Parameter	Unit	Value
1. Heat Diffusion in the Formation		
Density	kg/m3	2140
Thermal conductivity	W/m*K	1.5
Heat capacity	J/Kg*K	900
Heat diffusion constant	m2/s	7.78E-07
T well	deg	50
T Formation	deg	0
Rw	m	0.15
Dz	m	0.5
Dt	sec = 1 Day	86400
Diff_T		0.26

In the table; the heat diffusion constant is calculated by equation **3.1.1** while **Diff_T** (Temperature diffusivity) defines how the temperature diffuses. **Diff_T** = temperature diffusion constant * Dt/Dz^2**.**

This depth was selected as a representative depth for potential problems at high inclination based on field history, this data came from core measurements (Porosity, UCS, Friction

angle, bulk density, permeability, Young's modulus, Tensile strength, Poisson's ratio), and the remaining from the logs.

The effects are shown in **figure 17** and the results are as follow: (1) **figure 15** illustrates the temperature difference of 50 ºC will change over time and distance, dropping quickly to a lower level. With time, the temperature decreases, the range of temperature decrease is maximum at the borehole wall, and the range of temperature change towards the inside of the formation will decrease gradually. The reduction rate of the temperature is the highest at the beginning and decreases with time. The temperature will approach a certain constant value after some time. (2) The temperature continues to decrease so that after some times (10 days for example), the heat front at 1 meter will have temperatures around 11 degrees, comparing to previous situation (1 day) the heat front at 1 meter with temperature of almost zero; The temperature continues to decrease after 10 days, but at an even slower rate.

Over all it can be seen that the 50 degrees temperature will diffuse from the near-well region to r/Rw=30 into the formation in 20 days when it reaches reach the equilibrium (constant temperature of zero).

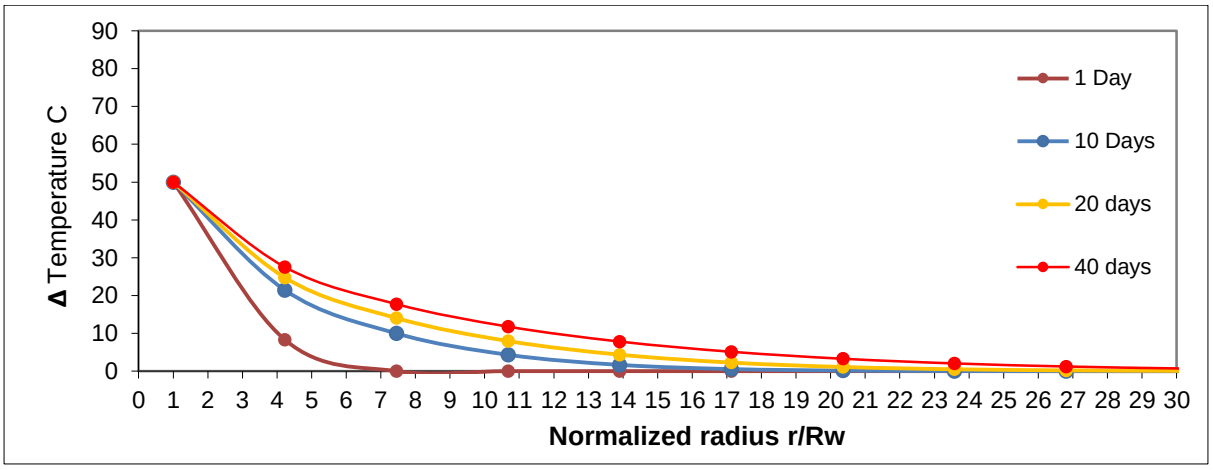

Figure 15 the temperature diffusion into the formation after several days. (Modified from Bauer 2014)

Figure 16 illustrates the pore pressure variation as result of temperature changes in the formation, and the input parameters used for the model are in **table 4B**. Assumption has to be made regarding Grain moduli, Viscosity, Bulk moduli of the fluid, drained Poisson ratio and Frame rock moduli; the parameter **dP/dT** is equal to term **c** in equation **3.4** its 0.4 MPa/deg value was resulted as assumption made for the above parameters for its calculation. The assumed values in the input parameters are for shales and allow the solution of **eq.3.4.2** which is an input to equation **3.4.** The undrained Poisson ratio was calculated from sonic data. The pressure diffusion constant is obtained from equation **3.3 Diff_P** (Pressure diffusivity) defines how the pressure diffuses. **Diff_P** = pressure diffusion constant * Dt/Dz^2. As stated early heating the wellbore will generate an induced pore pressure, which starts to build up

Table 4B Input parameters used for modelling the Pressure distribution

2. Pore pressure Diffusion	Units	Value
Fluid modulus	GPa	2.6
Porosity		0.4
Permeability	nDarcy	8
Viscosity	cp = [10-3 Pa sec]	1
Young's modulus	GPa	2.4
Poisson's ratio		0.44
Fluid modulus	Gpa	2.6
Grain modulus	GPa	37
Bulk modulus	GPa	7.38
Shear modulus	GPa	0.85
Biot alpha		0.98
Pressure diffusion constant	m2/sec	3.19E-09
P0	Mpa	0
Diff_P		0.01
dP/dT	Mpa/deg	0.4
Dz	m	0.5
Dt	sec = 1 Day	86400
Rw	m	0.15

first with the maximum induced pore pressure generated around the wellbore area and after it has reached its maximum as shown on the figure, for each period (1, 10, 20, 40 Days) it decrease with time and the pressure front location moves further away until the equilibrium is reached.

With time, around the borehole the rapid drainage of the rock will cause reduction in the pore pressure when compared to the initial time (20 MPa on Day One to almost 16 MPa after 10 Days), since the diffusion distance is shortest close to the borehole, and this will have a direct impact on the stress concentration at this point.

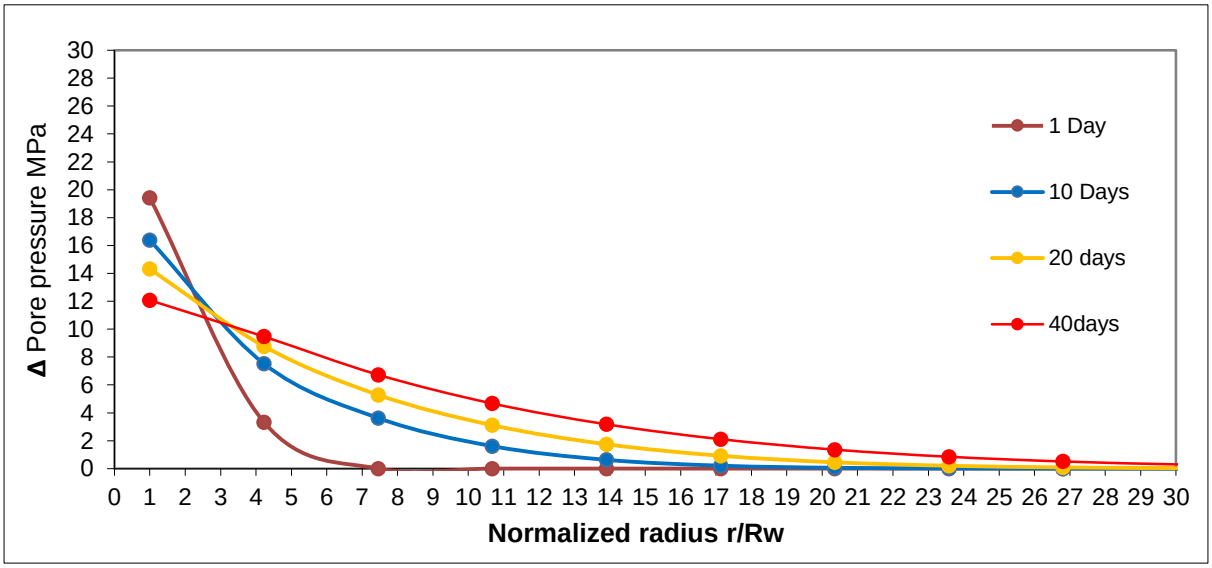

Figure 16 Induced pore pressure diffusion into the formation after several days. (Bauer 2014)

From the previous section we know that, circulation of the "cold / hot" mud into the well results in the stress alteration at the borehole wall due to the formation temperature changes, and the temperatures changes will result in direct thermally induced stress, as well as in transient pore pressure variations. **Fig 17** shows the stress induced into the formation as result of temperature changes, the thermally induce radial stresses at the borehole wall is equal to zero due to the fact that the borehole wall is a free surface, then the radial stress is equal to zero since there is no thermally induced stress at the borehole, but the maximum additional thermally induced radial stress occur at some distance away from the borehole wall. The maximum additional tangential stress and axial stress are at the borehole wall, and because the extent of the heated zone goes to few meters away from the borehole, thus the maximum thermally induced stress (tangential and axial) generated, decrease with time and their locations move further away from the borehole wall. From the figure it can be seen that increasing the temperature creates a high hoop stress (tangential and axial).

Further, the thermal stress is stacked with the pure mechanical stress near wellbore and finally, the effect of the thermal stress on the wellbore stability is analysed using the Mohr-Coulomb criterion for any drilling condition and any time.

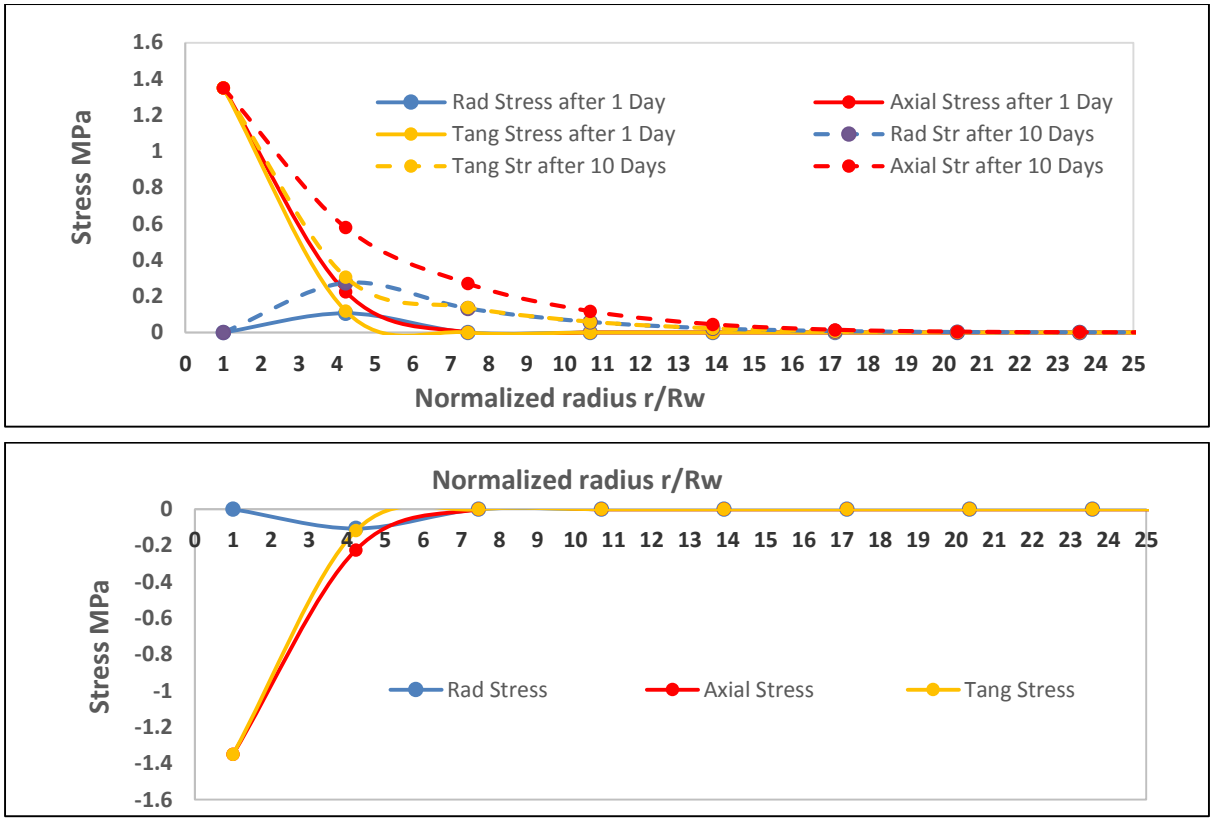

Figure 17 Thermal induced stress around the borehole wall predicted by numerical model for formation parameters as follow: E=2.4 GPa, Poisson Ratio=0.44, Thermal Expansion coefficient=1.89 10^{-5}, the formation temperature was 64 degrees and heated the formation 114 degrees. (Upper) increased temperature (Lower) reduced temperature.

At this point, only the heating of the well have been looked at and not the cooling, despite that the drilling mud is usually cooler than the rock formations. And the reasons are as follow:

As suggested by the field cases most instabilities are related to heating than cooling. Maury [1989] suggested that cooled drilling mud may enhance stability in an abnormally warm formation. The second reason is because at bellow certain depths, mud circulation also induces heating of the upper part of the open hole (Maury and Guenot, 1995). However the cooling of the formation will produce the opposite results than the heating as seen in the **lower fig 17** (reduces the tangential stress).

3.5.2. Thermal effects Discussion

By looking at the gamma ray and calliper log reading, easily seen that our well is comprised of shale and sand section. Chen and Ewy, 2005 provides the clue on how temperature affect the wellbore stability in both situations. In the shale section due to its low permeability, thermal diffusion is faster than hydraulic diffusion and the former can dominate the pore pressure and stress changes. The thermal effects were considered for both shales (660-885 m) and sand sections (1586-1950 m), for shales temperatures changes will result in direct thermally induced stress as well as in transient pore pressure variations. For sand section since the borehole wall was assumed to be impermeable then thermal diffusion effect will be the same as for shales section (Chen and Ewy, 2005), since the temperature distribution will remain the same and then the pore pressure will depend only on the temperature changes. However in the sand section due to its permeability factor the influence of temperature changes on the in situ pore pressure variation may be considered as negligible and the pore pressure variation may be considered as independent of temperature changes. In other words the pore pressure front moves much faster than the temperature front, or the localized

pore pressure has reached the equilibrium before the temperature changes (Chen and Ewy, 2005). Then, in case of high permeable conditions the effect of temperature changes on pore pressure variation is negligible and this occur because any thermally induced pore pressure variation is quickly dissipated by pressure diffusion (Chen and Ewy, 2005)

Increasing the temperature of the borehole wall, a compressive stress is applied on the borehole wall and the three principal's stresses (Hoop stress) around the borehole increase. The radial stresses at the borehole wall and at infinite distance should be equal to the well pressure and to the minimum horizontal stress respectively. The maximum additional tangential stress and axial stress are at the borehole wall, and away from the borehole it will be equal to minimum horizontal stress **fig (17).**

When the temperature at the borehole wall increases, the fracture pressure and collapse pressure will increase simultaneously (slightly decrease the fracturing mud weight), and thus, the safe mud window density becomes wider **fig 24**. When the temperature at the borehole wall decreases, the fracture pressure and collapse pressure will decrease simultaneously (slightly increase the fracturing mud weight), and, thus, the safe mud density window becomes narrower fig **24A.** This is because cooling the wellbore decrease both the pore pressure and tangential stress near the borehole wall but the amount of pore pressure reduction is less than reduction in the tangential stress at specific time and radial location. Therefore the effective tangential stress may increase even though the wellbore is cooled.

If the temperature at the borehole wall decreases, a tensile stress is applied on the borehole wall and the three principal's stresses around the borehole decrease, causing a reduction in the near-wellbore stress concentration, thus preventing the stresses in the rock from reaching their limiting strength. This acts as a strengthening of the borehole with respect to collapse (McLellan, 1994a; Maury and Guenot, 1995). Deliberate cooling of the mud can be a practical approach to mitigate stability problems. This was applied with success in the field (Guenot and Santarelli, 1989; Maury and Guenot, 1995).

However, since cooling reduces the tangential stress, it not only reduces the risk of shear failure, but it also promotes fracturing, and may hence be a destabilizing factor with respect to lost circulation problems, since the extent of the cold zone is however limited, and this may limit the growth of the fracture. Shear failure will occur when the Mohr's circle, which is constituted by the maximum and minimum effective principal stress on the borehole wall, exceeds the failure strength.

Thus, cooling reduces the pore pressure, which in general improves stability. Rock properties (strength, stiffness) may be altered as a result of temperature changes. Normally rock strength and stiffness will increase with decreasing temperature; the thermal effect is proportional to rock stiffness, which means that it is more significant in hard than soft rocks. Finally, mud properties are also temperature dependent: Cooling the mud will lead to a slight mud density increase due to thermal contraction, again resulting in improvement of stability with respect to borehole collapse conditions.

3.5.3. Thermal effects Conclusion.

Formation contraction will be generated as the temperature decreases, a tensile stress is applied on the borehole wall, and the fracture pressure and collapse pressure will decrease simultaneously. The drilling fluid density should be decreased properly in order to prevent drilling fluid leakage. Temperature increases will cause formation expansion and a compressive stress is applied on the borehole wall, and the fracture pressure and collapse pressure will increase simultaneously, and thus, increasing temperature will widen the safe mud density window, while decreasing temperature will narrow the safe mud density window. Generally heating the wellbore decrease stability by increasing the pore pressure and tangential stress and rise the fracturing and collapse mud weight.

As it has been remarked that temperature changes has a great impact on stress variation, and eventually the combined effect of such induced thermal stress and the original stress at

the borehole wall **(figure 28)** may exceed the rock strength and cause the borehole to collapse or fracture (Fjaer, 2008) when the circulation occurs as well as if the tangential stresses has to become lower than the pore pressure the well will fail.

4. Wellbore stability Interpretation, Results and Discussion

4.1. Interpretation

Complete data was supplied by Statoil SA and are available from a north sea well for this analysis. Hence all calculations were performed for this well. Since no core data was available from the well empirical correlations were performed.

The wellbore stability modelling was performed with a PC-based code described by Fjær et al. (2002). Overall, the code is based on a combination of well-established analytical solutions, specially developed approximate solutions, and numerical solutions. The strong point about the PSI is the possibility to study in details the stability of a well at any given depth.

Casing depth selection

The sonic velocities have supported the choice of casing depths a schematic casing design is illustrated by **the fig 18**. For a given lithology, sonic velocities usually depends on porosity: the greater the porosity the lower the velocities. In normally compacted sediments compaction increase with depth, porosity in turns decrease with depth and so the velocities of sonic waves travelling through the formation generally increase with depth. Deviations from this trend can often be attributed to layers of sediments that have not compacted signalling abnormally high pressure also called overpressure. In summary abnormally pressured formations can often be identified using sonic velocities, this information allows the casing shoe to be placed significantly closer to the overpressure zone to improve the safety and drilling efficiency of subsequent borehole section. This will be later confirmed and validated by the Output from the wellbore stability model.

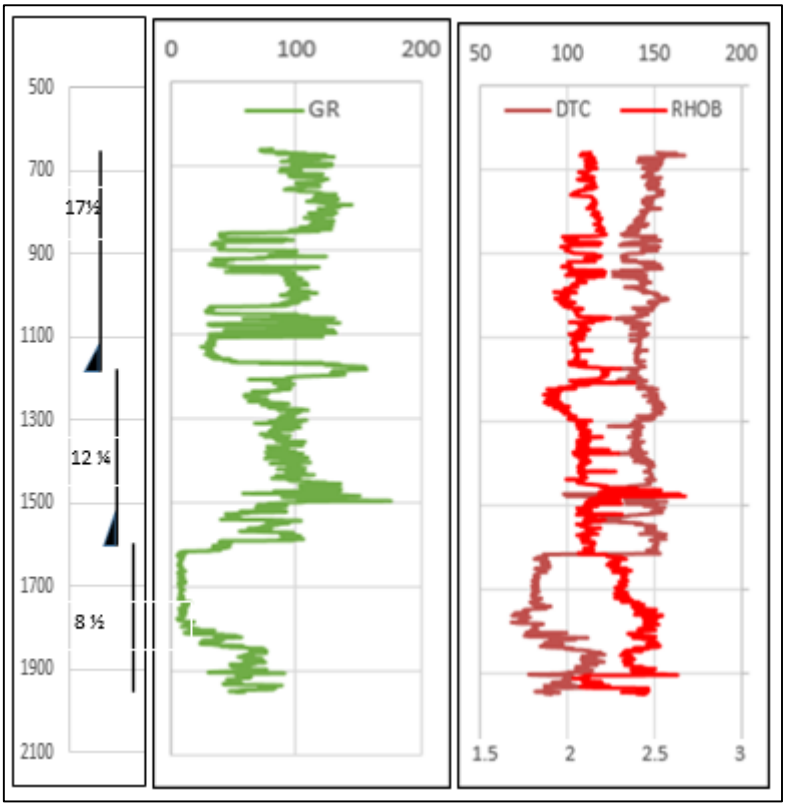

Figure 18 Casing design based on sonic velocity

Pore pressure

The Sonic velocity increases with increasing depth and increases with increasing density **Fig 18.** The sonic velocity is clearly indicating the pattern of change in pore pressure**.**

From the calculated normal compaction profile, over-pressured zones are spotted from depth 1630-1950 meters (Total depth) as seen in **Fig. 10.**

The hydrostatic, fluid pressure gradient (Normal pore pressure) cannot exceed the pressure gradient of the total overburden stress. Thus, any reservoir with a normal pore pressure gradient between 0.465 and 1.0 Psi/ft (1.5255 and 3.2808 Psi/m) is considered to have an abnormally high pressure (Chilingar, 2002).

The predicted pore pressure can be observed in detail in **figure 10,** which is plotted with normal pore pressure, mud density and overburden pressure. The pore pressure is equal to normal pore pressure value on zones where the formations were compacted normally **fig 10 centre**. On the other hand, in the zone where overpressure is observed, pore pressure is higher than normal pore pressure but lower or comparable to the mud weight. Pore pressure itself will not extend higher than the total overburden pressure because pore pressure and rock effective pressure will add up to the value of the overburden stress.

In case that the pore pressure is significantly higher than the mud weight one may expect a kick. But a kick or blowout during drilling does not happen merely because the pore pressure is higher than the mud weight. It depends on the rock mechanical properties and permeability, and might cancel out the effects of each other. Rock with higher permeability will have a good mudcake built during drilling, hence a slight increase of pressure differential during drilling will not cause formation fluid to enter the wellbore and vice versa.

Rock mechanical properties

Due to the content of shale, sonic compressional waves will travel slower compared to the sonic velocity in stiffer rock. This resulted in higher compressional transit time and even higher shear transit time, which are the components required for the Poisson's ratio calculation, as seen in the shaly section with higher Poisson's ratio. However, Young's modulus is lower on shaly formation.

The rock strength value results are presented on **figure 12**. Horsrud (2001) rock strength is depended on the sonic compressional travel time value as shown on **equation 2.61** above. On the other hand, the Horsrud calculated Young module and shear module resulted in slightly lower values compared to the values calculated from sonic velocities. Both results has lower value for the shaly above the section and has higher value for less shaly section below.

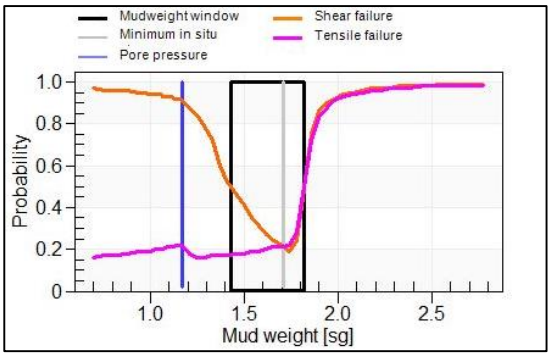

Figure 19 Modelled stable MW (Probability of failure) at 1589m one day after drilling using physical criteria. The stable MW as defined by 0.5 probability for failure is indicated in black line Minimum and Maximum). Note that the maximum MW is limited by the minimum horizontal stress (1.82sg)

4.2. Wellbore Stability Results

Wellbore stability analysis was carried out in the 17 ½, 12 ¼ and 8 ½ in hole sections although the 17 17 ½ in section was first drilled as 12 ¼ for data collection reasons and then opened up to 17 ½, drilled vertically from 657-1601m to 1601-1950m TVD respectively, based on the integrated methodology described above, wellbore stability analysis for this north sea well was conducted using Mohr-Coulomb failure criteria.

A detailed investigation was carried out and well-logging data was analysed to diagnose the troubles encountered during the drilling. Since this is a tight well the only data available is sonic data. The integration of all the data made the diagnostic process slower and time consuming. The aims of this diagnosis are to identify the formation and lithology that may complicate drilling operations and the non-productive time (NPT) due to the wellbore stability if any, and can be eliminated.

The rock mechanical parameters have been calculated and integrated to the overburden stress to perform the wellbore stability analysis. The analysis was carried out in PSI (SINTEF Software) at 5 different depths **(See section 4.1)** for each hole section, and the input parameters are in **table 5** giving corresponding recommended mud weight values as output as well as the probabilities estimation for failures, collapse, mud loss and stuck pipes. PSI estimates the mud weight ranges where the probabilities for collapse and mud loss are both less than 0.5.

Table 5 Input parameter used in PSI for WBS modelling

Depth_mTVD	Depth_mMD	CALI_in	DT_µs/ft	DTS_µs/ft	GR_API	RHOB_sg	VSH_-	E Gpa	UCS Mpa	Poisson	Sv sg	Sh sg	PP sg	Inc	Azi
688	688	12.979	154.162	430.914	104.477	2.104	0.845	3.003	5.6738	0.4226	1.84	1.55	1.07	0	0
780	780	12.862	147.764	387.163	127.271	2.149	0.851	3.768	6.4241	0.4147	1.87	1.58	1.08	0	0
833	833	13.245	145.344	366.371	128.511	2.18	0.99	4.244	6.7426	0.4066	1.89	1.6	1.09	0	0
1279	1279	13.018	152.011	375.454	108.746	2.005	0.99	3.705	5.9123	0.4019	1.95	1.68	1.15	0	0
1589	1589	12.867	152.628	483.188	96.07	2.137	0.99	2.456	5.8426	0.4445	1.97	1.71	1.17	0	0
1645	1645	8.704	85.241	152.749	6.274	2.287	0	23.2	32.1998	0.2738	1.99	1.75	1.25	0	0
1700	1700	8.343	80.689	148.001	8.819	2.295	0.001	25.084	37.8171	0.2885	2	1.75	1.25	0	0
1825	1825	8.434	94.821	213.413	42.118	2.481	0.568	13.937	23.568	0.377	2.03	1.77	1.26	0	0
1850	1850	8.466	119.568	289.347	75.546	2.321	0.99	7.196	11.9465	0.397	2.03	1.77	1.26	0	0
1900	1900	8.425	97.39	205.894	48.957	2.47	0.623	14.678	21.7925	0.3558	2.04	1.78	1.26	0	0

On this basis for a vertical well drilled with OBM the results predicted mud density window in terms of maximum and minimum mud density as in the **fig 19** the 0.5 probability of shear failure for the mud density of 1.43sg using physical failure criteria. Here physical failure criteria is estimated on the basis of the local stress pore pressure and selected shear failure criteria (Mohr Coulomb).

The **Fig 20** is the prognosis pressure model for the well, shows the mud density window (lower and upper limit) for effective drilling. However the maximum allowed mud density for effective drilling is limited by the minimum horizontal stress in case fractures are present.in this figure the difference in the pore pressure reading values between PSI and the numerical calculations (using equations **2.49** for $\mathbf{S_v}$, **2.50** for **PP** and **2.53** for $\mathbf{S_h}$) might be most probably due to the assumption made for DTC_n (Eaton 1975) when calculating pore pressure since PSI uses different approach.

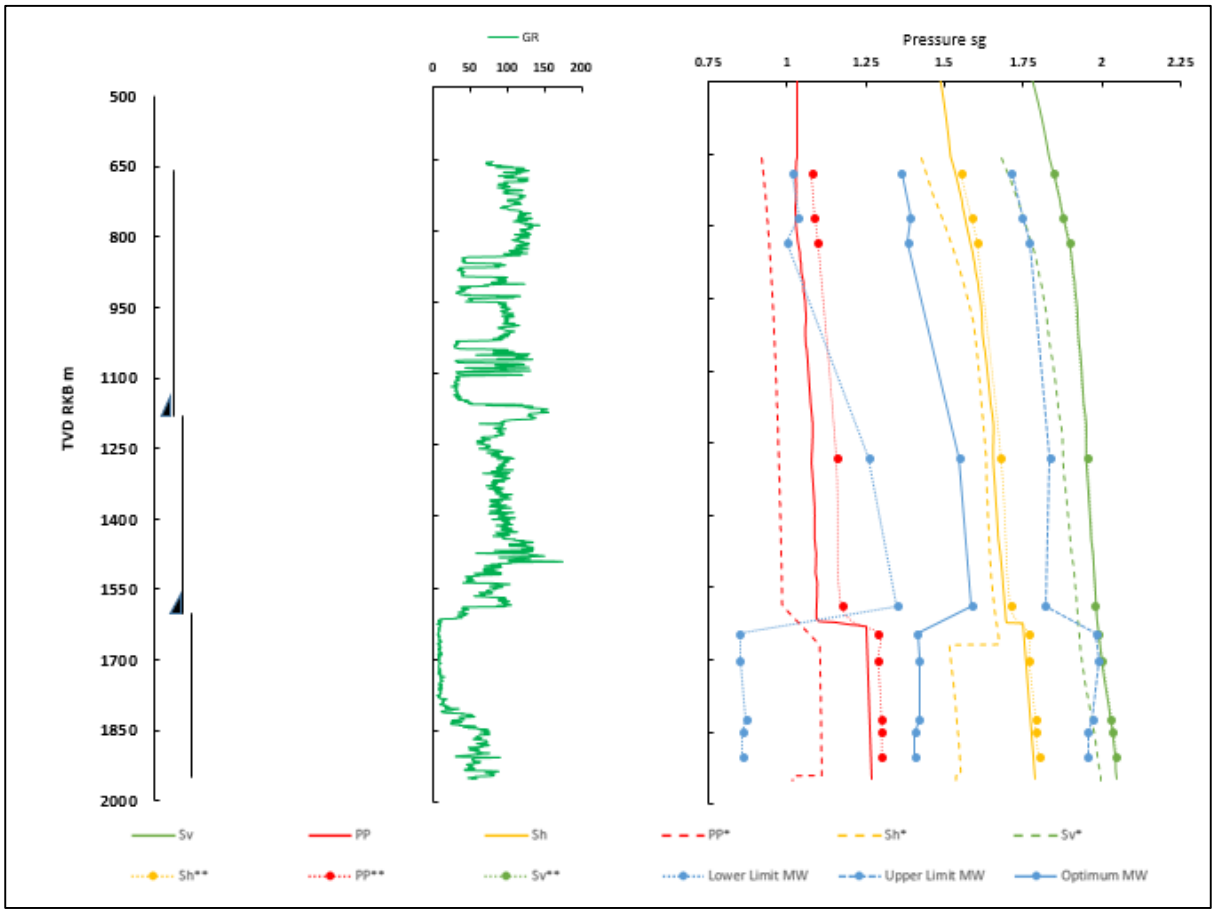

*Figure 20 Prognosis of the pressure model for the well. The plot is showing the predicted stable mud density window one day after drilling using 1.43 – 1.82sg and average of them. The red curve is pore pressure, the yellow minimum horizontal stress while the green is overburden stress and the blue is the MW. The * are estimated from offset well while the ** are from PSI and finally the numerically calculated.*

Fig 21 shows the predicted probability for failure when using the upper, lower and optimum (being the average) mud density. Here the probability for failure is calculated on the basis of the physical failure criteria. The figure **21** shows that the model predict a stable drilling condition with probability for failure of 0.5 or less when using the average mud density (Optimum). And the failure probability with optimum mud weight show remarkable low values for the entire depth interval (657-1950).

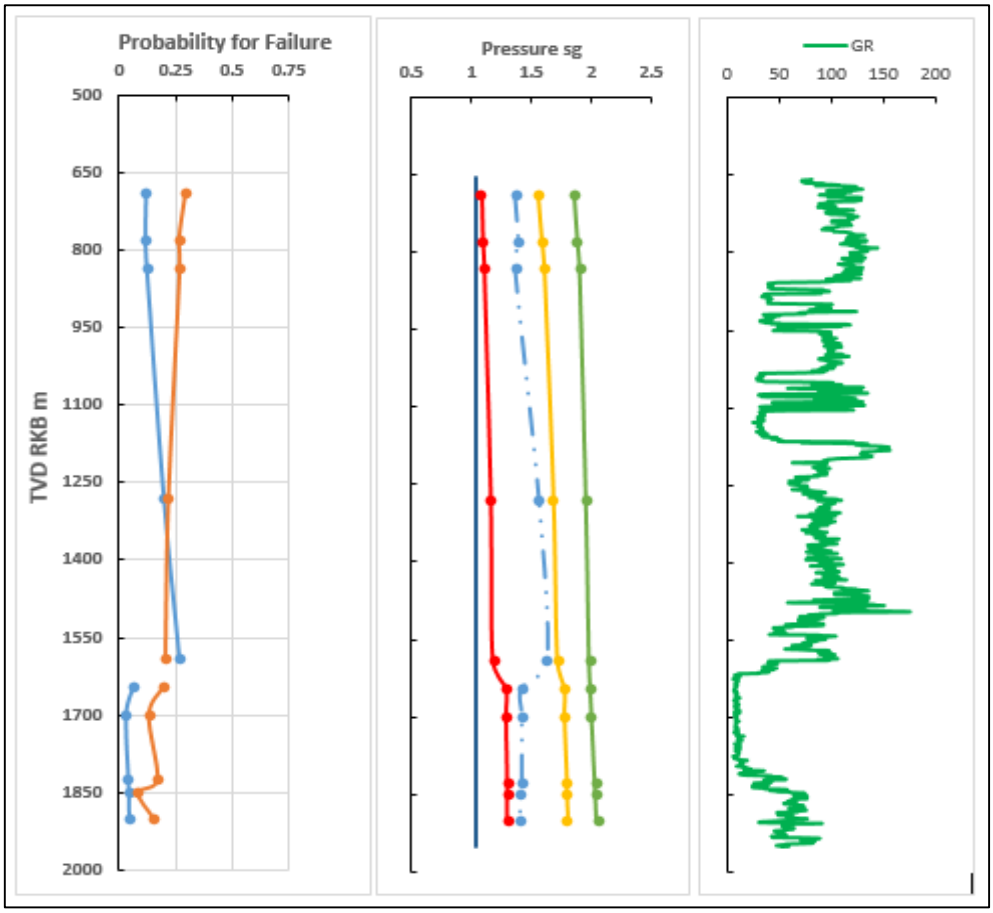

Figure 21 Plot showing the probability for Shear and Tensile Failure (Left) when using average MW of 1.62 sg for the upper part (12 ¼ in section) and 1.4 sg for the lower part (8 ½ in section). The orange line represent the probability for tensile failure and the blue line shear failure. The centre plot shows the pressure gradient and the average MW represented by the dash dot dot blue line and finally GR plot.

As illustrated by the **figure 21** the window between the pore pressure and the minimum horizontal stress is the 'safe' (Optimum) mud window. If the mud weight is allowed to fall below the pore pressure borehole wall break out can occur. Break out refers to additional formation or caving invading the drilled wellbore that requires removal during the drilling and circulating periods. If the mud weights exceeds the minimum horizontal stress fracturing of the formation can be expected. In case where the formation is naturally fractured then it's wise to stay below the minimum horizontal stress otherwise drilling fluid losses will be experienced.

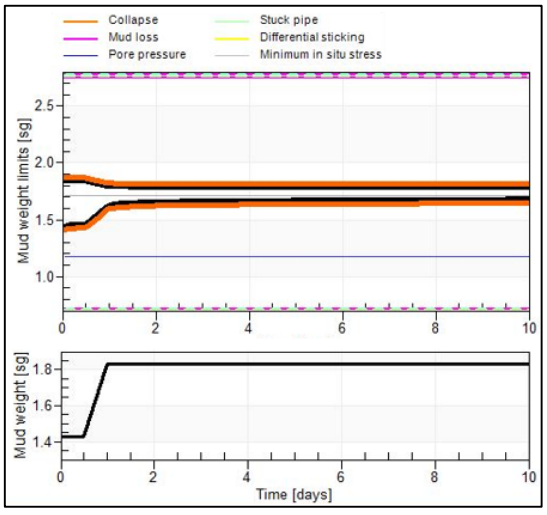

Figure 22 Time dependence effect. MW window after 0.5 days when the pressure in the well change by 0.4sg. The orange line is the collapse, blue the pore pressure and the grey the horizontal in situ stress.

Generally the stable mud density window show no time dependence here since oil based mud were used such that the chemical fluid-shale interaction is negligible, but if the pressure in the well changes then there will be time dependence effect after some time since the well has been drilled, this is illustrated in the **fig 22** Where the well is stable for the first few hours

after drilling but not after the pressure in the changes 0.4sg for the next 12 hours. This situation can still occur at approximately few meters below casing shoe after the casing has been set. The main time dependence here is the reduction in the maximum allowed mud density associated with tensile failure around the borehole. However the stable mud density window shrinks completely after 24 hours after drilling, the **figure 23** shows how mud windows close with time. The **fig 23A** illustrate the probability for borehole failure if the well pressure is increased by 0.4sg for some period of time and it show that after 12 hours the probability for failure by collapse is over 0.5 while for caving is 0.5. The final conclusion is that once the well pressure is changed there is no significant increase in the probability of failure with time for the changed well pressure, but this will depend on the capillary pressure for the drilling fluid (OBM, the oil based mud are not pure oils, so some water phase may be expected).

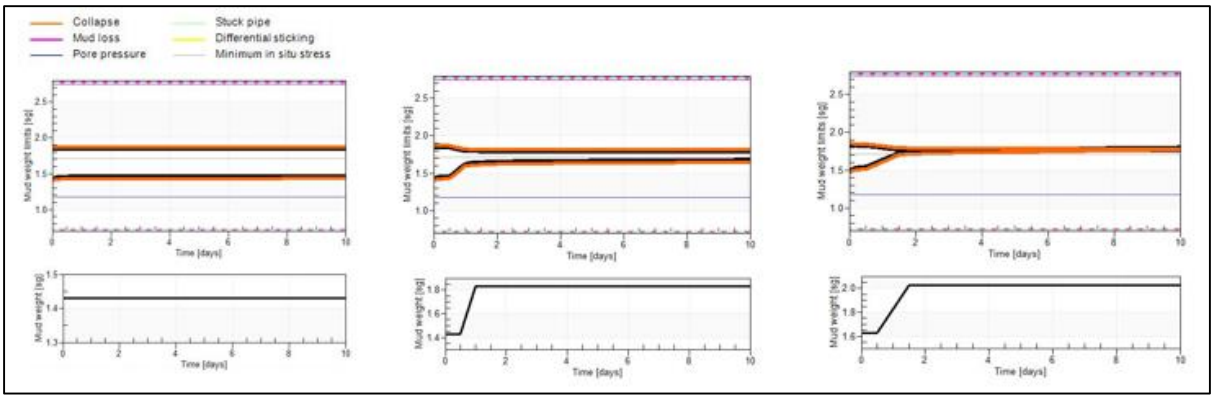

Figure 23 Time dependent effect. Different figures correspond to different time after drilling (3, 12 and 24 Hours) after the well pressure has changed by 0.4sg. Using 1.43sg on the first scenario and after the increasing the well pressure by 0.4sg during 12 and 24 hours.

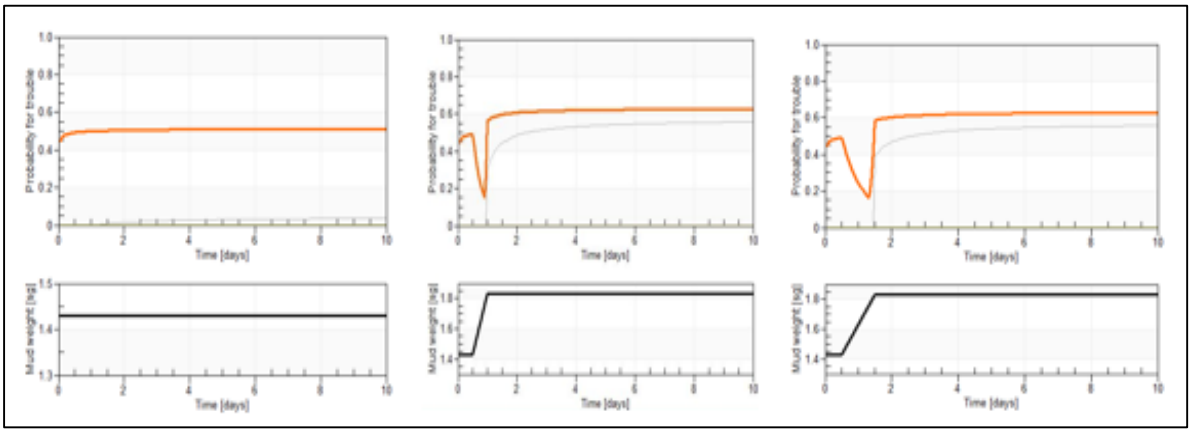

Figure 23A Probability for failure versus time since drilled when the well pressure is changed by 0.4sg during 12 and 24 hours the stable MW is 1.43sg. The orange curve is the probability for collapse and the grey one is for cavings. (Centre) for the 12 hours and (right) for 24 hours the left one is for the first few hours after drilling.

The stable mud window is also sensitive to temperature changes **fig 24**. The well is stable for the first few hours after drilling but if the temperature difference at the borehole wall increase to 50 degrees for the next 24 hours then the mud density window starts to shrink and shrinks completely after 5 days after drilling. Here as well the main time dependence here is the reduction in the maximum allowed mud density associated with tensile failure around the borehole.

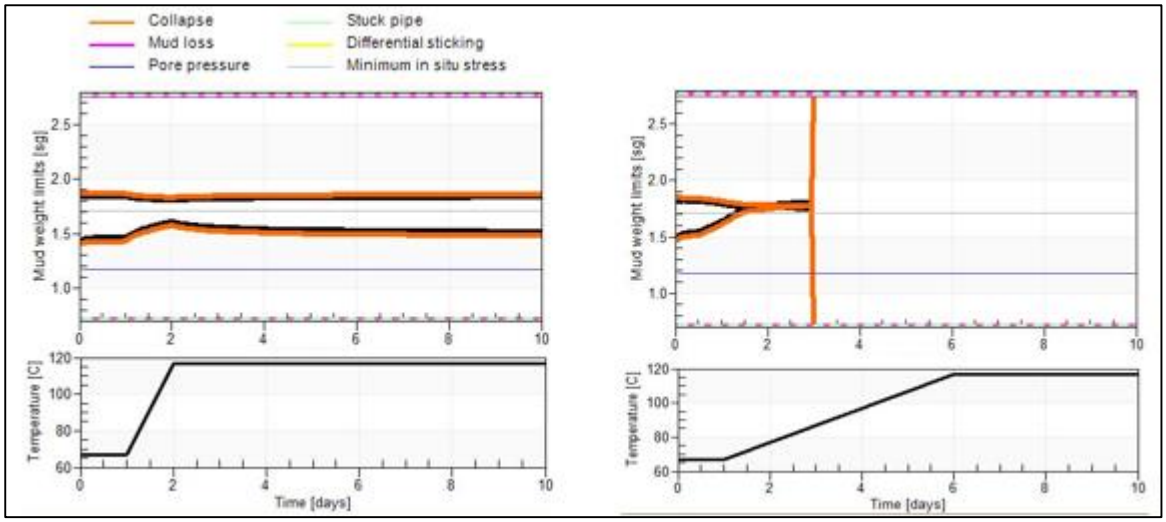

Figure 24 Time dependent effect. Different figures correspond to different time after drilling (1, 5 days) after the well temperature has increased by 50 degrees. Using 1.43sg.

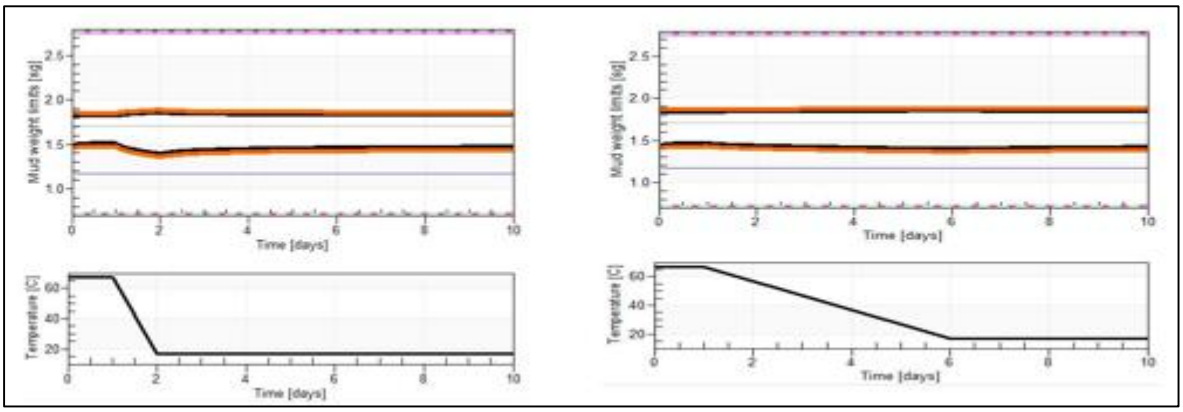

Figure 24A Time dependent effect. Different figures correspond to different time after drilling (1, 5 days) after the well temperature has decreased by 50 degrees. Using 1.43sg.

The **fig 24A** shows the behaviour of the mud weight window if the temperature is reduced. The effect here is opposite than when the mud weight is increased, resulting in increasing the mud weight window therefore its probability reduce as seen in the **fig 24B (Right)** while the probability for increase temperature **24B (left)** is very high since heating the wellbore is favourable to instability. Here this probability will decrease with time since after sometime the temperature will reach the equilibrium, and will be inverse when cooling (reducing temperature) with time the probability will increase.

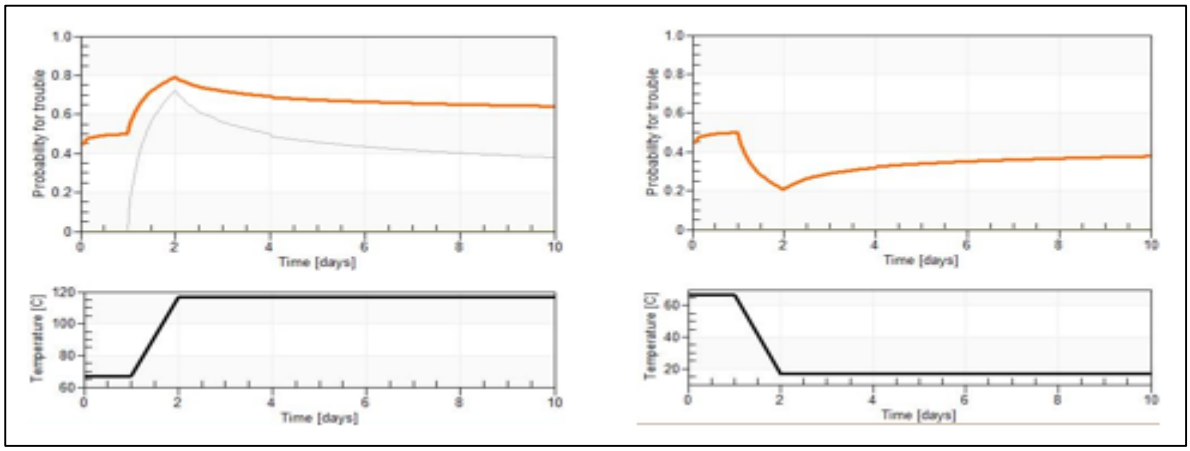

Figure 24B Probability for failure versus time since drilled when the well temperature is increased by 50 degrees during 1 day and 5 days the stable MW is 1.43sg. The orange curve is the probability for collapse and the grey one is for cavings. (Left) when temperature increase and (right) temperature decrease.

Fig 25 shows the stress around the borehole during the situation when the drilling fluid is in balance with the pore pressure. The stresses and pore pressure remains constant over the time. With those recommended (Optimum) mud weights, the wellbore stress distribution analysis has been done and the magnitude of tangential stress and the radial stress distribution have been shown in the **fig 25**. In the figure we see that the tangential stress around the borehole is higher compared to the radial stress and the former start to decrease while the late increase until get to the same value which is the far field horizontal stress.

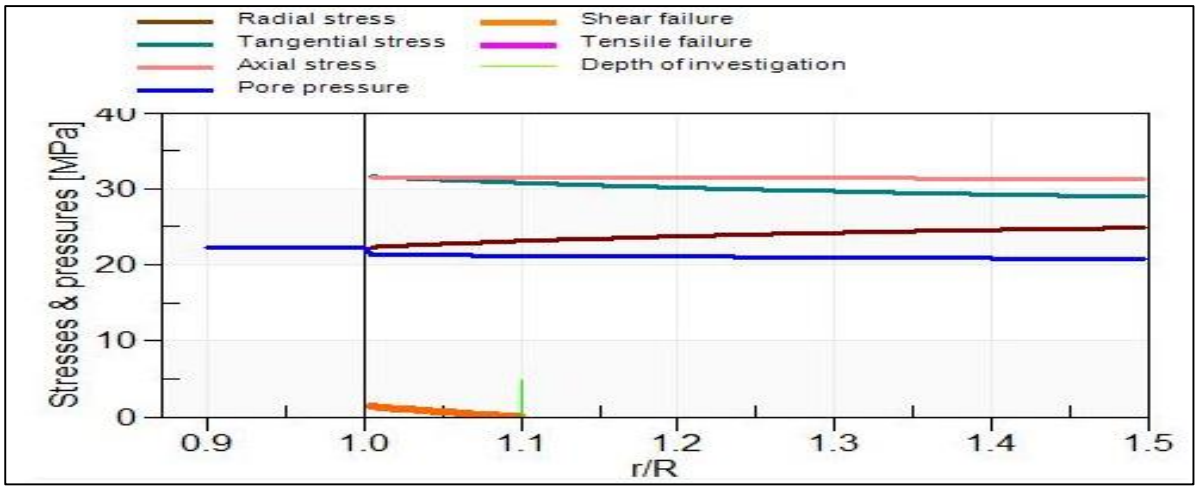

Figure 25 Stress distribution around the borehole when the drilling fluid is in balance with the pore pressure. Here the minimum allowed mud weight was used. The green line (Depth of investigation) is where PSI is looking for instability, and is taken to be 0.1R.

4.2.1. Borehole Failure Mechanism

When the formation rock is subjected to sufficient large stress a failure of any kind may occur. Failure criteria define the limit of deformation before the rock fails due to the induced stresses.

The borehole may fail because of too low or too high well pressure. Failure may occur during drilling or sometime after drilling. Here we will look at the shear failure mode of a borehole. It may take place because the Mohr-Coulomb criterion (**Eq. (2.25)**) is violated. Since the shear stress is a maximum at the borehole wall, this is where failure will be initiated.

Taking into account different possibilities for shear failure, depending on which of the principal stress components at the borehole wall are largest and smallest. Using the data in the **table 6,** the well pressure required to fulfil the Mohr-Coulomb criterion in this case can be calculated from **equation 2.26.** But since it's not possible to tell in advance which of the cases it would be relevant, it was necessary to calculate the critical well pressure at depth of 1589m from one of the 2 equations **(2.26 or 2.27)**, then calculating the corresponding borehole stresses **equations 2.7-2.9** to see if the initial assumption **(a or b)** is fulfilled. It was found out that this correspond to case **(a)** $\sigma_\theta > \sigma_v > \sigma_r$.

Parameter	Value
Cohesion (S0)	2.26
Tensile Strength	0.5
Friction Angle (φ)	14
Tang (φ)	0.24
Failure Angle (β)	52
Tang (β)	1.27
Tan^2 (β)	1.63
Sh	26.64
Sv	30.82

Table 6 Input parameters for minimum well pressure calculation as well as for Mohr Coulomb parameters calculation.

The **equation 2.26** gives the lower limit to the mud weight or well pressure. Since the calculated well pressure is

higher than the pore pressure, thus it represents the minimum permitted well pressure or mud weight.

We have seen that there is a mud weight window, which the borehole can be drilled in a stable manner. The window also changes with time, if any of the borehole conditions change and it is also found in the field that drilling instabilities occurs sometime after drilling.

On the other hand, the minimum horizontal stress should not be exceeded if fractures are present, and here since there is no information about the presence on natural fracture then the safest choice for the maximum well pressure is the magnitude of Sh. But if the absence of fracture is known then the maximum well pressure is given by **equation 2.33.**

Based on the Mohr-Coulomb diagram for stress was constructed for 1589m depth as illustrated in the **figure 26**, the diagram shows the stability of the borehole with respect to possible shear failure, since the Mohr circle lies below the failure envelope.

The figure reflect the initial stress state at the borehole wall and the effects of pore pressure change, if the exact fluid composition in the prognosed reservoirs are not known, then the presence of fluid lighter than water will cause additional pressure at the top of the structure (reservoir) resulting in overpressure due to density difference. The pore pressure increase will result in decreasing the effective stress which in turn will increase the probability for borehole failure in shear, moving the stress state close to the shear failure. In the **Fig.26**, the Mohr circle is shifting to the left as result of the pore pressure increasing. But as result of temperature changes the total stresses (the tangential and vertical total stresses) change as well, which result in changing of the radius of the Mohr circle, although not well clear in the figure.

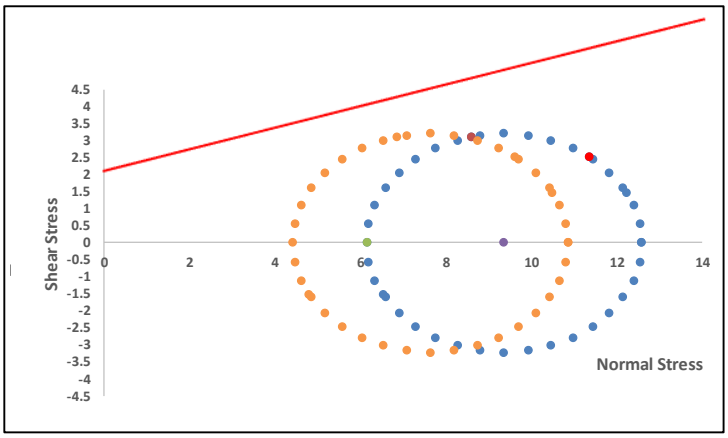

Figure 26 Mohr circle plot showing schematically the initial stress state at the borehole wall (Blue) and the effects of pore pressure change (increase) in orange. Here the effective stress law was used. The well pressure was 22.42 MPa and the rest of input parameter found in the table above.

4.3. Wellbore Stability Discussion

Typically, the magnitudes of the in-situ horizontal stresses and their difference from the overburden stress magnitude were addressed in wellbore-stability analyses using numerical models **(**See section **2.4.2** in chapter **2).** However, the physic and chemical interaction of formation and the drilling fluid, as well as with the formation temperature alterations induced during drilling also have significant impact on the net stress concentrations at the wellbore wall. Numerically was considered that the formation behaves linearly elastic, then the largest stress differences occur at the borehole wall, hence rock failure is expected to initiate there, while PSI use the same assumption but calculate the failure probability at some distance away from the borehole wall.

No significant wellbore-stability related issues were encountered during drilling of this well and not even spotted in the model, and analysing the data, it is assumed that the reasons for absence of any wellbore stability challenges while drilling this well, are the lithology and low inclination.

It is important to notice that hole issues, such as overpulls, torque, sloughing and bit balling may occur / increase, in the intervals that are represented by shale (Low GR in the log).

However, these shale dominated intervals are not thick enough; therefore shale sloughing may not be an issue here. The calliper data in **fig.10** confirms by reading lower than the bit size that we may have possible wellbore sloughing.

Overall, the sections needs to be checked for clay mineralogy. There is a high possibility that the clay in this horizon is less reactive or potassium/uranium enriched, which can be a reason for the absence of wellbore-stability issues at the drilling stage. But, since the shaly formation thickness at certain depth are only few meters, there won't be any significant wellbore-stability problems except for some probably overpulls.

Even though no problems were encountered at this well, while drilling, overgauge or possible washouts shown in **fig.10** suggest that this formation could contribute to the hole-cleaning issues during drilling. A close look at the sections of wide wellbore shape as per the calliper, indicates that the overgauge occur in the shale sections, some minor overgauge also occur in the sand sections. The shale section with significantly lower UCS values, could explain one of the causes for major overgauge which might be possible caving.

Within the sand section the large window between pore pressure and minimum horizontal stress trend represent additional challenge as the mud weight required for borehole stability is significantly higher than the calculated pore pressure, this could potentially lead to differential sticking as a result of overbalance in the wellbore. Differential sticking may occur if high permeability, mud cake formed and the well pressure is larger than the pore pressure.

The mud weight utilized must also take into account the pressure drop in the annulus above the point being considered and is referred to as ECD. The actual mud weight is adjusted to account for expected ECD so that minimum stress is not exceeded during drilling and circulating. If the ECD exceed the minimum horizontal stress losses are likely to occur. It is possible where the margin is not exceeded significantly for the leaked off fluid to be returned to the wellbore when the ECD drops below the minimum horizontal stress.

If the well pressure is allowed to fall below the pore pressure and in presence of damaged rock, these may cave in and the conditions for failure are likely to be fulfilled, leading to a continuous production of cavings for the newly exposed rock until the well collapse. If the well pressure is larger than minimum horizontal stress the mud may propagate into the rock and creating hydraulic fracture resulting in mud loss.

The time-dependent nature of the stress and pore pressure distributions influenced by temperature, manifests as time-dependent wellbore stability. Here time-dependency was observed in the failure analysis, in estimations of critical regions around the wellbore. The time effect implies formation weakens or strength due to continuing increase or decrease of temperature or pressure after some period of the formation-fluid contact. The presence of shale at around 750-850m could trigger and accelerate the formation-failure process due to due to continuing temperature oscillation since the thermal effects is the repeated cycle effects (alternate cooling and re-heating) during the drilling process. Then the wellbore may be subjected to the fatigue failure especially in shale, as the thermal effect is associated with low permeability of the shale. The conclusion is that once the well temperature is changed the probability for instability will increase at the beginning and for some time and will decrease with time since after sometime the temperature equilibrates with surroundings over time, so recovering its initial stability state.

As stated, the temperature changes has a great impact on stress variation, and eventually the combined effect of such induced thermal stress and the original stress at the borehole may change **(figure 28)** and cause the borehole to fail or if the tangential stresses has to become lower than the pore pressure the well will fail.

Taking into account the thermal effects on WBS, the stress around the borehole wall must be evaluated accounting the pre-existing stresses, a detailed evaluation of the stress showed that heating or cooling borehole walls could be responsible for various instabilities.

Since cooling reduces the tangential stress, it not only reduces the risk of shear failure, but it also promotes fracturing, The fractures created by the cooling effect are susceptible to spalling as consequence of wellbore pressure penetration into this fractures, where this occurs the fractured blocks are no longer subjected to the mud overbalance pressure and the destabilised blocks can cave into the wellbore as result of swabbing pressure.

Another consequence of fluid penetration in the fracture network is that the normal effective stress on the joints are much smaller and that the joint openings become much larger than when the cake is perfectly impermeable. Santarelli et al, (1992). Deliberate cooling of the mud can therefore be a practical approach to mitigate stability problems. This was applied with success in the field (Guenot and Santarelli, 1989; Maury and Guenot, 1995).

4.3.1. Comparison between PSI and Numerical model results

The comparison between these two analyses does not occur in the same level when the aim is the accuracy and solve the thermal effects issues since most of the tools for wellbore stability analyses has no feature for thermal analyses problem, thou, PSI has this feature incorporated, but is based on the assumption that the wellbore is permeable until the mud cake has been formed, and another assumption is that temperature changes suddenly and remain constant after that, also taking into account the initial state condition at the borehole and far field stress, whereas doing it numerically which consists in a huge calculation sheet with wide possibilities, thing that has allowed to perform the thermal effect analyses taking into account linear elasticity theory plus the factor that the temperature in fact vary after sometime (gradual process), and getting pretty good match between the two results but with differences on the assumptions and processes which are pronounced.

Numerically it was done step by step and the focus was to provide the solution to the diffusion problem (thermal and hydraulic) in general and in particular giving solution to thermal effects on stresses across the direction of changing temperature gradient, and the results as well as the methodology is accurate and easily built. Therefore, PSI shows the values of the solutions fluently, without taking care of previous effects and which factor has a great contribution to the results.

One of the main differences of these results is the time needed to describe and solve the problems. PSI does not need a lot of specifications in all the areas, just using the wide range of options for input and output the tool offers. Thus, the time the user spends in every step is insignificant compared with the numerical model, which the user have to set the formulas and conditions.

The thermal stress contribution on WBS may be very significant. And to illustrate the consequences of thermal effects for wellbore stability the model result from PSI and numerical model results can be compared and its strength and shortcoming evidenced.

The **fig 27** shows the stress around the borehole in the situation when the drilling fluid is in balance with the pore pressure and temperature, the **upper** figure is from numerical model (the axial, tangential and radial stress were calculated using **equations 2.5-2.6**) while the **lower** one is from PSI. As remarked above PSI model uses assumption that wellbore is permeable until the mud cake has been formed, the reason why in the **figure 27 (lower)** the borehole and formation are in communication as we can see that the well pressure is influencing the pore pressure and the pressure decrease from left to right; while in the **upper figure** there is no influence of the well pressure in the pore pressure, and the stresses and pore pressure remains constant over the time. **Fig 28 (Lower)** shows the stress around the borehole after the temperature has increased 50 degrees.

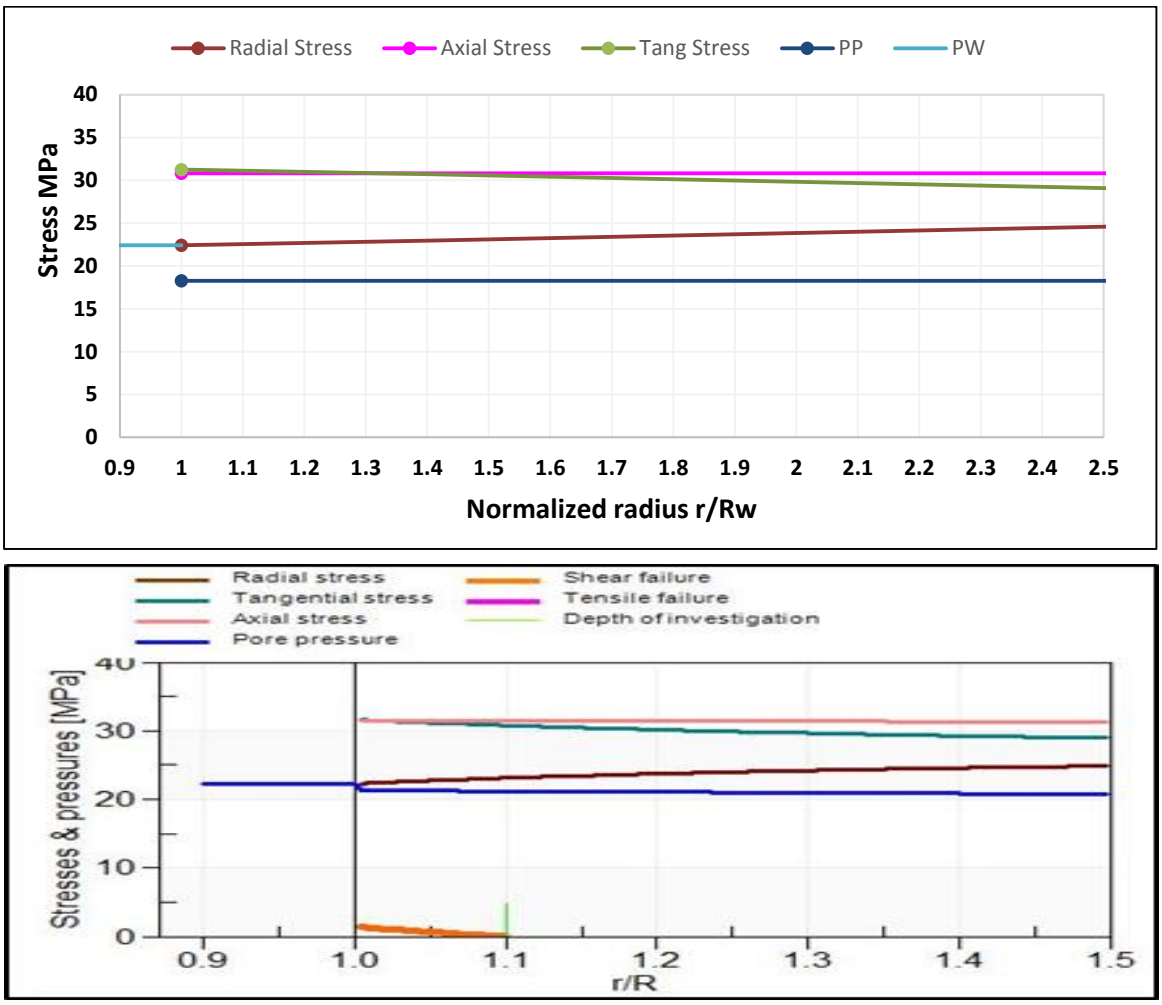

Figure 27 Initial stress distribution around the borehole when the drilling fluid is in balance with the pore pressure. Here the minimum allowed mud weight was used. The green line (Depth of investigation) is where PSI is looking for instability, and is taken to be 0.1R. And the input parameters are: Sv=30.82MPa, Sh=26.64MPa, Pw=22.42MPa and PP=18.27MPa

The **fig 28 (Upper)** shows the calculations results from the numerical model using mostly the same input as the software but different assumption. The figures shows the effect of temperature on WBS but the difference between **Lower** and **Upper** plot in the **figure 28** is once again the fact that in the software the borehole is assumed to be permeable, while the numerical ones always consider the borehole as impermeable. For PSI the main effect of the change in temperature is however seen at some distance at the borehole and not at the borehole wall. The explanation of this is as follows:

A change in temperature has two effects: the first one is the generation of thermal stresses, and the second one is generation of a pore pressure changes. The first effect is larger at the borehole wall, and disappears quickly with distance from the borehole as seen in the **upper fig** where impermeable borehole is assumed. The second effect is larger at some distance around the borehole as seen in the **Lower fig.**

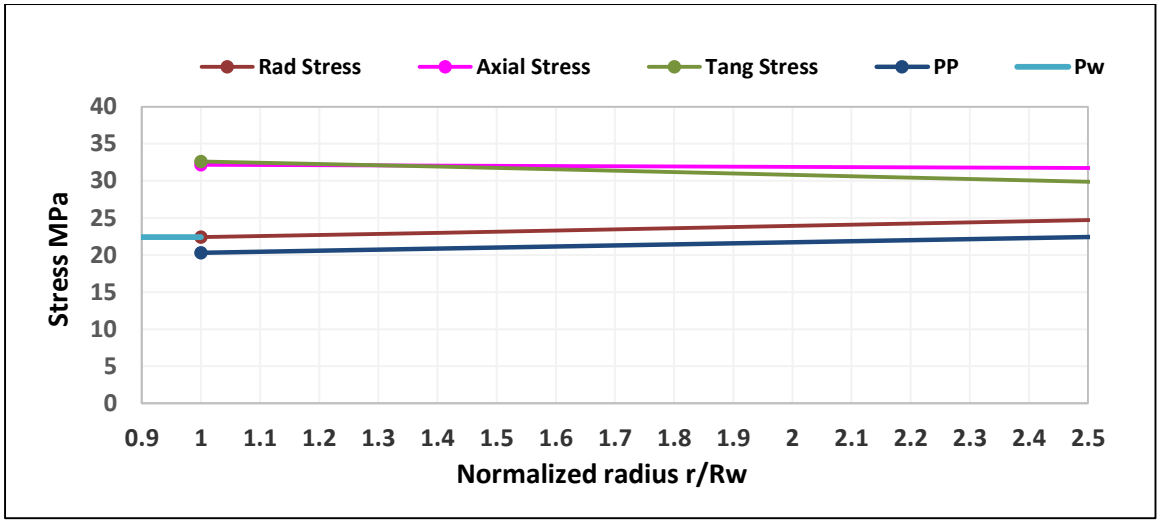

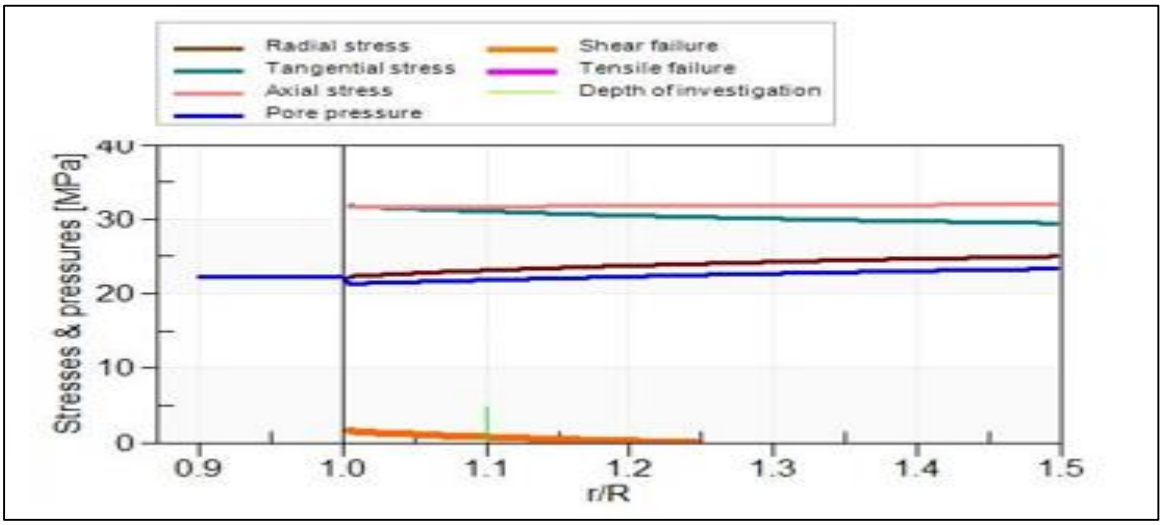

Figure 28 Plot showing schematically the stress state around the borehole wall after temperature change (increase). (Upper) from numerical model and (Lower) PSI. The input parameters used for the modelling is: E=2.4 GPa, Poisson Ratio=0.44, Thermal expansion coefficient=0.0000189 degrees, Sv=30.82MPa, Sh=26.64MPa, Pw=22.42MPa and PP=18.27MPa while the formation temperature was 64 and temperature difference of 50 degrees.

At the borehole wall, the pore pressure is equal to the well pressure (unless the borehole is completely impermeable as we assumed here) and hence the second effect disappears there, reason why not seen in the **Upper fig.**

For a low permeable formation, the second effect is much larger than the first one. Hence what is seen on the **Lower fig** is dominated by the second effect.

In the numerical **Upper fig.** the excessive tangential stress at the borehole wall may cause the near wellbore region to fail in tensile mode according to **eq 2.32.** This failure can then result in filling on the bottom of the well and cause packoff problems.

In the PSI case **Lower fig** as the near-wellbore pore pressure increases, changes in the effective stress distribution eventually leads to time-delayed near-wellbore deterioration. It is done by small and slow fluid filtrate invasion (Oil based muds are not pure oils ,so some water phase may be expected) which gradually equilibrates the mud pressure and the near-wellbore pore pressure, so effective mud pressure support will be lost with time. And this

may result in shear or tensile failure in shale (possible collapse) due to this pore pressure elevation **(eq, 2.34).** The elevation reduces the near-wellbore effective stresses that hold the material together, thus resulting in delayed failure.

From a physical point of view this result can be explained as follows: If the well pressure is higher than the pore pressure, fluids filtrate are injected into the formation and the pore fluid pressure is increased around the well. This will give a tendency for the material to expand and the stresses increase. If on the other hand the well pressure is allowed to fall lower than the pore pressure. The lower fluid pressure around the well will make the formation shrink, and hence the corresponding reduction in the tangential and axial stress.

The final conclusion for **Lower fig** is that once the well pressure is changed there is no significant increase in the probability of failure with time for the changed well pressure, but this will depend on the capillary pressure for the drilling fluid (OBM). While for the **Lower fig** is that the probability will increase at temperature increase and decrease with time since after sometime the temperature will equilibrates with surroundings over time and reach the initial stability state.

The model uses analytical solution and some of this solutions are exact only at and around the borehole wall and have reduced precision deeper into the formation, (Fjaer et al,. 2002). This is not considered to be a problem for the model as a tool for WBS analysis as the critical events with respect to stability occur around the borehole wall (Fjaer 2008).

4.4. Sensitivity Analysis of input parameters

A sensitivity analysis is conducted to a certain input factors that are most responsible for output variability. The analysis is required to understand how the model predictions respond to changes in input variables. In this analysis, the input parameter that is considered uncertain assumes a probability distribution, while other parameters are treated as fixed factors. This analysis highlights the importance of accuracy of each input parameter in the model used for wellbore stability analysis.

This sensitivity analysis gives the feeling about the stability of the mud weight with respect to different input parameters, it's calculated for any parameters and in general the most common is the one that has pronounced uncertainty. The parameters used here are pore pressure, maximum horizontal stress, minimum horizontal stress, vertical stress, well temperature and formation temperature. In most of the cases this can be used to see how the mud weight window changes as those parameters changes.

To understand safe mud weight windows sensitivity towards the maximum, minimum horizontal stress, well and formation temperature let's look at the 1589m TVD RKB. At this depth the well is stable with the (1.43sg) 22.3 MPa mud density, as seen in the **figure 19** where the mud density window is given for about 1 to 2 hours after drilling. The sensitivity analysis results are presented in **figure 29**. In this figure, in the "Y" axis is the mud weight window sensitivity with respect to the one of any input parameter listed above and the "X" axis is the input parameter. The tensile (Pink) and shear (Orange) failure limit the upper and lower mud weight window, the blue line represent the value used in the calculations.

In general the safe and stable mud window narrows down with increase in maximum horizontal stress and well temperature and gets wider with increasing in formation temperature and minimum horizontal stress. It's possible to see by reducing the S_H by certain amount will lead to an increasing in the minimum mud weight while increasing the S_h will give the opposite response.

When sensitivities are larger in magnitude the output may be significantly affected even by a small perturbation in the input parameter.

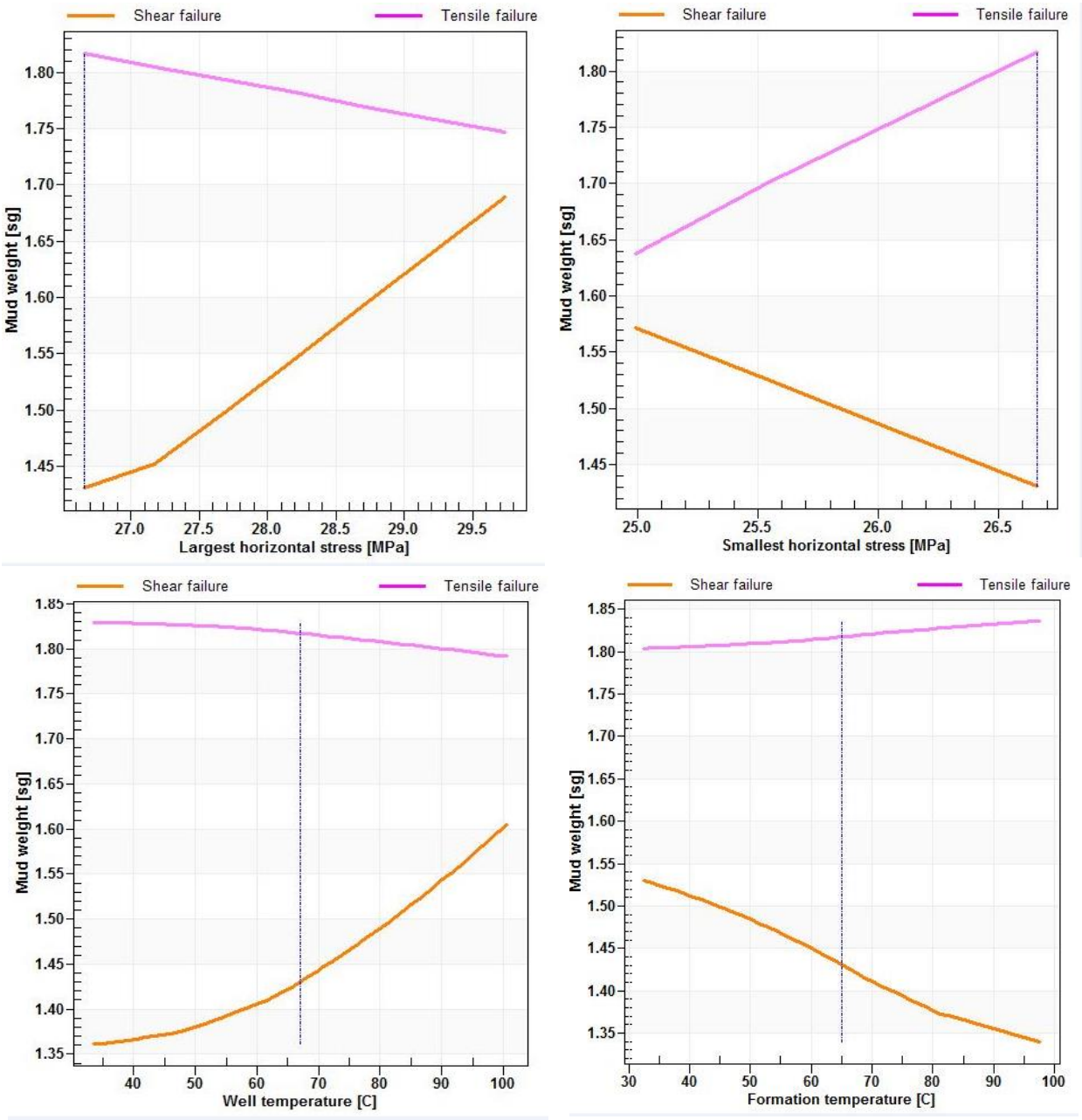

Figure 29 Sensitivity of the calculated stable mud window as function of maximum, minimum horizontal stress, well and formation temperature. At 1589m the orange curve is the lower limit (shear failure) and the pink upper limit (tensile failure) the blue vertical line indicated the value used for stability.

4.5. Uncertainty in wellbore stability analysis

One issue with wellbore stability analysis lies in the degree of uncertainty of the rock strength parameters and stresses. While measurement and analytical techniques have been developed for determination of these inputs, their actual values cannot be solved precisely (Morita, 1995).

The words ‘uncertainty’ and ‘risk’ are sometimes used interchangeably and are synonymous with decision-making. In 1921, F. H. Knight, distinguished the difference between the two concepts. According to him, risk deals with randomness with knowable probabilities, whereas uncertainty deals with randomness with unknowable probabilities.

Uncertainty in wellbore stability analyses have been discussed in previous studies (Morita 1995; Mostafavi et al., 2011; Ottesen et al. 1999; Liang 2002; de Fontoura et al. 2002; Sheng et al. 2006). Here is just an overview for this study using simple math calculation for error and uncertainty.

Handling uncertainty and lack of data in wellbore stability analysis, in case like this where no wells have been drilled or you have scarce data from one offset well in the area, with very few measurements from the offset well, developing a reliable wellbore stability analysis will be a challenge.

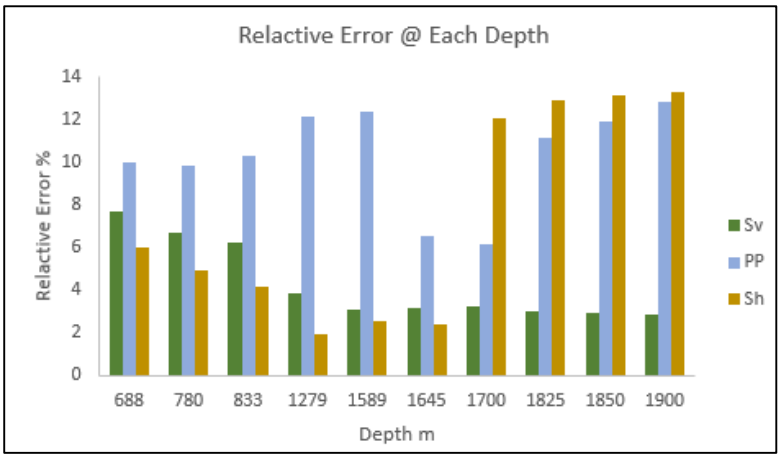

Figure 30 Relative error percentage for Sv PP and Sh at each depth. The error is given by the difference between the pre-drill predicted value from offset well and the calculated value dived by calculated value.

In this case, estimation of the required mud weight can have considerable uncertainties. It is, however, possible to quantify those uncertainties and also to learn what measurements are required to provide the maximal improvement in prediction accuracy, using simple math calculation, the analyses can be carried out at each single depth.

Measurement errors and misinterpretation errors are the major sources of input parameter uncertainties. The input uncertainties may also be due to scarcity of data, and there is a human error as well when calculating the input parameters from indirect measurements. Where input data are scarce, interpolations and assumptions are often introduced in the analysis. *Errors are measure of the estimated difference between the observed or calculated value of a quantity and its true value.*

Table 6 Uncertainty range for each parameter at each depth. The uncertainty is given by the standard deviation of the mean.

Parameters						
	Sv (Overburden)		PP (Pore Pressure)		Sh (Min Horiz Stress)	
Depth	Likely Value	% Uncertainty	Likely Value	% Uncertainty	Likely Value	% Uncertainty
688	1.774	±4	0.978	±5	1.487	±3
780	1.815	±3	0.989	±5	1.529	±2
833	1.837	±3	0.997	±5	1.553	±2
1279	1.914	±2	1.041	±6	1.648	±1
1589	1.952	±2	1.057	±6	1.68	±1
1645	1.959	±2	1.106	±3	1.691	±1
1700	1.969	±2	1.138	±3	1.624	±6
1825	1.999	±2	1.175	±6	1.653	±7
1850	2.005	±1	1.181	±6	1.658	±7
1900	2.015	±1	1.189	±7	1.666	±7

Here, the well was drilled vertical, based on error and uncertainty calculations from expected results (pre drill: calculated from offset well) versus calculated results (drilled), by using simple math calculation, the optimum mud weight required to drill the well without instability is 22.3 MPa for the upper section. The error results at each analysed depth is shown in the **figure 30** and it's related to difference between the pre-drill predicted value from offset well and the calculated value and the uncertainty given by the standard deviation of the mean is shown in **the table 7.** If at the time of analysis no well had been drilled in the area, there would have been large uncertainties in the magnitudes of the horizontal stresses, and there may also be large uncertainties in the overburden stress, **Sv**.

As it can be seen that the largest uncertainty is in the minimum horizontal stress and it might be associated with the lack of XLOT data to calibrate the calculated values since the estimated S_h values is a best-fit curve based on all available stress measurements, essentially extended leak-off tests taken in the area. In addition, the large variation in the magnitude of the pore pressure will produces a similarly large uncertainty in the recommended mud weight.

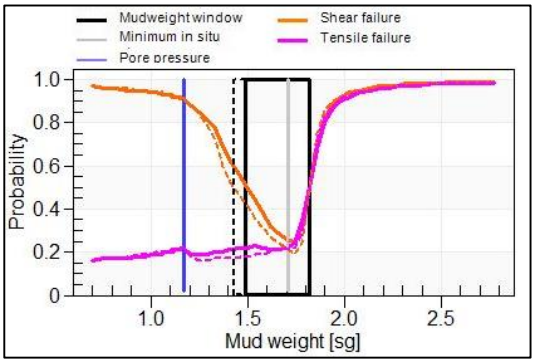

Figure 31 Uncertainty in the modelled stable MW (Probability of failure) at 1589m one day after drilling using physical criteria. After 6% uncertainty in the pore pressure has been introduced. The stable MW as defined by 0.5 probability for failure is indicated in black line Minimum and Maximum). Note that the dashed line is with no uncertainty. With the same 1.43sg

Here uncertainty in stability calculations is introduced through an uncertainty in the pore pressure. To illustrate the dependence of the output to the input uncertainty like pore pressure and vertical stress at 1589m TVD RKB. The uncertainty in the pore pressure curve might be due to lack of direct measurements in the overburden, as well as there is also a lithology change at this depth, going from non-reservoir into reservoir, but it is not clear how much this affects the curve. The **Fig 31** shows how an 6% in pore pressure uncertainty introduces nearly 0.5 MPa uncertainty in the lower limit stable mud density, and decreases in the minimum mud weight window, when compared to **fig 32 (Left)** where no uncertainty was used **(Right).**

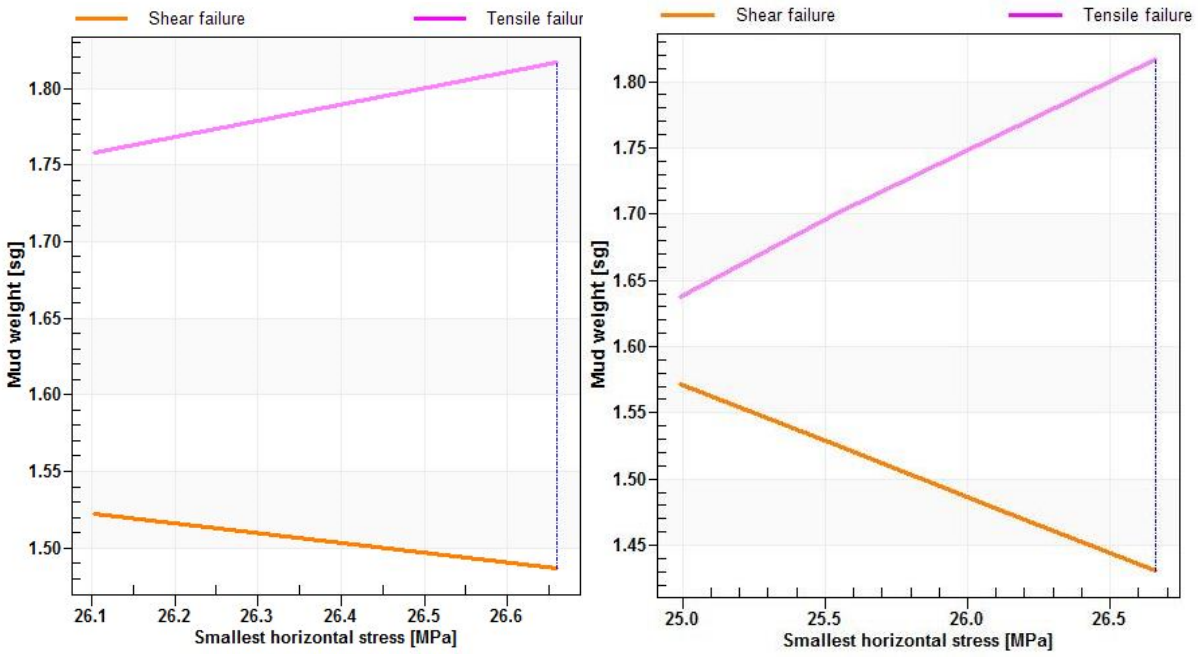

Figure 32 Mud weight window sensitivity to pore pressure (Left) with 6% uncertainty in the pore pressure (right) with no uncertainty in pore pressure.

In summary the overall uncertainty depend on the model and quality of the input parameter and there is higher uncertainty in the estimation of the rock mechanical properties such as cohesive rock strength, young modulus, and Poisson ratio and shear modulus from indirect measurements (sonic logs).

5. Conclusions

Important factors that contribute to wellbore instability were discussed. The key parameters that influence wellbore instability are pore pressure, rock strength, in-situ stresses, and based on the acoustic data (sonic), estimate of dynamic rock properties were presented. And the time dependent nature of the wellbore instability problem was presented in for a North Sea case well. In the example case time-dependency was observed in the failure analysis, in estimations of critical regions around the wellbore, and mud weight-window analyses.

As a result of the analysis, the safe mud density window was computed. And the results indicates that the well should not face any wellbore failure problem with the recommended mud weights, at which the borehole can be drilled in a stable manner.

The conclusions of this study are as follows:

1. A special wellbore-stability problem-diagnostic scheme was first used to identify problematic horizons. The possible causes of wellbore stability issues were narrowed down. It's possible to suggest that the well trajectory, drilling fluid density, and types of oil-based mud have the major impact on the fact that has not occurred any instability problems.

2. Even without any core measurements, formation conditions or properties it is feasible to obtain reliable required input data only utilizing available well log (Sonic), to solve wellbore-stability issues. It should be emphasized that availability of the key wells with critical well-log data is of utmost importance to conduct wellbore-stability studies without available core measurement data.

3. A comparison of the numerical modelling for thermal effects results with the PSI observations implies that obtained wellbore-stability input data and the output results is in an acceptable range even with some data uncertainty.

4. The wellbore-stability model developed in this study can be potentially applied to other fields in the North Sea Basin using a similar approach which might be adjusted to the particular field specifications and requirements.

5. This study neither has considered chemical interactions between drilling fluid and shale.

6. Formation contraction will be generated as the temperature decreases, a tensile stress is applied on the borehole wall, and the fracture pressure and collapse pressure will decrease simultaneously. The drilling fluid density should be decreased properly in order to prevent drilling fluid leakage.

7. Temperature increases will cause formation expansion and a compressive stress is applied on the borehole wall, and the fracture pressure and collapse pressure will increase simultaneously, and thus, increasing temperature will widen the safe mud density window, while decreasing temperature will narrow the safe mud density window. Generally heating the wellbore decrease stability by increasing the pore pressure and tangential stress and rise the fracturing and collapse mud weight.

5.1. Recommendations

The recommendations for future work from this analysis are as follows:

1. All the relevant data should be available to enhanced the model and for better visualizing the problematic horizons and populating of the obtained wellbore-stability input parameters.

2. The laboratory geomechanical parameters when available has to be correlated to the petrophysical parameters to derive these geomechanical parameters from well logs and to reduce costly geomechanical laboratory measurements in the life cycle of the field.

3. Rock strength parameters such as poisson's ratio (ν), young module (E) and uniaxial compressive strength (UCS) when estimated from processed sonic data, must be compared with available core data of the reservoir section, to check for comprehensive match with each other.

4. Extended leak-off tests should be conducted at various intervals to calibrate the calculated magnitude of the minimum horizontal stress.

5. In addition, to build a solid WBS analysis the professional software has to be used instead of student version due to its inability to effectively handle log based data and only single depth based data, and up to five single depth based data, which can pose great degree of difficulties when comes to interpret the results since it extrapolates what is happening in between two depths.

6. It is recommended a complete risk management flow chart integrating the wellbore stability and fault stability along with analysing the drilling problems that have been occurring. It will serve as road map to manage drilling hazards and risks through recommended prevention, mitigation and best practices.

6. Nomenclature

$\sigma; S$ = Formation Stress

τ = Shear Stress

σ' = Effective Stress

$\sigma(T)$; σ_T = Thermal Stress

T^*= Formation tensile strength

$P; PP$ = Pressure; Pore Pressure

ε = Strain

S_0 = Cohesion

C_0 = Shear strength parameters (Rock strength)

T; T_0 = Temperature; Initial Temperature

$Tcool$ = Temperature of the cooled region

t = Time

ρ_w = Mud Density, controls the pressure in the well

ρ = Density of the Rock

d = Diameter of the hole

D = Vertical depth

g = Acceleration due to gravity

h = Thickness of the formation

C_n = Relactive pressure amplitude = 0.046 MPa/K

ε_{ch} = Strain induced by ion exchange, at saturation, 10^{-3}

RT = The molar gas constant (8.31 J/(molK)),

Vw = The molar volume of water (0.018 l/mol).

α_{df}; $\alpha_{w,df}$ = Chemical activity of the Drilling fluid

α_{sh}; $\alpha_{w,sh}$ = Chemical activity of the Shale

$\Delta\Pi$ = Osmotic Potential

v = Poisson ratio

E = Young Modulus

G = Shear Modulus

K = Bulk Modulus of the Rock

M = Dynamic Compressive modulus

DTC = Compressional travel time

DTS = Shear travel time

V_c = Compressional Velocity

B = Skempton Parameter

β_T = Volumetric Thermal Expansion

α_T = Linear Expansion Coefficient

α_m = Volumetric Expansion Coefficient

k = Thermal conductivity

C_p = Specific heat capacity

c = Coupling coefficient

$\propto_0$ = Hydraulic diffusivity

$\propto$ = Thermal diffusivity constant

δ = Permeability Coefficient (Mobility)

k_* = Permeability

μ = Viscosity

α = Biot coefficient

β = Failure angle

φ = Friction angle

η = Poro-elastic stress coefficient

r; R = Radial Distance

Δ = Difference

Subscripts

r = Radial

θ = Tangential

v = Vertical

n = Normal

w = Well

f = Formation

fl = Fluid

u = Undrained

fr = Drained

z = Axial

vol = Volumetric

n = Normal

o = Observed

p = Pore

H; h = Max Horizontal; Min Horizontal

1; 3 = Max; Min

SI Metric Conversion Factors

sg x 1 = g/cc

ft x 0.3048 = E - 01 m

sg x 1.422 x TVD = Psi

psi x 6.894757 = Kpa

psi/ft x 22.62 = Kpa/m

7. References

Bell, V.: 1996, Rock Mechanics and Rock Engineering.

Chen, G. and Ewy, R.T.: 2005, “Thermo-poroelastic Effect on Wellbore Stability,” SPE 89039

Chi, A. et al.: 2013, The Effects of Pore Pressure and Temperature Difference Variation on Borehole Stability. CSCanada: Advances in Petroleum Exploration and Development, Vol 6

Chilingar, G. V.: 2002, Introduction to Abnormally Pressure formations

Coates, G. R. and Denoo, S. A.: 1980, Log Derived Mechanical Properties And Rock Stress. SPWLA-1980-U

Detournay, E. and Cheng, A. H-D.: 1988, Poroelastic response of a borehole in a non-hydrostatic stress field. Int. J. Rock Mech. Min. Sci. & Geomech. Abstr. Vol. 25, No. 3, pp. 171-182, 1988 (12 pp.)

Eaton, B.A.: 1975, The Equation for Geopressure Prediction from well logs. SPE-5544

Fjær, E. and Holt, R.M.: 2008, Petroleum Related Rock mechanics, Elsevier. Ch.4: Stresses around boreholes – Borehole failure criteria; pp. 135-174

Fjær, E. and Holt, R.M.: 1999, Rock mechanics - relevant for the Petrophysicist

Fjaer, E. et al,: 2002, Mud chemistry on time delayed borehole stability problems in shale. SPE/ISRM 78163

Jaeger, J. C. and N. G. W. Cook.: 1976, Fundamentals of Rock Mechanic. Chapman and Hall

Lal, M.: 1999, Shale Stability: Drilling Fluid Interaction and Shale Strength. SPE 54356

Majidi, R. et al.: 2010, Quantitative analysis of mud losses in naturally fractured reservoirs: The effect of rheology. SPE Journal, December 2010, 509-517 (8 pp.)

Maury, V. and Guenot, A.: 1995, Practical advantages of mud cooling systems for drilling. SPE Drilling & Completion, March 1995, 42-48; 7 pp

Maury, V. and Zurdo, C.: 1992, Drilling-induced lateral shifts along pre-existing fractures - A common cause of drilling problems. SPE Drilling & Completion, March 1996, 17-23; 7 pp

Maury, V.M. Sauzay, J.-M.:1987, Borehole instability: Case histories, rock mechanics approach, and results. SPE/IADC 16051.

McLellan, P.:1994a, Assessing The Risk of Wellbore Instability in Horizontal and Inclined Wells. HWC94-14 SPE/CIM/CANMET

McLean, M.R. Addis, M.A. (1990): Wellbore Stability Analysis: A Review of Current Methods of Analysis and Their Field Application. IADC/SPE 19941

Mody, F.K. and Hale, A.H.: 1993, Borehole stability Model to couple chemistry of drilling fluid shale interactions; JPT (November) 1093-1101; 8 pp

Morita, N. et al.: 1990, Theory of lost circulation pressure. SPE 20409; 15 pp.

Morita, N., 1995. Uncertainty Analysis of Borehole Stability Problems, SPE Annual Technical Conference and Exhibition.

Mostafavi, V. et al.: 2011, Based Uncertainty Assessment of Wellbore Stability Analyses and Downhole Pressure Estimations

Nes, O.M. et al.: 2005, Drilling time reduction through an integrated rock mechanics analysis. SPE/IADC 92531, 7 pp.

Nes, O. et al,: 2012, Borehole instability in tertiary shales in the Nowergian North Sea. SPE 150714

Nes, O. et al,: 2013, Borehole shale stability analysis to facilitate successful drilling of a horizontal well in the North Sea. ARMA 13346.

Nguyen, D.: 2010, Modelling thermal effects on wellbore stability. SPE 133428

Økland, D. and Cook, J.M.: 1998, Bedding related borehole instability in high angle wells. SPE/ISRM 47285. 10 pp.

Oort, V.: 2003, On the physical and chemical stability of shales. J Petr Sci Eng; pp. 213-235 (23 pp.)

Horsrud, P.: 2001, Estimating Mechanical Properties of Shale from Empirical Correlations. SPE 56017

Outmans, H.D.: 1958, Mechanics of differential pressure sticking of drill collars. AIME Petr. Trans. 213, 265-274, 10 pp.

Perkins, T.K. and Gonzalez, J.A.: 1984, "Changes in Earth Stresses around a Wellbore Caused by Radial Symmetrical Pressure and Temperature Gradients," SPE, April 1984

Santarelli, F.J. et al.: 1992, Mechanisms of borehole instability in heavily fractured rock media. Int. J. Rock Mechanics, Min. Sci. & Geomech. Abstr. 29, 457-467; 11 pp

Stjern, G. et al.: 2000, Improving drilling performance in troublesome clay formations in the Heidrun Field. IADC/SPE 59219; 10 pp

Tang, L. and Luo, P.: 1998, "The Effect of Thermal Stress on Wellbore Stability," SPE 39505

Thiercelin, M.J. et al.: 1997, Cement design based on cement mechanical response. SPE 38598; 12 pp.

Willson, S.M. et al.: 1999, Drilling in South America - a wellbore stability approach for complex geologic conditions. SPE 53940; 10 pp

Pasic, B. et al.: 2007, Wellbore Instability: Causes and Consequences

Yan, C. et al,:2013, Borehole Stability in High-Temperature Formations

Zoback, M. D.: 2007, Reservoir Geomechanics. Cambridge University Press

8. Appendices

8.1. Concepts for useful terms

Re-entry drilling: Is a process of revisiting existing wellbore to save the expense of drilling entire new well, provides a means to reduce horizontal well costs. In addition to boost well productivity, re-entry drilling can also tap bypassed reserves.

Extended-reach Drilling / well: Is a high-angle (with an inclination of generally greater than 85°) directional well drilled to intersect a target at a point.

Extended reach wells can be extremely long (measured depth) and relatively shallow vertically, the extremely long reach wells are typically drilled to distant reservoirs to reduce the infrastructure and operational footprint that would otherwise be required to access the resource.

Multilateral wells: are new evolution of horizontal wells in which several wellbore branches radiate from the main borehole. Is the ability to create wells with multiple branches that can target widely spaced reservoir compartments.

Bottom hole assembly (BHA) is the lower portion of the drill string, consisting of (from the bottom up) the bit, bit sub, a mud motor (in certain cases), stabilizers, drill collar, heavy-weight drill pipe. The bottom hole assembly must provide force for the bit to break the rock (weight on bit). While drill string is the combination of the drill pipe, the bottom hole assembly and any other tools used to make the drill bit turn at the bottom of the wellbore.

Wellbore instability: is recognised when the hole diameter is markedly different from the bit size and the hole does not maintain its structural integrity (Osisanya,2012).

The Equivalent Circulating Density (ECD) is defined as the increase in density due to friction and it is normally expressed in pounds per gallon.

$$ECD = MW + \frac{Pa}{1.4223 * TVD}$$

Where; ECD = Equivalent circulating density (ppg), Pa = Annular friction pressure (psi), TVD = True vertical depth (m), MW = Mud weight (ppg).

Osmotic pressure is the minimum pressure which needs to be applied to a solution to prevent the inward flow of water across a semipermeable membrane.(Voet, et al., 2001). In another words the minimum pressure required to prevent osmosis.

Osmosis is the spontaneous net movement of solvent molecules through a semi-permeable membrane into a region of higher solute concentration, in the direction that tends to equalize the solute concentrations on the two sides. (Haynie, D. T. 2001).

A **semipermeable membrane**, also termed a selectively permeable membrane, is a type of membrane that will allow certain molecules or ions to pass through it by diffusion. The rate of passage depends on the pressure, concentration, and temperature of the molecules or solutes on either side, as well as the permeability of the membrane to each solute.

Osmotic Potential is the potential of water molecules to move from a hypotonic solution (water > solutes) to a hypertonic solution (water < solutes) across a semi permeable membrane. Or it's a measure of the potential of water to move between regions of differing concentrations across a semi-permeable membrane.

A pure water contains no solutes, thus, it should have zero water potential. And also for this reason, the value of osmotic potential of a solution is always negative since the presence of solutes will always make a solution have less water than the same volume of pure water. In application, when two solutions are isotonic (same proportion of solute and water) the osmotic potentials will be equal, and there will be no net movement of water molecules. But if the solution is hypotonic (diluted solution, solutes < water) will have higher osmotic

potential (less negative) whereas the solution that is hypertonic (concentrated solution, solutes > water) will have lower osmotic potential (more negative). Difference in osmotic potentials will cause water molecules to move from a hypotonic solution to a hypertonic solution.

Thermal expansion: Is the tendency of matter to change in volume in response to a change in temperature through heat transfer.

Thermal Expansion Coefficient

The thermal expansion coefficient is one of the important parameters influencing the calculation of thermal stress around a borehole. It describes how the size of an object changes with a change in temperature. Specifically, it measures the fractional change in size per degree change in temperature at a constant pressure.

Heat transfer: Describes the exchange of thermal energy, between physical systems depending on the temperature and pressure, by dissipating heat.

The fundamental modes of heat transfer are conduction or diffusion, convection and advection.

Diffusion: Is the net movement of a substance (e.g., an atom, ion or molecule) from a region of high concentration to a region of low concentration.

Thermal or heat advection: is the transport of heat by a moving fluid. A special form of advection is convection, where the fluid motion is itself driven by temperature differences.

Convective heat transfer, or convection: is the transfer of energy between an object and its environment, due to fluid motion, a process that is essentially the transfer of heat via mass transfer.

The difference between thermal conduction, advection and convection is based on fact that for diffusion the transfer of energy is within a solid or between objects that are in physical contact, and convection is usually the dominant form of heat transfer in liquids and gases. The difference between convection and advection heat transfers is the direction of the exchange.

Convection heat transfer involves the transfer of heat through the movement of the medium's particles, this medium must be a gas or liquid. Convection always transfers heat in the vertical plane, this movement is driven by variations in the medium's density and, therefore, buoyancy. Heated particles expand, causing them to decrease in density; these particles become more buoyant than surrounding particles, causing them to rise. As they rise, their heat is transferred to cooler portions of the medium located above them.

Advection heat transfer differs from convection in that the movement of heat is confined to the horizontal plane. This type of heat transfer is not powered by variations in density, but rather requires an outside force, such as wind or currents, to displace the particles of the medium. As the particles move horizontally into systems that are hotter or colder, heat is transferred.

Temperature: Is defined as the average molecular kinetic energy of a substance.

Thermal conductivity: is the intrinsic property of a material which relates its ability to conduct heat, as well called the thermal conductivity coefficient.

It can also be defined as the quantity of heat transmitted through a unit thickness in a direction normal to a surface of unit area due to a unit temperature gradient under steady state conditions and when the heat transfer is dependent only on the temperature gradient.

Thermal conductivity of materials is temperature dependent. Birch and Clark (1940) suggested that the reciprocal of thermal conductivity (thermal resistivity) might be a linear function of the temperature. Blesh et al. (1983) found that the agreement between the best-

fit line and experimental data for several rocks for temperatures up to 300 C is acceptable, and does not vary by more than 3 %.

Please take into account that measured conductivities and some other thermal properties of rocks observed in various regions and or even within the same regions may vary due to influence of different physical-chemical factors.

The thermal conductivity of formations is dependent on temperature, pressure, porosity, composition, and properties of pore-filling fluids and gases. Values of thermal conductivity coefficients range widely for rocks and pore-filling substances.

All pore-filling fluids have lower thermal conductivities values than rocks and this causes the overall thermal conductivity to decrease with increasing porosity. Poelchau et al,. (1997).

Heat capacity: of a defined system is the amount of heat needed to change by raising the system's temperature by one degree. The heat capacity is therefore an extensive variable since a large quantity of matter will have a proportionally large heat capacity. A more useful quantity is the specific heat (also called specific heat capacity), which is the amount of heat required to change the temperature of one unit of mass of a substance by one degree.

Density: The density, or more precisely, the volumetric mass of a substance is its mass per unit volume. It is a physical property of matter, as each element and compound has a unique density associated with it. Density defined in a qualitative manner as the measure of the relative "heaviness" of objects with a constant volume.

Leak off Test (LOT) is a test to determine the strength or fracture pressure of the open formation, usually conducted immediately after drilling below a new casing shoe. During the test, the well is shut in and fluid is pumped into the wellbore to gradually increase the pressure that the formation experiences. At some pressure, fluid will enter the formation, or leak off, either moving through permeable paths in the rock or by creating a space by fracturing the rock. The results of the leak off test dictate the maximum pressure or mud weight that may be applied to the well during drilling operations. To maintain a small safety factor to permit safe well control operations, the maximum operating pressure is usually slightly below the leak off test result.

The differences between Formation Integrity Test (FIT) and Leak Off Test (LOT) is that in Leak Off Test the pressure test is performed on shoe and formation until formation break down, while for Formation Integrity Test is to test the strength of shoe and formation to designed pressure. FIT is performed to ensure that you will be able to drill to section target depth and will be able to control the well in case of well control situation without underground blow out.

Table 8 thermal expansion of rocks for temperature interval 20-100 deg C

Rocks	Volumetric thermal expansion[1] (10^{-5} per °C)
Sandstone	3
Quartzite	3.3
Limestone	2.4
Marble	2.1

1 Mean volumetric thermal expansion, (X = (1/V_0) (ΔV / ΔT), in units of 10-5 per °C, from Skinner (1966).